

UNIVERSIDADE DE SÃO PAULO
INSTITUTO DE GEOCIÊNCIAS

EVOLUÇÃO DO MÉDIO RIO TOCANTINS DURANTE O QUATERNÁRIO TARDIO

JANDESSA SILVA DE JESUS

Dissertação apresentada ao Programa de
Geociências (Geotectônica e Geoquímica)
para obtenção do título de Mestra em
Ciências.

Área de concentração: Geotectônica

Orientador: Prof. Dr. Fabiano do
Nascimento Pupim

SÃO PAULO
2020

Autorizo a reprodução e divulgação total ou parcial deste trabalho, por qualquer meio convencional ou eletrônico, para fins de estudo e pesquisa, desde que citada a fonte.

Serviço de Biblioteca e Documentação do IGc/USP

Ficha catalográfica gerada automaticamente com dados fornecidos pelo(a) autor(a)
via programa desenvolvido pela Seção Técnica de Informática do ICMC/USP

Bibliotecários responsáveis pela estrutura de catalogação da publicação:
Sonia Regina Yole Guerra - CRB-8/4208 | Anderson de Santana - CRB-8/6658

Jesus, Jandessa Silva de
Evolução do médio rio Tocantins durante o
Quaternário tardio / Jandessa Silva de Jesus;
orientador Fabiano do Nascimento Pupim;
coorientador André Oliveira Sawakuchi. -- São Paulo,
2020.
108 p.

Dissertação (Mestrado - Programa de Pós-Graduação
em Geoquímica e Geotectônica) -- Instituto de
Geociências, Universidade de São Paulo, 2020.

1. Rio Tocantins. 2. Marabá (PA). 3. Geomorfologia
Fluvial. 4. Datação OSL. 5. Paleoclima. I. Pupim,
Fabiano do Nascimento, orient. II. Oliveira
Sawakuchi, André, coorient. III. Título.

UNIVERSIDADE DE SÃO PAULO
INSTITUTO DE GEOCIÊNCIAS

"Evolução do médio Rio Tocantins durante o Quaternário Tardio"

JANDESSA SILVA DE JESUS

Orientador: Prof. Dr. Fabiano do Nascimento Pupim

Dissertação de Mestrado

Nº 849

COMISSÃO JULGADORA

Dr. Fabiano do Nascimento Pupim

Dr. Mario Luis Assine

Dr. Carlos Henrique Grohmann de Carvalho

SÃO PAULO
2020

À minha família
José Martins, Elzanira e Taís

AGRADECIMENTOS

Ano de 2014, rio Xingu, minha irmã (Taís de Jesus) estudante de biologia na UFPA-Campus de Altamira, em uma campanha de campo conheceu um geólogo na equipe. Nesse período (2013-2014) fui presidente do CA da Fageo/Marabá e estávamos organizando a Semana de Geologia. Compartilhei com minha irmã que nosso objetivo era levar para a referida Semana de Geologia pesquisadores das diversas áreas das geociências. Então ela comentou de um geólogo que estava pesquisando sistemas fluviais na Amazônia. Ora, perfeito! Entramos em contato, o geólogo era o André, que prontamente aceitou o convite e assim apresentamos o Paleocanal do Tocantins.

A convite do André para uma atividade de campo no Rio Xingu, ainda em 2014, conheci Henrique, Dailson, Mauricio, Geovan e Fabiano. Mais contatos estabelecidos e mais elos construídos. Vínculos acadêmicos fortalecidos, Fabiano e André pousaram em Marabá, final de 2015 para participar o campo do meu Trabalho de Conclusão de Curso no médio rio Tocantins. Foram dias de muito aprendizado. Meu horizonte como pesquisadora se expandiu em meados de 2016 quando fui a São Paulo para “rodar” as amostras para datação. Continuei a conhecer pessoas maravilhosas que foram e são fundamentais nessa etapa da vida, Eurides e Dilce que me deram abrigo e muito afeto. Sim, existe amor em SP. Thays e Luciana duas humanas lindas, em todas as dimensões e profissionais competentíssimas foram vitais nessa etapa de “paixão pela datação OSL”. Conhecer esse mundo, o método, as pessoas, o ambiente, tiveram consequências, o espírito curioso de criança reviveu. TCC defendido em dezembro de 2016. Vários percalços vencidos até a prova do mestrado no 2º semestre de 2017. Ano de 2018, eu, mestrandona no IGc/USP. Égua, foi demais!

Agradecimento relevante ao Programa de Pós-Graduação em Geociências (Geotectônica e Geoquímica) especialmente a Profª. Drª. Juliana pelo empenho de aplicar a prova fora do IGc/USP e pelo CPG que aprovou o pedido. Gratidão ao Prof. Cláudio Lamarão e a Gisele Marques, muito solícitos, que me receberam na UFPA para aplicar a prova de seleção. Tudo isso com a intercessão deles, a dupla, André e Fabiano. São seres humanos e profissionais que me espelho. Obrigada por terem acreditado em mim, pela oportunidade. André por todo apoio e confiança, pelas valiosas e numerosas contribuições neste trabalho. Ao Fabiano que é um grande

orientador. Pesquisador que instiga, perspicaz e dedicado. Quem dera todo pós-graduando tivesse a sorte que tenho. É inenarrável a gratidão!

À USP, pela oportunidade de conviver e aprender com os melhores pesquisadores do mundo. Ao IGc pelo ambiente criativo e amigável que proporciona, e pelo seu corpo docente, direção e administração por abrir a janela pela qual hoje vislumbro um horizonte superior, baseado em uma produção científica ética e saudável. Ao INPA, excelência em ensino e pesquisa na Amazônia, pela experiência de disciplinas com feras desse universo verde e azul. À Unifesspa, pelo apoio logístico durante a etapa de campo. A Prefeitura Municipal de Anapu pela oportunidade de concluir esse mestrado com tranquilidade.

Ao Prof. Léo, pioneiro, por ter me apresentado a área de estudo, pela oportunidade de começar na Iniciação Científica e incentivo a continuar a pesquisa. Valeu, Gordo! A Kelly Cruz, a vida da pós nos uniu, obrigada pelo compartilhamento mútuo dos medos, das frustrações do inglês, alegrias e dilemas da vida adulta. A Elianne, companheira fiel, exemplo de dedicação, obrigada pela ajuda imprescindível durante o campo e abrigo afetuoso da sua família durante os voos de madrugada para SP. Ao Josiel, agora parceiro de pesquisa, obrigada pelo apoio no campo, por abraçar o desafio. Ao Romário por contagiar com seu entusiasmo pela pesquisa, e na preciosa ajuda com os clastos junto com o Ricardo. A Érica e a Paula, por sermos testemunhas da nossa evolução, por dividir a vida mesmo de longe. Ao Guano por disponibilizar equipamento para finalização dos mapas. Ao Messias pelo incentivo e revisões em inglês. Aos meus colegas de trabalho da SEMMAT pela ajuda e palavras de incentivo nos dias de cansaço, em especial ao Pereira, amigo de lutas diárias por uma Amazônia sustentável. Ao Marksuel que tornou essa trajetória mais suave com paciência e amor. Aos amigos que fiz nessa fase Ian, Paty, Caio, Cláudia, Fernanda Piotto, Fernanda, Isaac e Potien. Meus sinceros agradecimentos a todas as pessoas e entidades que contribuíram para que este trabalho. A CAPES pela bolsa.

Finalizo com a responsável pelo primeiro elo do laço, minha irmã-amiga, testemunha da minha vida. Aos meus pais, pelo incentivo e amor aos nossos sonhos (até coleta para datação OSL eles já acompanharam), desculpa pela ausência dedicadas ao estudo. “*Tudo que nóiz tem, é nóiz*” (*Emicida*).

A Nossa Senhora de Nazaré, nossa mãezinha intercessora.

A Deus, por ter cuidado de todos os elos desse laço lindo da minha vida.

*“Eu posso acreditar que ainda dá pra gente
viver numa boa. Os rios da minha aldeia são
maiores que os de Fernando Pessoa*

*Molhando meus olhos de verde-floresta
sentindo na pele o que disse o poeta
eu olho o futuro e pergunto pra insônia
será que o Brasil nunca viu a Amazônia?”*

Nilson Chaves & Celso Viáfora

RESUMO

Jesus, J. S., 2020, Evolução do médio rio Tocantins durante o Quaternário tardio [Dissertação de Mestrado], São Paulo, Instituto de Geociências, Universidade de São Paulo, 108 p.

O rio Tocantins drena a área mais oriental da Amazônia. A maior parte de sua bacia hidrográfica é representada por vales rochosos, mas o trecho médio é marcado pelo acúmulo de sedimentos, que mostra um conjunto diversificado de formas fluviais, grandes planícies de inundação e níveis de terraço, chamados Paleocanal do Tocantins e Bico do Papagaio. No entanto, a história quaternária do rio Tocantins é pouco conhecida devido à falta de estudos geomorfológicos condicionados por dados geocronológicos. Portanto, caracterizamos os depósitos sedimentares do médio Tocantins e aplicamos datação por luminescência opticamente estimulada (OSL), a fim de entender como essa paisagem fluvial evoluiu durante o Quaternário tardio. Os resultados desta pesquisa são apresentados em dois artigos. O primeiro consiste no mapeamento geomorfológico na escala de 1:100.000 da planície fluvial no médio rio Tocantins. Foram definidas três unidades geomórficas principais: (i) planície aluvial, (ii) terraços fluviais e (iii) paleoleque aluvial. Nossos resultados oferecem insights sobre os complexos processos geomorfológicos e sedimentológicos que moldam a paisagem fluvial atual. O mapa apresentado oferece um produto cartográfico detalhado, que pode ser de utilidade para planejadores e tomadores de decisão em projetos de desenvolvimento regional e conservação. O segundo artigo apresenta os resultados da análise morfosedimentar integrada à datação OSL, que permite interpretar a evolução da paisagem entre 661 ± 42 e $160 \pm 16,3$ ka. As idades OSL permitem identificar três fases principais de deposição e duas fases de incisão. A fase deposicional mais antiga formou os Terraço Altos (T1) e parte do Paleoleque aluvial entre 160 a 32 ka. Posteriormente, ocorreu um evento de incisão em torno de 31 ka, resultou no abandono do T1, seguido de uma segunda fase de deposição que construiu os Terraços Baixos (T2) e promoveu a reativação dos Paleoleques aluviais de 31 a 6 ka. A incisão mais recente ocorreu de 6 a 5 ka, permitindo o abandono do T2 e a redução do nível da base local até sua posição atual. A moderna planície de inundação é construída desde 5 ka até o presente, com deposição de sedimentos devido à frequente migração lateral do rio Tocantins. Os resultados obtidos neste trabalho apresentam uma paisagem altamente diversificada em termos de suas geoformas, aspectos sedimentares e geocronológicos resultantes dos vários momentos de sua evolução geomorfológica ao longo do Quaternário tardio. Os resultados foram correlacionados com dados paleoclimáticos regionais e apontam que as mudanças climáticas foram o principal impulsionador da dinâmica fluvial do médio Tocantins nos últimos 160 ka. A evolução dos terraços dessa região da Amazônia se assemelha a formação dos terraços fluviais na Amazônia Central e Ocidental descritos na literatura e apontam que os sistemas fluviais da Amazônia Oriental, que drenam terrenos do Brasil Central apresentam respostas fluviais semelhantes aos rios com cabeceiras em terrenos andinos. Reforçam assim, que as flutuações climáticas são o principal fator responsável pela formação de sequência de terraços fluviais amazônicos e que responderam de forma similar as essas mudanças registradas no Quaternário tardio.

Palavras-chave: Rio Tocantins, Marabá (PA), Geomorfologia Fluvial, Datação OSL, Paleoclima.

ABSTRACT

Jesus, J. S., 2020, Evolution of the middle Tocantins River during the late Quaternary [Master's Thesis], São Paulo, Instituto de Geociências, Universidade de São Paulo, 108p.

The Tocantins River drains the easternmost area the Amazon. Most of its upper catchment is represented by bedrock channel, but the middle reach is marked by the extensive sediments accumulation, that show a diverse assembly of channel fluvial forms, wide floodplains and terrace levels, which is called Paleocanal do Tocantins and Bico do Papagaio. However, the Quaternary history of the Tocantins River is poorly understood due lack of geomorphological studies constrained by geochronological data. Therefore, we characterize the sedimentary deposits of the Middle reach of the Tocantins River and we applied optically stimulated luminescence dating (OSL) to understand how this fluvial landscape evolved during the Late Quaternary. The results of this research are presented in two articles. The first consists of mapping geomorphology on a scale of 1:100,000 of the fluvial plain in the Middle Tocantins. Four main geomorphic units were included: (i) aluvial plain, (ii) terraces and (iii) paleo-alluvial fan. Our results obtained insights into the geomorphological and sedimentological processes that shape the current river landscape. The presented map offers a detailed cartographic product, which can be useful for planners and decision makers in regional development and conservation projects. The second article presents the results of the morphosedimentary analysis integrated with the OSL dating, which allows to interpret the evolution of the landscape between 661 ± 42 and 160 ± 16.3 ka. OSL ages can identify three main deposition stages and two incision stages. An older position stage of the Upper Terrace (T1) and part of the Paleo-alluvial fan between 160 to 32 ka. Subsequently, an incision event occurred at around 31 ka, which resulted abandonment of T1, after a second phase of exposure that was created by Lower Terraces (T2) and promotes the reactivation of alluvial Paleo-alluvial fan from 31 to 6 ka. A more recent incision occurred 6 to 5 ka, allowing or abandoning T2 and reducing the local base level to its current position. The modern floodplain is built from 5 ka to the present, with sediment exposure due to frequent lateral frequencies of the Tocantins River. The results presented this work present a highly diversified landscape in terms of geoforms, sedimentary and geochronological aspects that are used in the various moments of its geomorphological evolution throughout the Late Quaternary. The results were correlated with regional paleoclimatic data and pointed out that climate change was the main driver of the Tocantins average river in the last 160 ka. The evolution of terraces this region of the Amazon is similar the formation of terraces in Central and Western Amazonia described literature and points out that the fluvial systems of the Eastern Amazon, which drain land from Central Brazil, present fluvial responses similar to rivers with headwaters in Andean lands. Reinforces that climatic fluctuations are the main factor responsible for the formation of a sequence of Amazonian river terraces and that responded in a similar way to these changes registered in the Late Quaternary.

Keywords: Tocantins River, Marabá (PA), Fluvial Geomorphology, OSL Dating, Paleoclimate.

SUMÁRIO

1	INTRODUÇÃO.....	14
2	CAPÍTULOS	17
3	CONTEXTUALIZAÇÃO DA PESQUISA	18
2.1	Paleocanal do Tocantins	18
2.2	Sistema Fluvial do Leste da Amazônia: Tocantins – Araguaia	18
2.3	Objetivos.....	20
4	CARACTERIZAÇÃO DA ÁREA DE ESTUDO	21
3.1	Clima	22
3.2	Geologia	23
3.3	Geomorfologia	25
5	GEOMORPHOLOGY OF FLUVIAL DEPOSITS IN THE MIDDLE TOCANTINS RIVER, EASTERN AMAZON	27
1	INTRODUCTION.....	28
2	PHYSICAL SETTING.....	29
3	METHODS AND DATA.....	31
3.1	Geomorphological Mapping and Classification	31
3.2	Remote Sensing	32
3.2.1	Image processing	32
3.2.2	Morphometric classification and topographic profiles	33
3.3	Field Surveys.....	33
4	DESCRIPTION OF THE GEOMORPHOLOGICAL MAP UNITS.....	33
4.1	Geomorphological Units	34
4.2	Alluvial Plain	35
4.2.1	Channel.....	35
4.2.2	Floodplain.....	37
4.3	Fluvial Terraces	40
4.4	Paleo-alluvial fan	42
5	DISCUSSION AND CONCLUSIONS.....	44
SOFTWARE	46	
FINANCING.....	46	
ACKNOWLEDGMENT	46	
6	LATE QUATERNARY EVOLUTION OF THE MIDDLE TOCANTINS RIVER IN EASTERN AMAZON	47

ABSTRACT.....	47
1 INTRODUCTION	48
2 THE TOCANTINS RIVER SYSTEM	50
3 MATERIAL AND METHODS.....	53
3.1 Geomorphic Mapping and Remote Sensing.....	53
3.2 Sedimentological Descriptions	53
3.3 Optically Stimulated Luminescence Dating	54
4 RESULTS.....	57
4.1 Alluvial Plain.....	60
4.1.1 Channel	60
4.1.2 Floodplain	62
4.2 Fluvial Terraces.....	64
4.3 Paleo-alluvial fan.....	69
5 DISCUSSION	71
5.1 Late Quaternary Evolution of the Tocantins River	71
5.2 Climate and Tectonic Controls on the Fluvial History	76
6 CONCLUSION.....	84
FINANCING	85
ACKNOWLEDGMENT.....	85
7 CONCLUSÕES	86
REFERÊNCIAS.....	88
APÊNDICE – Mapa Geomorfológico	105

ÍNDICE DE FIGURAS

CAPÍTULOS – INTRODUÇÃO

Figura 1 - Localização da área de estudo.....	21
Figura 2 - Imagens do Satélite GOES-13 sobre a localização e atuação da ZCIT na América do Sul.	22
Figura 3 - Contexto geológico regional e local.....	24
Figura 4 - Geomorfologia da área de estudo	25

CAPÍTULO 5 - GEOMORPHOLOGY OF FLUVIAL DEPOSITS IN THE MIDDLE TOCANTINS RIVER, EASTERN AMAZON

Figure 1 - Geological setting of the middle Tocantins River.....	31
Figure 2 - Geomorphological aspects of the middle Tocantins River.....	34
Figure 3 - Hierarchical classification of mapping units of the middle Tocantins River.	
.....	35
Figure 4 - Bedrock rapids upstream middle Tocantins River.	36
Figure 5 - Geomorphic features within the channel unit.....	37
Figure 6 - Geomorphic features of the floodplain.....	39
Figure 7 - Crevasse splay in DEM image.....	40
Figure 8 - Geomorphic features of the terraces and paleo alluvial fan.....	41
Figure 9 - General aspects of the paleo-alluvial fan geomorphological unit.....	43
Figure 10 - Geomorphic features of the paleo-alluvial fan unit.....	44

CAPÍTULO 6 - LATE QUATERNARY EVOLUTION OF THE MIDDLE TOCANTINS RIVER IN EASTERN AMAZON

Figure 1 - Geological and topographical settings of the middle Tocantins River.....	52
Figure 2 - Geomorphology of the middle Tocantins River.....	58
Figure 3 - Surface aspects of the fluvial channels in the study area.	60
Figure 4 - Characteristic of the geomorphologic unit Channel.	61
Figure 5 - Sedimentary sections described in the Floodplain units.	63

Figure 6 - Sedimentary facies of the Upper Terraces (T1)	65
Figure 7 - Geomorphic features and sedimentology of the Lower Terraces (T2)	67
Figure 8 - Features of the geomorphologic unit Paleo-alluvial fan.....	70
Figure 9 - Gravel bars from the tributary drainage that filled the paleo-alluvial fans..	74
Figure 10 - Schematic diagrams illustrating the geomorphological evolution of the middle Tocantins River during the Late Quaternary.	75
Figure 11 - Chronology of sediments of the geomorphologic units described in the middle Tocantins River compared with Quaternary climate records.....	82
Figure 12 - Synthesis of the chronological evolution of fluvial terraces in the study area and its comparison with Quaternary palynology and speleothem records of the Eastern Amazon.	83

ÍNDICE DE TABELAS

CAPÍTULO 6 - LATE QUATERNARY EVOLUTION OF THE MIDDLE TOCANTINS RIVER IN EASTERN AMAZON

Table 1 - Measurement protocol used for equivalent dose estimation in quartz grains of the studied samples..... 56

Table 2 - Data summary of the equivalent doses, dose rates and OSL ages. OD is the overdispersion of equivalent dose distributions.. 59

Table 3 - Summary of lithofacies characteristics of the Late Quaternary deposits in middle Tocantins River, with corresponding interpretation of sedimentary processes.
..... 68

LISTA DE ABREVIATURAS E SIGLAS

CAPES	Coordenação de Aperfeiçoamento de Pessoal de Nível Superior
De	Dose Equivalente
DEM	Digital Elevation Model
FCCM	Fundação Casa da Cultura de Marabá
HPGe	Detector de Germânio Hiperpuro
IBGE	Instituto Brasileiro de Geografia e Estatística
IDESP	Instituto de Desenvolvimento Econômico, Social e Ambiental do Pará
IGc	Instituto de Geociências
LABSED	Laboratório de Sedimentologia
LALLS	Low Angle Laser Light Scattering
Landsat	Land Remote Sensing Satellite
LEGaL	Laboratório de Espectrometria Gama e Luminescência
LGM	Last Glacial Maximum - Último Máximo Glacial
MERIT	Multi-Error Removed Improved-Terrain
NASA	National Aeronautics and Space Administration
OSL	Optically Stimulated Luminescence
PVC	Policroleto de Vinila
RADAM	Projeto Radar Amazônia
RGB	Red, Green, Blue
RHTA	Bacia Hidrográfica Tocantins-Araguaia
RPM	Rotação Por Minuto
SAR	Single-Aliquot Regeneration
SMAS	Sistema de Monção da América do Sul
SRTM	Shuttle Radar Topographic Mission
TD	Taxa de Dose
TL	Termoluminescência
ZCAS	Zona de Convergência do Atlântico Sul
ZCIT	Zona de Convergência Intertropical

1 INTRODUÇÃO

A própria natureza de um sistema fluvial é produzir sedimentos que registram a variabilidade dos processos através do tempo e espaço (Gupta, 2007). As análises da evolução do rio a longo prazo e as respostas do sistema às mudanças ambientais fornecem um contexto importante com o qual pode se interpretar a dinâmica contemporânea e pretérita do rio. Na escala de tempo de longo-prazo (10^3 - 10^6 anos), fatores como controle tectônico, mudanças climáticas e no nível de base desempenham papel fundamental na dinâmica e desenvolvimento desses sistemas (Maddy et al., 2001). Mudanças nessas variáveis alteram o volume de água e o suprimento de sedimentos, resultando em fases alternadas com predomínio de incisão ou agradação, o que pode conduzir para a formação de terraços e planícies fluviais ao longo da história evolutiva dos sistemas fluviais (Bull, 1991; Bridgland e Westaway, 2008). Contrastos nas características morfológicas e sedimentares entre diferentes níveis de terraços fluviais e a planície moderna de um rio indicam a ocorrência de mudanças nas condições ambientais regionais (Pazzaglia, 2013). Portanto, o estudo geomorfológico e sedimentológico de depósitos sedimentares preservados em terraços e planícies fluviais, acoplados a geocronologia, são importantes ferramentas para a compreensão da resposta dos sistemas fluviais a mudanças ambientais ocorridas em escalas temporais de longo-prazo, principalmente durante o Quaternário (Merritts, 2007).

O sistema fluvial formado pelo rio Amazonas e seus afluentes têm sido alvo de muitos esforços com o objetivo de compreender sua evolução geológica ao longo do Quaternário. A maioria desses estudos está concentrada na porção oeste da bacia (Pupim et al., 2019 e referências). No extremo oeste (May et al., 2008; Rigsby et al., 2009), sudoeste (Latrubesse, 2002; Rossetti et al., 2012, 2014; Bertani et al., 2015), noroeste (Latrubesse and Franzinelli, 2005; Cremon et al., 2016), região central da Amazônia, no rio Solimões-Amazonas (Latrubesse e Franzinelli, 2002; Soares et al., 2010; Nogueira et al., 2013; Gonçalves Júnior et al., 2016), onde a ocorrência de depósitos fluviais em diferentes níveis de terraços é mais abundante.

No entanto, os fatores que governam as mudanças nesses grandes sistemas fluviais ainda são controversos. Muitos autores argumentam que as flutuações climáticas seriam o principal fator responsável pela formação de sequências de

terraços nos rios da Amazônia ocidental ao longo do Quaternário tardio (Räsänen et al., 1990; Latrubesse, 2003; Rigsby et al., 2009).

A alternância entre períodos úmidos e secos associados a mudanças na cobertura vegetal (florestas mais ou menos densas ou floresta *versus* savana) (Hammen et al., 1992; Bush et al., 2004; Cheng et al., 2013; D'Apolito et al., 2013) levariam a perturbações no suprimento de sedimentos e no fluxo desses rios, promovendo fases de gradação (período seco) e degradacional (período úmido) (Latrubesse, 2003).

Registros palinológicos e geoquímicos importantes no leste (Absy et al., 1991, 2014; Sifeddine et al., 1994; Cordeiro et al., 2008; Hermanowski et al., 2012, 2014; Guimarães et al., 2013, 2016, 2019a; Sahoo et al., 2015; Reis et al., 2017), sul (Fontes et al., 2017), oeste (Behling and Hooghiemstra, 1999; Seltzer et al., 2000; Baker et al., 2005; Cordeiro et al., 2011a; Groot and Bogot, 2011; Cohen et al., 2014), central (Behling, 2001; Moreira et al., 2009; Zocatelli et al., 2016) e noroeste (Behling, 2001; Sifeddine et al., 2003; Zocatelli et al., 2013; Häggi et al., 2017; Augusto-Silva et al., 2019) da Amazônia contribuem para evidências de alterações paleoambientais e de vegetação que provavelmente refletem as mudanças climáticas ocorridas durante o Quaternário tardio na região. Por outro lado, há uma expressiva lista de publicações que indicam a influência de processos tectônicos recentes na configuração e geometria do sistema de drenagem da Amazônia (Costa et al., 2001; Franzinelli e Igreja, 2002; Almeida-Filho e Miranda, 2007; Rossetti et al., 2014, 2017, 2019).

A formação de terraços também foi associada a mudanças relativas no nível do mar desde o LGM. Irion et al., (2009) argumenta que a incisão que originou a atual planície e afluentes do rio Amazonas ocorreu durante o LGM, devido a condições de nível relativo do mar inferior ao atual. Depois, a elevação do nível do mar no Holoceno teria afogado os vales esculpidos, gerando espaço de acomodação para a deposição de sedimentos que preenchem a planície atual.

Apesar dos recentes avanços no entendimento dos fatores que influenciam os sistemas fluviais na Amazônia Ocidental, existe uma lacuna no entendimento dos depósitos fluviais do rio Tocantins que drena o extremo leste da Amazônia. Os dados geológicos disponíveis são escassos e muitas questões ainda estão em debate, principalmente sobre quais são os fatores alogênicos e/ou fatores autogênicos mais importantes para a evolução desses sistemas. As escalas temporais e espaciais em que atuam e se as mudanças na precipitação, cobertura vegetal, regime de fluxo,

calibre e disponibilidade de materiais trouxeram mudanças significativas na morfologia dos sistemas fluviais na Amazônia durante o Quaternário.

No entanto, dados paleoambientais indicam que o padrão de precipitação e vegetação não foi homogêneo em toda a região drenada pelos rios amazônicos, pelo menos nos últimos 100 ka, com diferenças marcantes entre leste-oeste e norte-sul (Bush et al., 2004a; Cheng et al., 2013; Zhang et al., 2016; Wang et al., 2017). Assim, a segunda hipótese de trabalho é que os sistemas fluviais do extremo leste da Amazônia, que drenam terrenos do Brasil Central (Sawakuchi et al., 2015; Pupim et al., 2016; Bertassoli et al., 2019) como o rio Tocantins, apresentam respostas diferentes dos rios que drenam terrenos andinos, no extremo oeste da Amazônia.

Embora reconhecendo o imperativo das mudanças regionais ou específicas de ajustes geomórficos no final do Quaternário, é instrutivo considerar a natureza e extensão da perturbação e sistema associado (Gupta, 2007). Neste contexto o objetivo foi a elaboração de um modelo de evolução geológica-geomorfológica para os depósitos fluviais no médio rio Tocantins baseado na análise geomorfológica, sedimentológica e geocronológica. Isto visa compreender os principais fatores responsáveis pela evolução durante o Quaternário tardio

A escolha da área de estudo deve-se à localização, pois esse trecho do rio Tocantins recebe água e sedimentos de áreas de transição entre os biomas Amazônia e Cerrado, assim, os depósitos sedimentares têm grande potencial para registrar flutuação nesses ambientes, e a existência de uma lacuna de estudos que abordam a evolução geomorfológica dessa região, com exceção de Valente e Latrubesse (2012). O mapeamento geomorfológico por meio de produtos de sensoriamento remoto e análise de fácies sedimentares possibilitaram compreender a distribuição espacial e características dos ambientes e subambientes deposicionais atuais e pretéritos. Detalhada cronologia absoluta dos depósitos sedimentares por meio de datação por OSL permitiram determinar a idade de soterramento dos sedimentos, assim como definir fases com domínio de processos agradacionais e degradacionais ao longo da evolução da planície. Esse conjunto de dados forneceu subsídios para a elaboração de um modelo geológico-geomorfológico evolutivo da planície fluvial do médio rio Tocantins e das mudanças ambientais que podem ter influenciado o fluxo de sedimentos e o desenvolvimento dos sistemas fluviais situados na região leste da Amazônia.

2 CAPÍTULOS

Os resultados desta dissertação são apresentados na forma coletânea de artigos. Desta forma, o corpo central deste documento apresenta dois artigos científicos, sendo os mesmos apresentados na forma de capítulos (Capítulos 5 e 6) e estão formatados segundo as normas do PPGG/IGc/USP. Os capítulos com os artigos são precedidos por um texto integrador, em um capítulo introdutório, que inclui a apresentação, contextualização da área e da pesquisa, bem como o breve histórico do Paleocanal do Tocantins, os objetivos e aspectos físicos. O capítulo final, sumariza de forma integrada as conclusões alcançadas nos dois artigos científicos e no desenvolvimento da dissertação como um todo. Os artigos serão apresentados de acordo com a seguinte ordem:

CAPÍTULO 5: Artigo 1 – GEOMORPHOLOGY OF FLUVIAL DEPOSITS IN THE MIDDLE TOCANTINS RIVER, EASTERN AMAZON. Em processo de revisão (major review) no periódico *JOURNAL OF MAPS*. Este artigo apresenta o mapa geomorfológico na escala de 1:100.000 da região do médio Tocantins. O mapeamento permitiu definir as três principais unidades geomorfológicas, bem como detalhar os subambientes e propor eventos relativos de formação e/ou retrabalhamento superficial e desta forma especular sobre a história evolutiva desses depósitos fluviais. Nossos resultados oferecem insights sobre os complexos processos geomorfológicos e sedimentológicos que moldam a paisagem fluvial atual. O mapa publicado na escala original oferece um produto cartográfico detalhado da região, que pode ser de utilidade para planejadores e tomadores de decisão em projetos de desenvolvimento regional e conservação.

CAPÍTULO 6: Artigo 2 – LATE QUATERNARY EVOLUTION OF THE MIDDLE TOCANTINS RIVER IN EASTERN. Em preparação para ser submetido ao periódico *GEOMORPHOLOGY*. O artigo contempla os dados geomorfológicos, sedimentológicos e geocronológicos do médio rio Tocantins. Estes dados sugerem que a evolução geomorfológica dessa região desde 160 ka é resultante da interação dos canais tributários e canal principal impulsionadas por variações de vazão e sedimentos resultantes de mudanças climáticas. Foram reconhecidas 5 fases de evolução, três deposicionais e dois eventos de incisão associados a alternâncias de períodos úmidos e secos registrados em dados paleoclimáticos na Amazônia e no Cerrado.

3 CONTEXTUALIZAÇÃO DA PESQUISA

2.1 Paleocanal do Tocantins

A região de interesse dessa pesquisa consiste em uma marcante expressão geológica-geomorfológica. São expressivos terraços com numerosas lagoas que podem estar relacionados com fenômenos localizados de endorreismo e com a natureza siltico-argilosa dos aluviões (RadamBrasil, 1974).

O Paleocanal do Tocantins foi classificado como Reserva Biológica (Área de Proteção ao Ecossistema para Preservação da Flora e da Fauna) em função das condições naturais representadas pelo ambiente físico e biótico oferecido pelas Florestas e Campos de Várzea (RadamBrasil, 1974), visando sobretudo, a proteção da flora e da fauna ribeirinha. Nessas áreas a existência de zonas inundáveis e mesmo lagoas, oferecem condições para a criação natural de larvas e alevinos.

Em 1984 Ab'Saber em visita a região de Carajás “batizou” a área de Paleocanal do Tocantins. O trecho do artigo escrito por Mattos (2014, p. 74) a partir da entrevista feita com Nôe Atzingen, ex-presidente da FCCM, instituição pioneira nos estudos do Paleocanal do Tocantins, relata o momento.

Ao passar pela PA-70 (atual BR-222), Nôe mostrou a área para o geógrafo Ab'Saber; este analisou a região e verificou que ela compunha o antigo leito do rio Tocantins, quando ele era mais largo, com nível mais alto de água, que posteriormente foi drenado, reduzindo-se ao leito atual. O rio teria uma largura de 10 ou 15 km: uma coisa imensa! Isso talvez, há 40 mil anos, no período do degelo.

Assim como o RadamBrasil, (1974), a FCCM, o IDESP (1992), Ab'Saber (2010) também propôs que esses paleocanais arenosos de grandes rios que mudaram de posição no entorno de tabuleiros necessitam de proteção sob planejamento inteligente. Contudo, apesar dos esforços e de vários projetos da FCCM a área continua sem proteção necessária.

2.2 Sistema Fluvial do Leste da Amazônia: Tocantins – Araguaia

Os grandes esforços para o entendimento do maior sistema fluvial do mundo têm resultado em significativos avanços sobre a evolução geológica e biológica Neogénica e Quaternária da Amazônia (Hoorn et al., 2010; Ribas et al., 2012; Pupim et al., 2019).

Contudo, o entendimento da dinâmica dos sistemas fluviais do leste da Amazônia ainda é incipiente e são, principalmente, registros restritos ao Holoceno

(Behling et al., 2001; Irion et al., 2006; Moreira et al., 2013; Souza, 2015; Zocatelli et al., 2016; Bertassoli et al., 2019).

Apesar da dimensão geográfica e do contexto socioeconômico e hidroelétrico, a bacia dos rios Tocantins-Araguaia é praticamente ignorada na literatura internacional sobre grandes rios (Latrubesse e Stevaux, 2002). Contudo esta região possui a principal bacia sedimentar quaternária do Brasil Central – Ilha do Bananal, localizada na região ecotônica do Cerrado - Amazônia (Oliveira e Marquis, 2002). A Ilha do Bananal apresentam evidências de sedimentação ativa há pelo menos 240 ka (Pleistoceno Médio), havendo importantes períodos de desenvolvimento de depósitos fluviais com predomínio de areia grossa e um sistema avulsivo entre 70 e 34 ka e entre 24 e 17 ka (Valente e Latrubesse, 2012). Os autores interpretaram que tais depósitos foram consequência de um sistema fluvial com alto aporte de sedimentos e baixa descarga de água, devido às condições regionais dominadas por vegetação de cerrado e pluviosidades inferiores às atuais. Mudanças significativas ocorreram durante a passagem do Pleistoceno para o Holoceno (cerca de 10 ka), sendo que o aumento da umidade e desenvolvimento da vegetação de floresta levou a uma maior estabilidade do sistema fluvial moderno, com menos eventos de avulsão e o desenvolvimento de depósitos lamosos nas planícies de inundação e consequente estabilização do sistema fluvial moderno (Valente e Latrubesse, 2012).

Apesar de drenarem predominantemente terrenos cristalinos ocorrem potenciais áreas que podem ter registros da dinâmica da bacia, principalmente no curso médio e baixo Tocantins. No trecho médio rio Tocantins, ocorre uma área com expressão geomorfológica e sedimentar peculiar na confluência do rio Araguaia e Tocantins, conhecida como Bico do Papagaio e o Paleocanal do Tocantins. Nesse trecho ocorre grande variação da dinâmica fluvial, extensas áreas dominadas por lagos estreitos e extensos, além de paleodiques e paleocanais inseridos em terraços e amplas planícies. O Paleocanal do Tocantins foi alvo de estudos geológicos e geomorfológicos por Felipe (2012) e Mascarenhas et al., (2015).

Posteriormente, Jesus (2016) integrou dados geomorfológicos, sedimentológicos e geocronológicos que possibilitaram concluir incialmente que os depósitos fluviais na região de Marabá foram construídos do Pleistoceno tardio ao Holoceno, com idades entre 31.1 ± 2.6 a 601 ± 0.4 ka e foram classificados como paleoleque aluviais, terraços fluviais e planície de inundação moderna. Nesse contexto, a área de estudo mostrou-se promissora no registro sedimentar, motivando

novas investigações para a compreensão da evolução geomorfológica regional e suas possíveis correlações com mudanças ambientais ocorridas durante o Quaternário tardio.

2.3 Objetivos

Esta pesquisa teve como objetivo principal a elaboração de um modelo de evolução geológica-geomorfológica para os depósitos fluviais no médio rio Tocantins, baseado na análise geomorfológica, sedimentológica e geocronológica. Isto visa compreender os principais fatores e processos responsáveis por essa evolução durante o Quaternário tardio.

Em decorrência disto, considerou-se os seguintes objetivos específicos:

- I) Caracterizar as feições geomorfológicas associadas à dinâmica fluvial com base nos aspectos morfológicos e morfométricos interpretados em produtos de sensoriamento remoto e mapeamento de campo;
- II) Analisar as fácies sedimentares para caracterizar os ambientes e processos deposicionais;
- III) Determinar a idade absoluta dos depósitos sedimentares por meio da técnica de datação OSL para caracterização dos principais episódios deposicionais; e
- IV) Correlacionar mudanças no sistema fluvial do médio rio Tocantins, representadas por períodos de agradação e incisão, com mudanças no clima, tectônica e/ou do nível de base ocorridas no Quaternário tardio.

4 CARACTERIZAÇÃO DA ÁREA DE ESTUDO

Os depósitos fluviais em estudo localizam-se no Submédio Tocantins da RHTA, o qual, segundo a classificação do Plano Nacional de Recursos Hídricos (MMA, 2006), corresponde à Mesorregião do Sudeste Paraense. A área está compreendida entre as coordenadas 5°10' e 5°30'S e 49°35' e 48°95'W, região historicamente denominada de Bico do Papagaio, confluência do rio Araguaia e Tocantins e o Paleocanal do Tocantins, expressão nominada por Ab'Saber (Mattos, 2014; Figura 1).



Figura 1 - Localização da área de estudo. A) Área de estudo com destaque para o Paleocanal do Tocantins e Bico do Papagaio, região da cidade de Marabá (PA). B) Localização da área de estudo na porção setentrional da Bacia Hidrográfica Tocantins-Araguaia e no ecótono Amazônia-Cerrado. Fonte: A) Bing Satellite, 2019; B) Landsat, 2019.

3.1 Clima

Região leste da Amazônia está inserida na Zona Equatorial próximo ao limite com Zona Tropical Equatorial. O clima da região é fortemente influenciado pelas condições atmosféricas e oceânicas do Atlântico Tropical (Molian, 1993; Nobre e Shukla, 1996) e SMAS (Zhou e Lau, 1998).

A ZCIT é o sistema meteorológico mais marcante próximo à região equatorial do Globo terrestre (Rosa e Silva, 2016). Esse sistema está localizada no ramo ascendente da célula de Hadley e consiste, no geral, numa região de baixa pressão, tendo convergência de escoamento em baixos níveis e divergência em altos níveis, sendo a fonte principal de modulação do regime pluviométrico distintos da região, um chuvoso, com elevada precipitação e diretamente influenciado pelo deslocamento sazonal da ZCIT para sul, período chuvoso na Amazônia (Figura 2A; janeiro a abril), e durante o inverno, desloca-se para norte, período menos chuvoso (Figura 2B; julho a outubro) (Fisch et al., 1998; Souza e Ambrizzi, 2003).

O SAMS está associado ao desvio da ZCIT para a ZCAS, que é intensificado durante o verão (Vera et al., 2006). A ZCAS parece não influenciar diretamente a região Amazônia, mas exerce forte influência nas cabeceiras da RHTA, pois estende desde o sul e leste da Amazônia até o sudoeste do Oceano Atlântico Sul (Kodama, 1992, 1993).

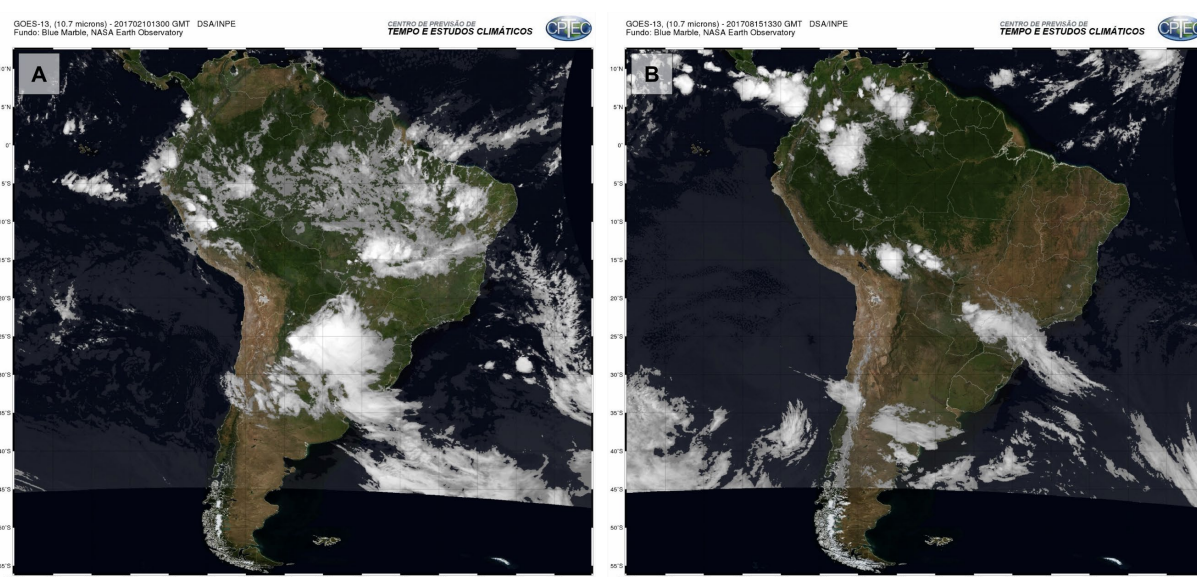


Figura 2 - Imagens do Satélite GOES-13 sobre a localização e atuação da ZCIT na América do Sul. A) ZCIT deslocada para Sul com nebulosidade sobre o Oceano Atlântico Equatorial e Região Norte e Nordeste (Data 10/02/2017); B) ZCIT deslocada para Norte com nebulosidade esparsa sobre Oceano Atlântico Equatorial. Fonte: Cptec/INPE.

3.2 Geologia

O contexto geológico da área compreende quatro domínios tectônicos: Cráton Amazônico, Província Tocantins, Bacia do Parnaíba e Bacia do Marajó (Figura 3).

O embasamento cristalino da área consiste em rochas paleoproterozóicas do Domínio Bacajá da Província Transamazonas (Santos et al., 2000) ou segundo a proposta de compartimentação tectônica do Cráton Amazônico de Tassinari e Macambira (1999), à Província Maroni-Itacaiúnas. Este Domínio tem sua evolução relacionada ao Ciclo Transamazônico (2,26 - 1,96 Ga) e destaca-se o predomínio de rochas de alto grau metamórfico, menor proporção de rochas supracrustais e uma notável tectônica transcorrente, marcada por zonas de cisalhamento NW-SE e WNW-ESE, paralelas e contínuas, que imprimem deformação dúctil nas rochas (Vasquez, 2006). Este domínio é representado na área pelo Complexo Cajazeiras que consiste em ortognaisses originalmente enderbíticos a charnockíticos, frequentemente retrometamorfizados, contendo localmente ortopiroxênio (Vasquez e Rosa-Costa, 2008) com idades de metamorfismo de 2.074 ± 8 Ma (Pb-Pb).

A oeste da área de estudo o limite do Cráton com a Província Tocantins é marcado pelo cavalgamento do Cinturão Araguaia (Vasquez, 2006). Consiste em Sequências Supracrustais do Grupo Baixo Araguaia, Proterozoica Inferior a Médio, com destaque para a Formação Couto Magalhães (Hasui et al., 1977). Esta, constituída essencialmente de rochas de baixo grau metamórfico representada por filitos pelíticos e filitos grafíticos, metarcósios, metassiltitos e lentes de quartzitos (Hasui et al., 1977). O arcabouço estrutural é marcado principalmente por um sistema de cavalgamentos regionais de direção aproximada N-S, suavemente inclinados para E e ESSE, que imprimem uma foliação pervasiva nas rochas. Lineações com cimento para SE, sugerem transporte tectônico para NW e colisão oblíqua com o Cráton Amazônico (Vasquez e Rosa-Costa, 2008).

Na porção norte e nordeste da área ocorrem rochas sedimentares cretáceas relacionadas ao Grupo Itapecuru (Rossetti e Truckenbrodt, 1997) e Formação Codó (Mesner e Wooldridge, 1964), da Bacia Sedimentar de Marajó (Villegas, 1994; Costa et al., 2002) e Bacia Sedimentar de Parnaíba (Bigarella, 1973).

Os estratos da Formação Codó, formados durante o Neoaptiano (Rossetti e Goés, 2004), afloraram em corpos restritos localizados na porção oriental da área de estudo, próximos a margem direita do rio Tocantins. São compostos por calcilutitos esbranquiçados, cremes e arroxeados com laminação plano-paralela com lentes de

arenitos com cimentação carbonática e folhelhos pretos betuminosos. Interpretados como de ambiente lacustre com breves invasões marinhas (Mesner e Wooldridge, 1964). Esta formação é recoberta por rochas sedimentares Albianas do Grupo Itapecuru. Goés (1981) descreveu o Grupo Itapecuru como essencialmente siliciclástico e formado por arenitos caulínicos finos, com níveis argilosos e conglomeráticos, que exibem, geralmente, abundante estratificação cruzada, e que foram depositados em ambiente continental fluvial.

Os depósitos quaternários que recobrem essas unidades são divididos em duas macro unidades, segundo Vasquez e Rosa-Costa, (2008): 1) terraços fluviais: compostos de argila, areia e cascalho não consolidada e semi-consolidada, topograficamente superior à atual planície aluvial; e 2) depósitos aluviais: compostos por argila e areia, relacionados às atuais planícies aluviais, que constituem depósitos de canais e planícies aluviais.

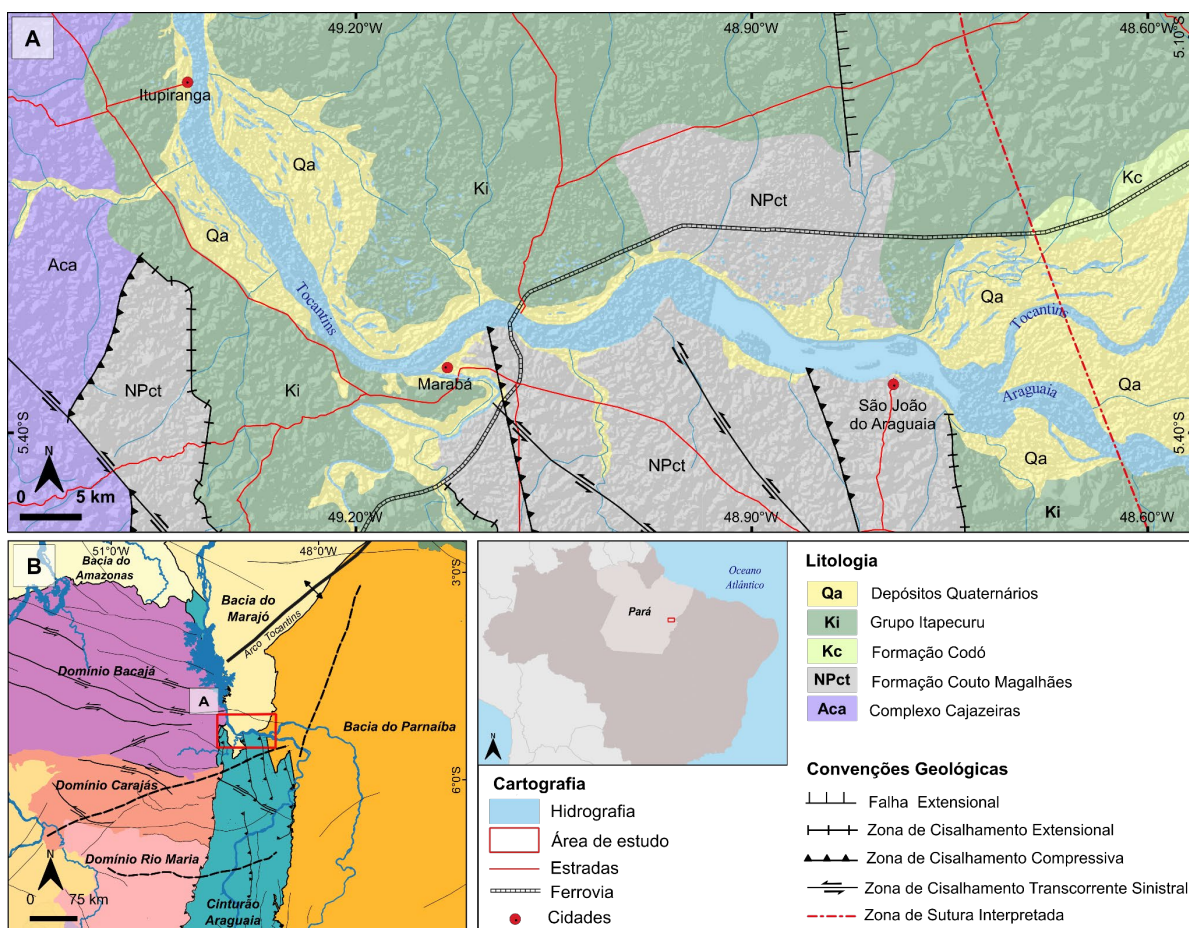


Figura 3 - Contexto geológico regional e local. A) Geologia local da área investigada; B) Domínios Tectônicos compreendidos na área de estudo. Fonte: Vasquez e Rosa-Costa, (2008).

3.3 Geomorfologia

Seis unidades geomorfológicas compõem o quadro regional (Figura 4). Na porção norte predomina o Patamar Dissecado Capim-Moju e no extremo leste Depressão de Imperatriz, a oeste a Depressão do Bacajá, a sul e sudeste a Depressão do Médio e Baixo Araguaia e Planalto do Interflúvio Tocantins-Araguaia, e nas margens das principais drenagens unidade Planície e Terraço Fluvial (IBGE, 2009).

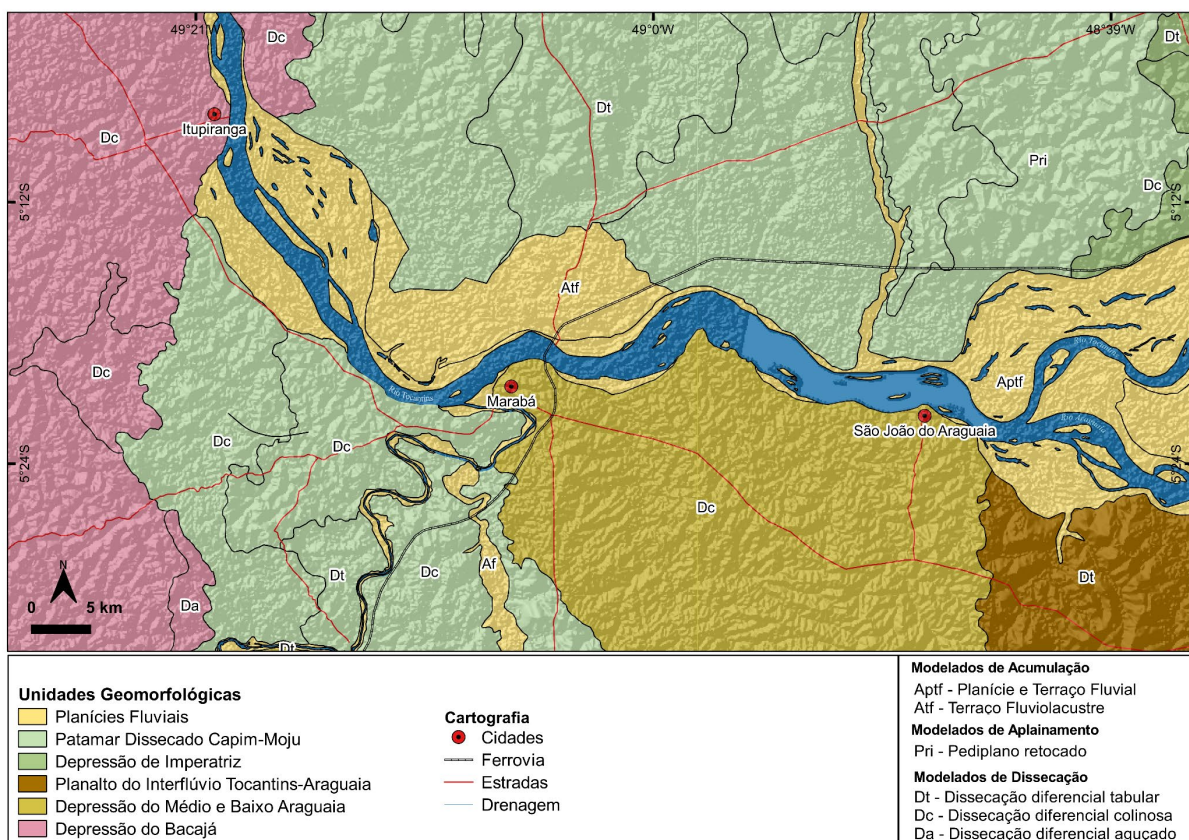


Figura 4 - Geomorfologia da área de estudo. Fonte: IBGE, (2009)

O Patamar Capim-Moju na porção norte corresponde a formas de dissecação diferencial de topos tabulares (Dt), conformando feições de rampas suavemente inclinadas e lombas esculpidas em coberturas sedimentares inconsolidadas, denotando eventual controle estrutural; ao passo que a nordeste ocorrem superfícies de aplainamento elaborada durante fases sucessivas de retomada dos processos de erosão (Pri), os quais geraram sistemas de planos inclinados, às vezes levemente côncavos. Vale ressaltar que essa unidade aparece inumada por coberturas detriticas e/ou de alteração; já a sul ocorre dissecação diferencial convexa (Dc) esculpidas em

rochas cristalinas e, eventualmente, também em sedimentos, às vezes denotando controle estrutural.

A Depressão do Bacajá, a oeste, é um setor topograficamente deprimido, sob o Domínio de Embasamentos em Estilos Complexos, pertencente ao conjunto das depressões (Dc) periféricas elaboradas na margem sul da Bacia Amazonas, aberta por processos de circundesnudação.

A Depressão do Baixo e Médio Araguaia possui forma de relevo com extensão de terrenos de superfície rebaixada e suavemente dissecada, com formas predominantemente tabulares (Dt) e convexas esculpidas em Faixas de Dobramentos e Coberturas Metassedimentares.

O modelado de acumulação denominado Planície e Terraços Fluviais (Aptf, Atf) são áreas periodicamente alagadas, comportando meandros abandonados e cordões arenosos. Os mesmos ocorrem nos vales com preenchimento aluvial, contendo material fino a grosseiro, pleistocênico e holocênico. A identificação é feita em conjunto devido à limitação de representação nesta escala de mapeamento (IBGE, 2009).

5 GEOMORPHOLOGY OF FLUVIAL DEPOSITS IN THE MIDDLE TOCANTINS RIVER, EASTERN AMAZON

Article Submitted to Journal of Maps

ABSTRACT

This paper presents the geomorphological mapping at a 1:100,000 scale of fluvial deposits in the middle Tocantins River, eastern Amazon. The region preserves an important sedimentary archive of environmental changes of the Amazon and Cerrado biomes during the Quaternary. Yet, the region is under influence of diverse anthropogenic activities, including deforestation, urban activities and planned or operational hydropower plants, and detailed geomorphological mapping in the region is lacking. The mapping combined interpretation of surface geomorphic features and morphometric analysis through remote sensing images, digital elevation model and field surveys. Three main geomorphic units were defined: (i) alluvial plain, (ii) fluvial terraces and (iii) paleo-alluvial fan. The detailed mapping survey allowed a hierarchical organization of geomorphological units as well as their relative chronology of formation, considering the topographic levels, truncation, and superposition of mapping units. This information supported the interpretation of landform genesis. Our results can be used to outline conservation strategies since they improve the understanding on the complex geomorphological and sedimentological processes which shape the current fluvial landscape. Specifically, improving the understanding of the Tocantins River floodplains is crucial to support conservation of flooded forests, sustainable use of natural resources and minimize socio-economic losses and damages.

Keywords: fluvial geomorphology, geomorphological mapping, digital elevation model, Tocantins River, Marabá

1 INTRODUCTION

Geomorphological mapping of floodplains, terraces and their associated sub-environments provides information for understanding the functioning of river systems (Lewin, Davies, and Wolfenden 1977; Nanson and Croke 1992; Brierley and Fryirs 2005), which is critical to decisions in territorial planning, flood risk assessment, surface water management and river restoration programs (Fryirs and Brierley, 2012). Additionally, floodplains of large tropical rivers host unique biodiversity adapted to flooding (e.g. Thom et al. 2020) and the detailed mapping of landforms and surface fluvial deposits is important to predict future landscape changes with implications for biodiversity conservation (e.g. Hamilton et al. 2007). These studies have been developed under a perspective of process-form relationships to support the interpretation of ancient fluvial sequences (Sinha et al., 2005).

Historically, studies about river terrace landform sequences significantly contributed to understand Quaternary landscape changes (Antoine et al. 2007; Bridgland and Westaway 2014; Rossetti, Toledo and Góes 2005). Detailed geomorphological maps are important components of such fluvial systems studies because they allow to connect surface landforms to fluvial processes (Miklín and Galia, 2017).

The detailed characterization of the fluvial systems in the Amazon is still a hard task due to the large extension of the area and ubiquitous forest vegetation cover, but the remote sensing data has allowed to improve the knowledge on the alluvial deposits (e.g. Passos et al. 2020; Rossetti, Toledo and Góes 2005). Currently, easy access to emerging remote sensing methods and tools such as high-resolution spatial data such as aerial and satellite imagery or digital elevation models provides enormous opportunities to produce more accurate and detailed geomorphological maps (Jones et al., 2007; Bangen et al., 2014; Williams et al., 2014).

The Tocantins River and its main tributary, the Araguaia River, are among the largest rivers in eastern Amazon (Figure 1) and they stand out due to host areas with significant accumulation of Quaternary sediments (MMA, 2006). The geomorphological history of the Tocantins River, in turn, is mostly associated with the geological evolution of the Brazilian Shield (Lima and Caires, 2011; Lima and Ribeiro, 2011). The middle stretch of the Tocantins River consists of wide floodplains and fluvial terraces with numerous lakes and wetlands that provide diverse wildlife habitats and

important ecological services (Merona, 1987) and due to its evolutionary history among Amazonian tributaries (Akama, 2017), has one of the highest endemicity and species richness rates (Dagosta and Pinna, 2019).

The middle Tocantins River also includes the Marabá city, one of the major cities of eastern Amazon, and extensive agriculture areas over wetlands experiencing seasonal flooding, which promote recurrent socio-economic damages (Deus et al., 2018).

Despite the ecological and socio-economic relevance of the middle Tocantins River and its floodplains, there are few studies needed for planning of conservation initiatives and there are still enormous gaps on detailed spatially-resolved geomorphological information about this area. Recent studies described the geomorphological aspects of the middle Tocantins River (Felipe and Morales 2017; Mascarenhas, Vidal and Silva 2015), but only in a regional scale, classifying the terrains as depositional, dissected and surface planation.

In this context, this study aims to produce a detailed geomorphological map (1:100,000) of the middle Tocantins River to improve the understanding between surface landforms and fluvial processes. Therefore, the geomorphological mapping of the middle Tocantins River was carried out through field surveys combined with remote sensing and geographical information system (GIS) methods. The results are discussed to constrain landform changes in terms of fluvial processes operating in large tropical rivers. Moreover, our results also have potential to support decision makers in conservation programs in a region over constantly threatens. The possibility of installing a large hydroelectric plant in the Tocantins River near the Marabá city (Brasil, 2012) reinforces the importance of this study because of predicted reduction of floodplains and unknown threats to the aquatic environments (Akama, 2017).

2 PHYSICAL SETTING

The Tocantins River watershed extends from 46° to 55° west and from 2° to 18° south, has a drainage area of 306,310 km², upstream the confluence with the Araguaia River and a total area of 764,996 km², including the drainage area of the Araguaia River (Figure 1, ANA 2017). The Tocantins River drains distinct biomes, which are mainly represented by savannas (Cerrado) of the Central Plateau of Brazil, the e

Amazon rainforest and a transition zone between both vegetation biomes (Figure 1B; Oliveira-Filho 1995).

The study area comprises a wide (20 km x 80 km) fluvial plain located downstream of the confluence of the Araguaia and Tocantins Rivers, until the Itupiranga city (Figure 1). This region is locally named “Bico do Papagaio” (Parrot beak; eastern area) and “Paleocanal do Tocantins (Tocantins Paleochannel; western area), which is characterized by a low-altitude (< 110m) and low relief terrains developed in fluvial sediments deposited during the Quaternary (Figure 1; RadamBrasil 1986). These deposits are incised by Tocantins River that flow over metamorphic rocks and alluvial beds. Vasquez and Rosa-Costa (2008) proposed two units for this Quaternary deposits: 1) fluvial terraces: composed of unconsolidated and consolidated clay, sand and gravel, topographically higher than the current alluvial plain; and 2) alluvial deposits: composed of grey clay and sand corresponding to channel and floodplain deposits related to the current alluvial plain. Upstream of the Marabá City, the riverbed is dominated by rapids and rocky islands that expose low-grade metamorphic rocks related to the Araguaia Fold Belt (Herz et al., 1989). Downstream, the channel of the Tocantins River is dominated by fluvial bars and forms a wide floodplain with lakes, paleo-channels and swamps (Ribeiro, Petrere and Juras 1995).

Regional geology is represented by four distinct geological units (Figure 1A): Archean high-grade metamorphic rocks of the Cajazeira Complex (Brito Neves and Cordani 1991); Neoproterozoic low-grade metamorphic rocks of the Couto Magalhães Formation (Almeida et al., 1977); Cretaceous sedimentary rocks related with the Itapecuru Group (Rossetti and Truckenbrodt 1997) and Codó Formation (Mesner and Wooldridge, 1964) of the Marajó Basin (Villegas, 1994; Costa et al., 2002) and; sandstones from Parnaíba Basin (Bigarella, 1973; Góes, 1995).

The rainfall in eastern Amazon is concentrated during the austral summer and autumn due to the activity of the South American Summer Monsoon (SASM, Zhou and Lau 1998) and the Intertropical Convergence Zone (ITCZ, Garreaud et al. 2009; Marengo and Espinoza 2016), whose southward shift during the austral summer bring moisture from the equatorial Atlantic to inland areas. The climate across the Tocantins watershed is tropical, with an annual average temperature of 26° C and two well-defined climatic periods: the rainy, October to April, with more than 90% of precipitation, and the dry one, from May to September, with low relative humidity (MMA, 2006). The average rainfall in the watershed is around 1,869 mm yr⁻¹ (ANA

2002), but can reach up to 2,565 mm near the river mouth on the estuary (ANA, 2005), and the average evapotranspiration is 1,371 mm yr⁻¹.

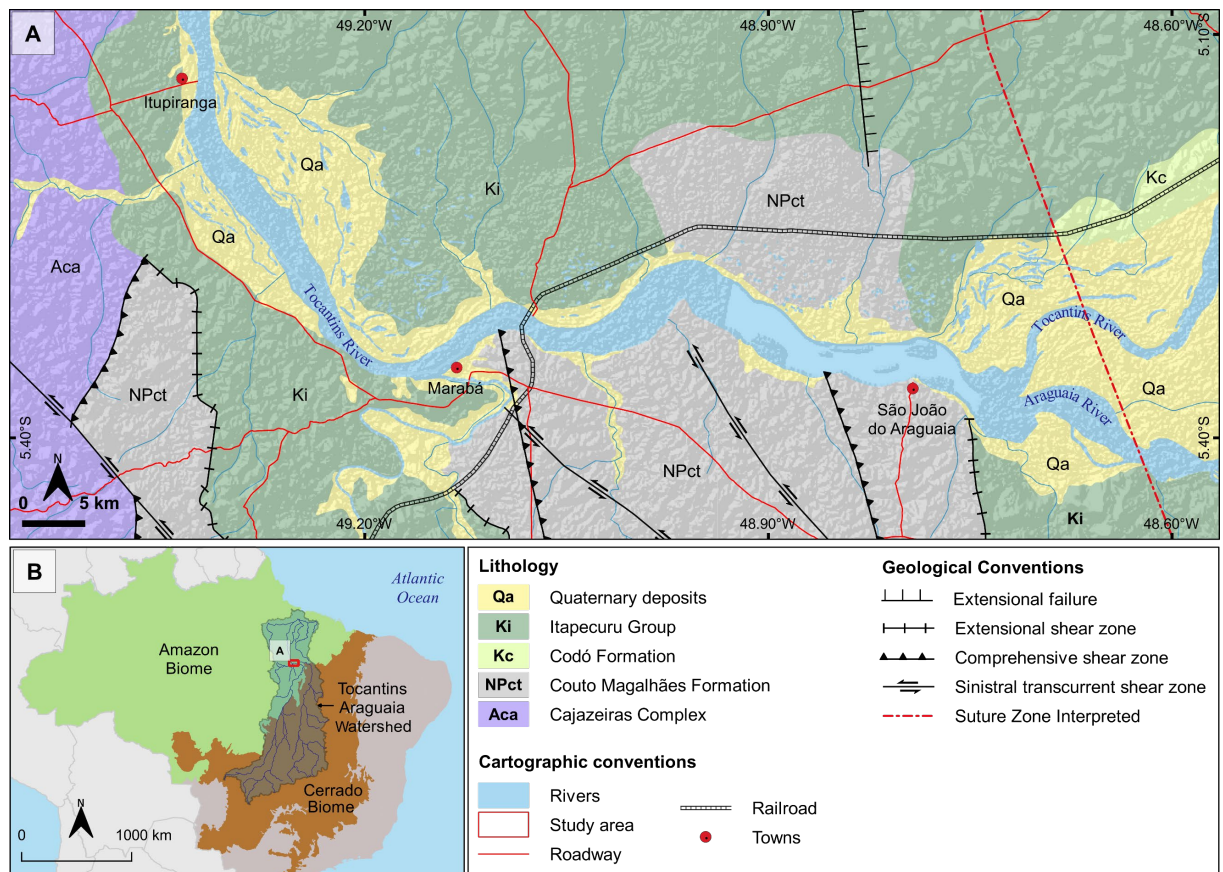


Figure 1 - Geological setting of the middle Tocantins River, including the study area. (A) Main geological units of the area include high-grade metamorphic rocks of the Cajazeiras Complex, low-grade metamorphic rocks of the Couto Magalhães Formation, sedimentary deposits of the Itapécuru Group and Codó Formation (Vasquez and Rosa-Costa 2008). (B) Location of the study area near the boundary between the Amazon and Cerrado biomes.

3 METHODS AND DATA

3.1 Geomorphological Mapping and Classification

Identification and mapping of surface landforms were based on visual interpretation of optical and radar satellite images from different sensors and resolutions based in an constructivist (building block) approach to reading the landscape (Fryirs and Brierley, 2012). To standardize the mapping on the scale of 1:100,000, it was used Tobler's rule (Tobler, 1987). Although remotely sensed or modelled data provide critical guidance in our efforts to interpret landscapes, it is

.highlighted that robust validation of surface features identified through remote sensing methods is derived from field-based analyses (Fryirs and Brierley, 2012).

The criteria for image interpretation and terminology of fluvial landforms were applied combination as suggested by Wheaton et al. (2015), Fryirs and Brierley (2012), John Lewin and Ashworth (2014) and Akter et al. (2018). Geomorphic units were defined by analysis of the drainage networks, erosive and depositional features, and visual interpretation of satellite images. The geomorphological classification was based on the hierarchical system proposed by Zinck (2016), which is constructed under the basic criteria of configuration, composition and hierarchical organization that reflects the level of the geomorphological units in the landscape.

3.2 Remote Sensing

3.2.1 Image processing

We use Landsat-8 images, Path 223 / Row 64, dated of on May 29th, 2018. Images were obtained from NASA's repository. Images resulting from the natural color composition bands 4 Red (640-690 nm), 3 Green (530-590nm) e 2 Blue (450-510 nm), with band 8 Panchromatic (500-680 nm) and final spatial resolution of 15 m, were particularly useful in obtaining a better contrast and enhancement of fluvial features due to its higher spatial resolution. High resolution imagery from the Google Earth Pro© (Google Earth Pro©, 2019) application and Esri World Imagery (Esri, 2019) were used to improve the remote sensing interpretation of smaller geomorphic features (e.g. paleo-channels, fluvial bars and small lakes). The Multi-Error Removed Improved-Terrain Digital Elevation Model (MERIT DEM), with 3 arc second resolution (~90 m at the equator), was used for identification and mapping of landforms, morphometric analysis, and elaboration of topographic profiles. The MERIT DEM was developed by processing existing spaceborne DEMs (MERIT DEM accessed on January 6th, 2019; Yamazaki et al. 2017). Processing techniques were applied to enhance landforms of low topographic amplitude, following Merino et al. (2015). The color palettes were customized with local elevation intervals between 3 and 15 m. Image processing techniques and the map design were performed in the software QGIS® (Version 2.18.19, QGIS Development Team, 2019). The graphic adjustments, as color enhancement and brightness, were made in the software Inkscape™ 0.92 (Inkscape,

2007) and the fusion of the optical images by the Spectral Transformer GUI Landsat-8 Imagery® (Geosage, 2018). The cross-section topographic profile was performed using the "Profile Tool" plugin in QGIS and exported to Inkscape™ to add lithological information and perform graphical adjustments.

3.2.2 Morphometric classification and topographic profiles

Morphometric characterization and topographic profiles were derived from MERIT-DEM. The determination of the relative chronology of mapping units was performed through the analysis of morphological and topographic attributes, such as the presence of active or paleo-channels and lakes, preservation degree of forms, forms superposition and truncations and topographic level of terraces surfaces (e.g. Verstappen 1977; Pupim, Assine, and Sawakuchi 2017). In general, higher topographic levels are older than lower levels, as well as more preserved morphological features are newer than more degraded features (Pazzaglia, 2013).

3.3 Field Surveys

Field surveys were performed to verify and improve the geomorphic interpretation through satellite images and aerial photographs. Fieldworks were carried out in September of 2018 and comprised the description of sedimentary deposits in outcrops and trenches using a facies analysis approach according to Miall (2014).

4 DESCRIPTION OF THE GEOMORPHOLOGICAL MAP UNITS

The presented geomorphological map integrates erosive and depositional landforms observed in the middle Tocantins River, at a 1:100,000 scale. The mapping units are organized into three categories based on interpreted active and paleo depositional environments: (i) alluvial plain; (ii) fluvial terraces (T1, T2) and (iii) paleo-alluvial fan (Main Map – Appendices). The distribution of these geomorphological mapping units is restricted to the Tocantins River valley (Figure 2).

4.1 Geomorphological Units

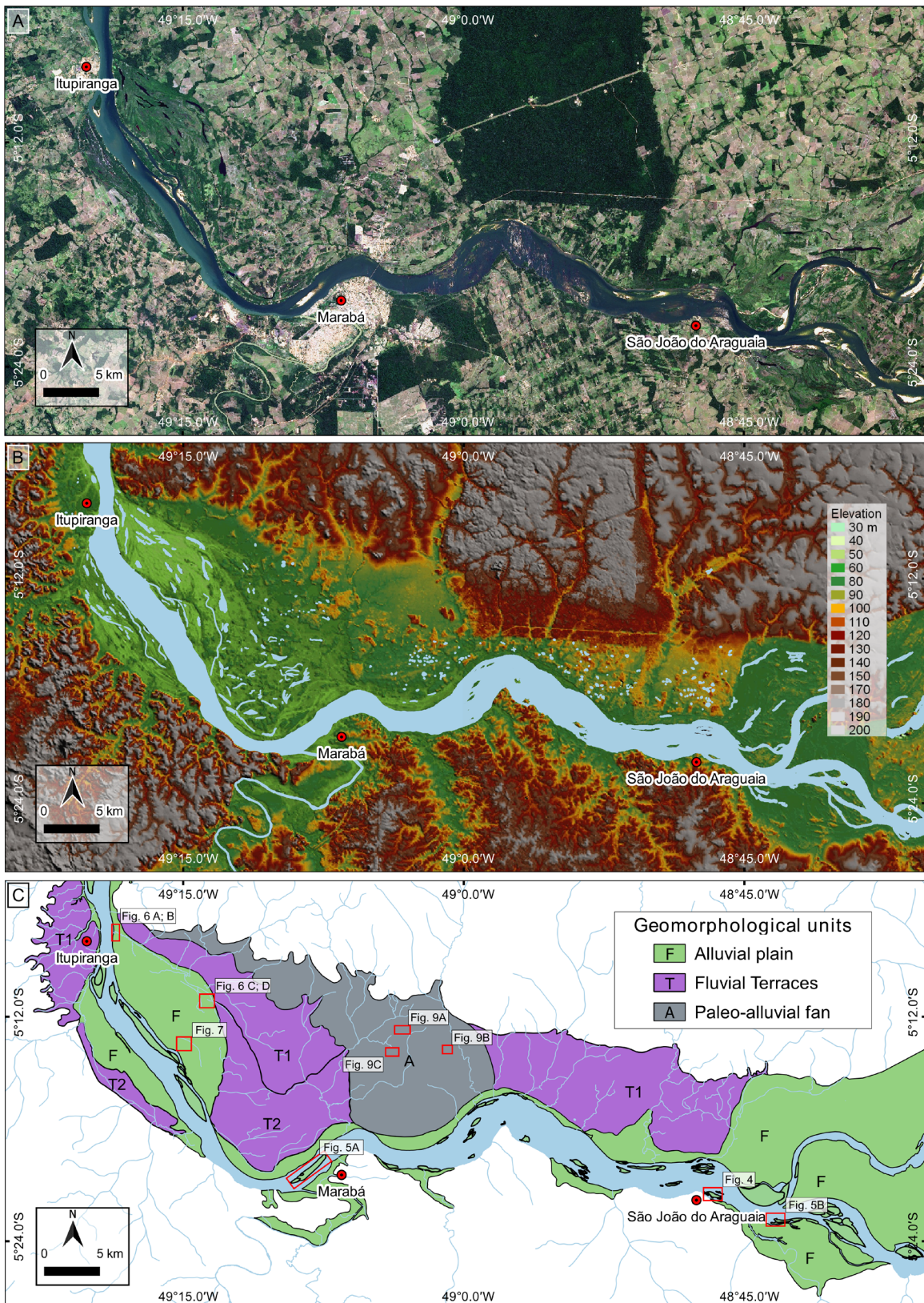


Figure 2 - Geomorphological aspects of the middle Tocantins River: (A) Landsat-8 image true-color (September 2018); (B) MERIT digital elevation model; (C) Main landform mapped that represents the relief/molding categorical level suggested by Zinck (2016).

GEOMORPHIC LANDSCAPE	RELIEF/MOLDING	TERRAIN FORM	
Alluvial plain (F)	(F1) Channel	(F11) Water body	
		(F12) Longitudinal bar	
		(F13) Lateral bar	
	(F2) Proximal Floodplain	(F21) Levee	(PC) Paleo-channel lakes
		(F22) Crevasse splay	
	(F3) Distal Floodplain		(PL) Paleo-levee
Fluvial Terraces (T)	(T2) Lower Terrace		
	(T1) Upper Terrace		
Paleo-alluvial fans (A)		(A11) Sand ridges	(L) Perennial lakes
		(A12) Ephemeral lakes	

Figure 3 - Hierarchical classification of mapping units of the middle Tocantins River.

4.2 Alluvial Plain

4.2.1 Channel

The studied reach of the Tocantins River comprises a mixed bedrock-alluvial channel. The main channel is cutting into bedrock substrates in the upstream reach (Figure 4), with rapids and some lateral sediment bars (Figure 5B). The river style changes to a predominately sand-rich channel and wide floodplain from Marabá to Itupiranga cities (Figure 2A). The smallest geomorphic units recognized within the channel are longitudinal and lateral bars. **Longitudinal bars** are elongated sand bodies in the direction of the water flow and with and/or without vegetation cover. The deposits are predominately sandy with decimetric sets of crossbedding, cross-lamination, and levels of well-selected and sub-rounded granules (Figure 5A). Vegetated bars associated with longitudinal bars, have accumulation of deposition build up leading to a relatively stable and high-altitude landform suitable for vegetation growth. This condition keeps the surface free of the inundation for long periods and supports the development of forest vegetation (Figure 5A). **Lateral bars** are sand bodies attached to rocky outcrops in the riverbed that consist in obstacles to accumulation of sediments. Vegetation cover is incipient but can occur in the wider bars (Figure 5B). The bars are composed of gravel in the bottom part and coarse sand in the upper portion whose morphology is controlled by joints, bedding and outcrops of

slates, shales and phyllites (Figure 5). This structural control is prominent in the upper reach of the mapping area, leading the development of irregularities in the channel substrate and the formation potholes, steps, and pools.



Figure 4 - Bedrock rapids upstream middle Tocantins River. Digital Globe, GeoEye, CNES/Airbus DS. Change updated: August 8, 2019 to Accessed: August 8, 2019.



Figure 5 - Geomorphic features within the channel unit. Location of photos and images in Figure 2C: A) Longitudinal bar attached in vegetated bar; B) Lateral bar with vegetated and non-vegetated. Digital Globe, GeoEye, CNES/Airbus DS Change updated: August 8, 2019 to Accessed: August 8, 2019.

5

6

7 **4.2.2 Floodplain**

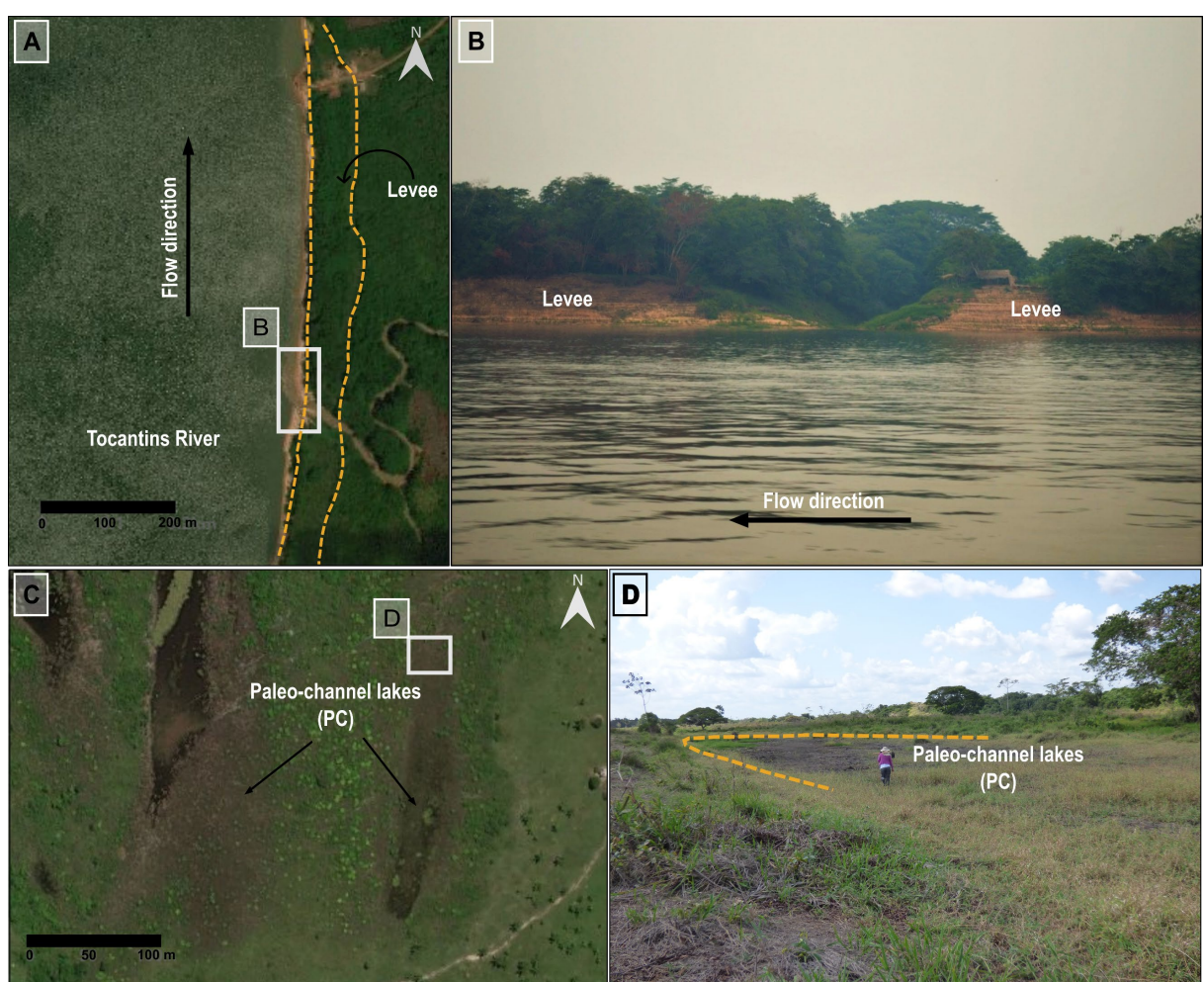
8 Floodplains were recognized in both margins of the Tocantins River, but the
 9 plain of the right margin is wider and more complex in terms of landforms, with the
 10 presence of numerous lakes, paleo-channels, swamp areas, levees, and crevasse
 11 splays. The terrain is almost flat, with smooth local relief in which the highest elevations

12 vary from 84 to 79 m.a.s.l. (meters above sea level) and the lowest from 78 to 66
13 m.a.s.l.. The floodplain areas have deposits of mud and fine sand due to seasonal
14 inundation. The alluvial plain was divided in proximal floodplain and distal floodplain
15 considering the presence of morphological elements as scroll bars, lakes and paleo-
16 channels. Lower level units were also mapped, reflecting the complexity of this
17 environment.

18 **Distal floodplain** is representing the lowest area of this geomorphic unit, with
19 elevation ranging from 66 to 78 m.a.s.l. The surface sediments are dominated by clay
20 and silt and the sedimentation occurs during high magnitude floods that reach the distal
21 parts of the plain. Perennial lakes, paleo-channels and ridge-and-swale are diagnostic
22 features of this geomorphic unit, but they also occur in proximal floodplains and
23 younger terraces. **Perennial lakes** are circular or semi-circular forms permanently
24 flooded. Perennial lakes have been described as “rounded lakes” which are particularly
25 important in geomorphic mapping, because they are the major “sink of sediment” in
26 the large fluvial systems of South America (Dunne et al. 1998; Mertes, Dunne and
27 Martinelli 1996). **Paleo-channels** are elongated features corresponding to abandoned
28 channels (Figure 4C and D). The paleo-channels are commonly formed through
29 channel avulsion that promotes the development of perennial or ephemeral lakes
30 (Slingerland and Smith 2004). They are filled with fine-grained sediments (silt and clay)
31 and organic matter supplied by the channel and nearby floodplain areas during
32 flooding. These forms can connect water between floodplains and main channel during
33 the flood seasons, playing a key role in ecological processes (Stevaux, Corradini and
34 Aquino 2013). This seasonal flood is complex process not only affect the floodplain
35 ecology but also controls hydrogeomorphology of the floodplains documented in Park
36 and Latrubblesse (2017). Ridge-and-swale is a landform consisting of regular, parallel
37 sand-ridges alternating with marshy depressions. **Paleo-levees** occur decoupled of
38 the main channel and they are frequently associated with paleo-channels in the
39 floodplains and lower terrace levels.

40 **Proximal floodplain** is periodically flooded terrains immediately adjacent to the
41 main channel. It has elongated shape parallel to the main channel, with changes in
42 width controlled by marginal bedrocks. Sedimentation in swampy areas is dominated
43 by silt and clay, but with presence of fine sands in other associated features as levees,
44 paleo-levees, and crevasse splays. **Levees** are narrow and elongated ridges that

45 occur irregularly along the main channel (Figure 6A and B). They have asymmetric
 46 morphology, with low angle slopes towards the floodplain and high angles to the
 47 channel, and are composed of clay, silt and very fine to fine sands. Levees crests have
 48 the highest elevation (from 85 to 90 m.a.s.l.) in the floodplain, and they are entirely
 49 covered by forest vegetation (Figure 6B). A **Crevasse splay** is recognized in the
 50 proximal floodplain (Figure 7). This landform is a local high and has three main lobes
 51 that probably were attached to a past position of the main channel (Figure 7). Rossetti
 52 et al. (2015) revealed paleoenvironments including active channel, abandoned
 53 channel, point bar, crevasse splay and floodplain, which are altogether compatible with
 54 meandering fluvial systems, thus indicating evolution processes of the evolution plan.
 55
 56



57
 58 Figure 6 - Geomorphic features of the floodplain. Location of photos and images in Figure 2C: A) Levee
 59 within the proximal floodplain; B) Levee located on the right bank of the main channel and covered by
 60 arboreal vegetation; C) Lakes formed by paleo-channels within the floodplain; D) Field view of paleo-
 61 channel. Figure A and B with images from Digital Globe, GeoEye, change updated: August 8, 2019 to
 62 Accessed: August 8, 2019.



63
64 Figure 7 - A) Crevasse splay in DEM image. B) Crevasse splay highlighted by denser vegetation cover
65 in Landsat 8 image true color (September 2018).

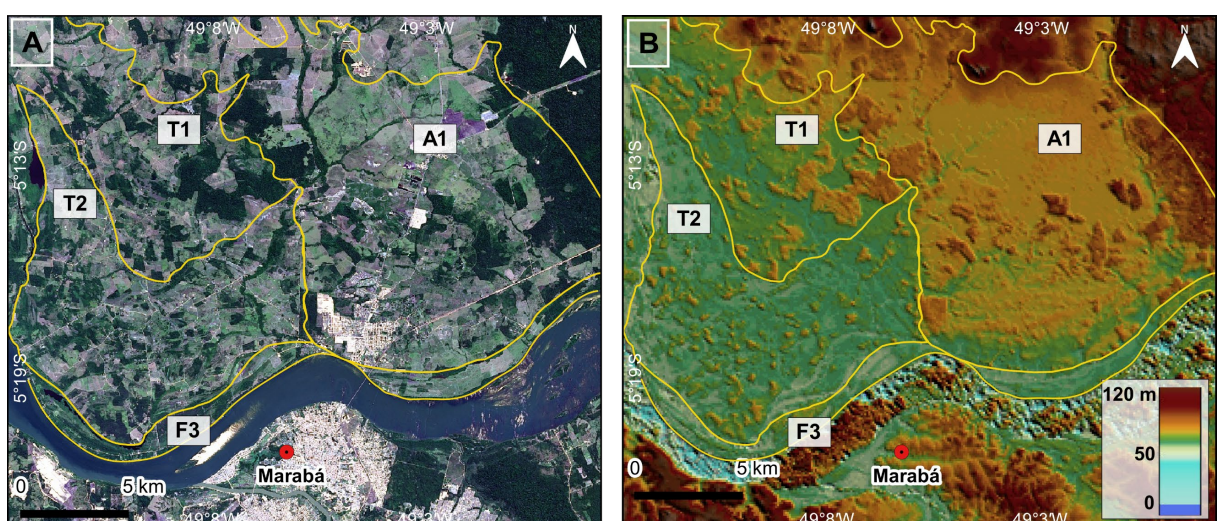
66

67 **4.3 Fluvial Terraces**

68 **Fluvial Terraces** are relatively flat terrains not susceptible to seasonal flooding.
69 In the studied area, three terrace levels were mapped based on their morphological
70 characteristics and elevation (Figure 8). The **Upper Terrace (T1)** level is related to
71 fluvial deposits occurring between 43 and 66 m above the water level of the Tocantins
72 River channel (105 -110 m.a.s.l.). The surface is almost flat with low drainage density
73 (70 m/km²) that carved narrow (17 m width) and shallow valleys (5 m depth). The
74 deposits are predominantly composed of massive medium sands. The sediment color
75 in outcrops varies from dark to light gray at the top and yellowish to the base,
76 suggesting pedogenetic processes, with an upper horizon rich in organic matter and a
77 lower horizon enriched in iron-minerals. The shallow water table (1.6 m depth at
78 September 2018) maintains numerous perennial lakes in this unit, displaying circular
79 morphology with average radius about 116 m. At the base of T1, there are
80 conglomerate layers with around 1 m thick, but eventually reaching up to 3 m.
81 Conglomerate layers are well- exposed at the base of terraces in the northwest and
82 west portions of the area. At the base of this unit, the conglomerates have polymictic
83 and well-rounded clasts and they occur as layers with incipient grading, tabular
84 geometry, and wavy top. Grain size of the framework varies from granules to cobbles
85 of sandstones, iron-rich duricrust, granites, gneiss and quartzite immersed in a reddish
86 matrix of sandy mud.

87 **Lower Terraces (T2)** are between 27 and 36 m above the river level (84 and 86
88 m.a.s.l.), with surface slightly tilted to the main channel. This unit is marked by high
89 density of paleo-channels that give origin to lakes in the modern floodplain. These
90 lakes can be connected to the main channel during the flood season. The paleo-
91 channels are gradually filled by suspended fine-grained sediments (clay and silt) during
92 flooding events and can show meander scrolls-bars in an advanced stage of
93 degradation. The drainage network has low density, with channels showing shallow
94 incision. The contact between lower level terraces and floodplains is marked by an
95 abrupt slope. Flooding of the lower terraces may occur during high magnitude
96 precipitation events. Most of the lower terraces are composed of massive fine sand
97 with clay. Sediment color ranges from red-yellowish at the top to yellowish at the
98 bottom.

99



100
101 Figure 8 - Geomorphic features of the terraces and paleo alluvial fan: A and B) Regional relationship
102 between fluvial terraces (T2 and T3), paleo alluvial fan and the alluvial plain, where an abrupt slope
103 break marks the inner boundary of the proximal floodplain. Image A from ESRI's World Imagery, updated
104 at Aug 8, 2019; Image B MERIT-DEM.

105

4.4 Paleo-alluvial fan

The paleo-alluvial fan unit is made up of unconsolidated massive medium sands accumulated in a relatively high topographic position (90 - 100 m.a.s.l.). These sediments appear to derive from streams that drain hillslopes in the north portion of the area, and which spread out over a gently slope surface related to the ancient floodplain of the Tocantins River. The present morphology includes deposits with a convex-up transversal profile between the Flexeiras and Geladinho Rivers and ephemeral lakes (Figure 10). **Ephemeral lakes** are semicircular closed depressions showing seasonal flooding, usually disappear during drought and fill up again with water in rainy seasons. The lakes are concentrated in the north portion of the unit and are filled by dark brown mud over grayish fine sands. The seasonal variation of water table controls the vegetation distribution, with grasses in the center and shrub in the margins of the lakes. This unit is dissected by low density drainage network, with streams incised in narrow (17 m) and shallow valleys (5 m). The sedimentary deposit consists of metric-thick layers of quartz-rich white sands intercalated with three horizons of the 10-20 cm organic paleosols. The sandy layers are dominated by well-sorted fine to medium sands, with well-rounded grains. An upper layer of medium sands occurs in the paleo-alluvial fan unit as well as in the surrounding fluvial terraces (T2). This upper **sand sheet** might represent the eolian or alluvial reworking of the underlaying units (Figure 9B).

Most of the paleo-alluvial fan surfaces are covered by patches of diverse vegetation that comprises a mosaic of grasslands, shrubs and arboreal forest spots (Figure 10A and C). The sand ridges arboreal spots are small areas (10^3 - 10^5 m 2) with substrates with elevation higher (~1 m higher) than adjacent grasslands and supporting a dense forest cover (Figure 9A). The forests spots are developed over soils with an upper thin layer of gray mud covering quartz-rich sands (Figure 8B). Open vegetation areas have been identified across the Amazon and they can be associated with the development of alluvial fans (Cordeiro et al., 2016) and eolian deposits (Zular et al., 2019).

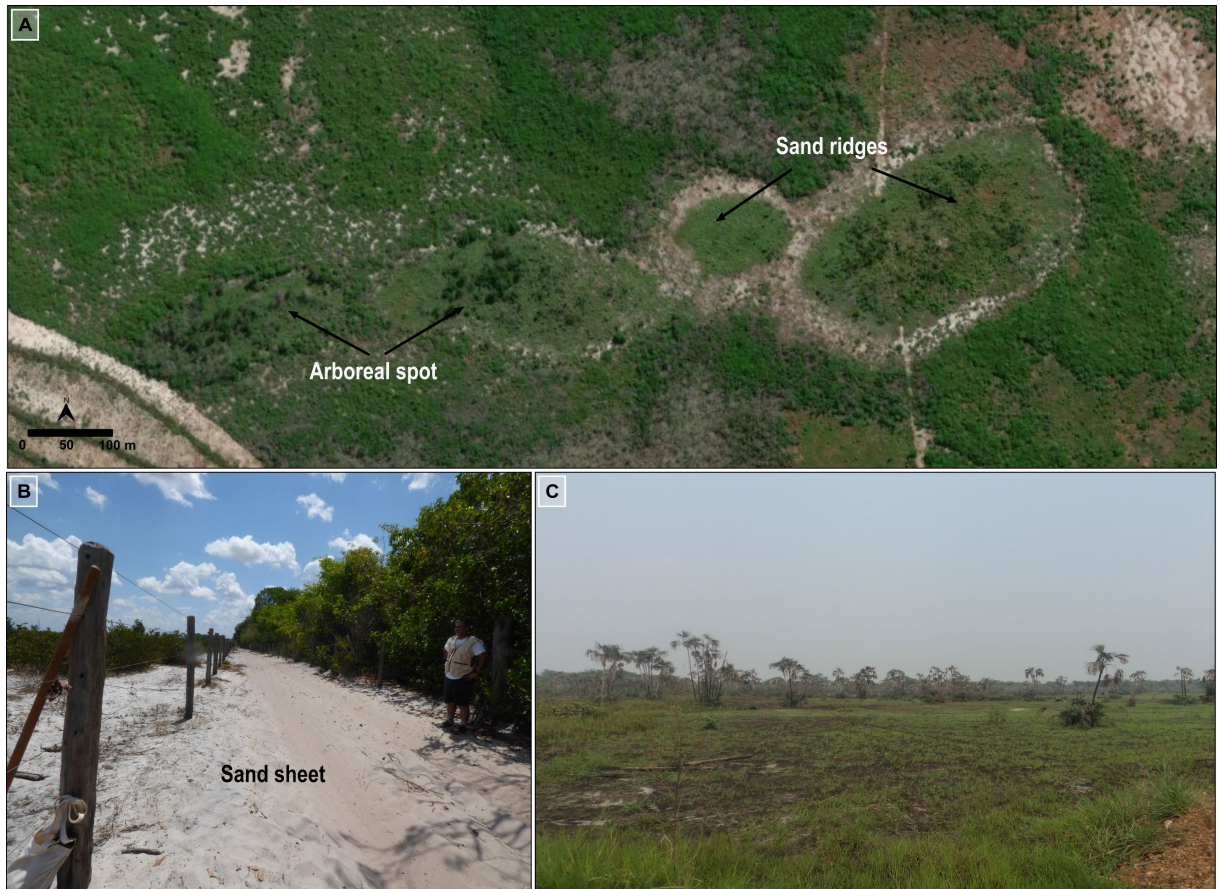


Figure 9 - General aspects of the paleo-alluvial fan geomorphological unit. A) Patches of diverse vegetation that comprises a mosaic of grasslands, shrubs and arboreal forest spots; B) Partial view of the sand sheet; C) View of grasses and palm trees.

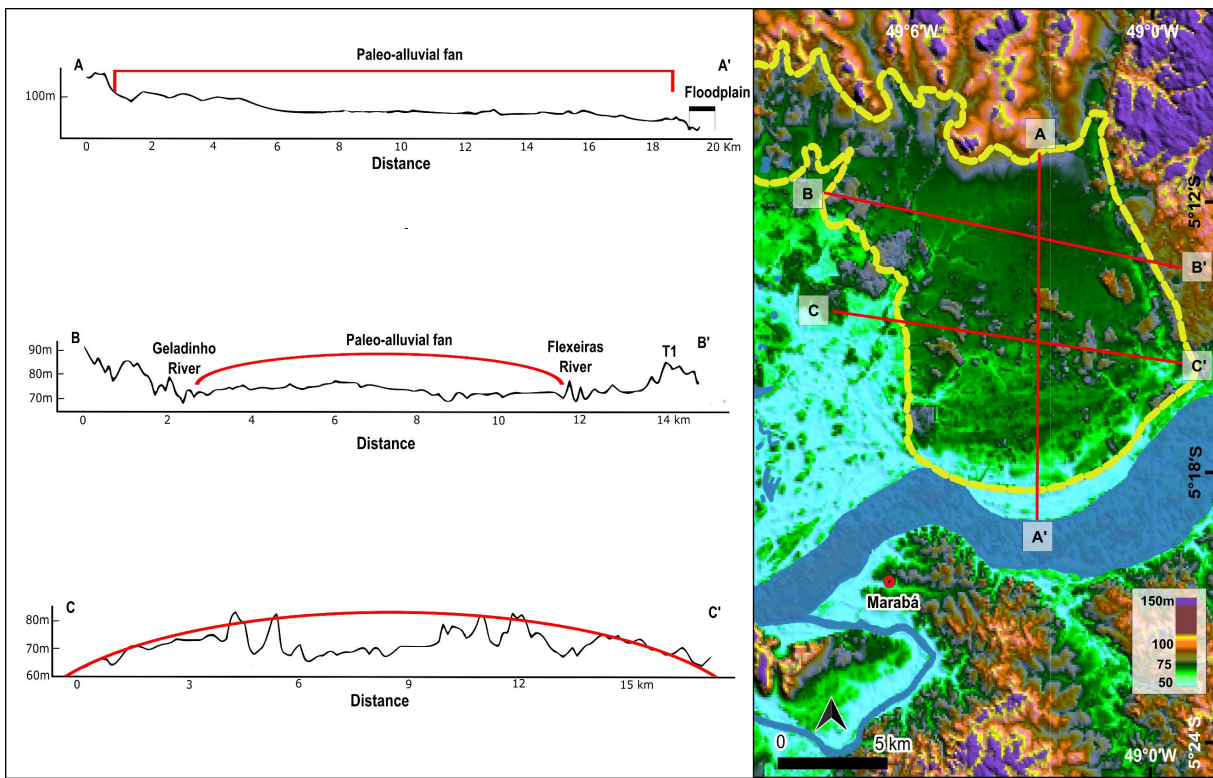


Figure 10 - Geomorphic features of the paleo-alluvial fan unit. Longitudinal and transversal topographic profiles showing upward convex shape. Map showing the boundaries of the paleo-alluvial fan, with indication of the longitudinal (line A -A ') and transverse (line B-B' and line C-C') profiles. Topographic data are from MERIT-DEM.

5 DISCUSSION AND CONCLUSIONS

Three mapping categories representing different depositional environments and their specific landforms were described in the middle Tocantins River. The mapping and elevation surveys of landforms suggest that the evolution of the plain comprised stages of sediment aggradation and erosion. In addition, the tributaries of the Tocantins River influenced the physiography of the modern and ancient alluvial valley by segmenting the floodplain into patches of different environments, including the development of a paleo-alluvial fan, which contrasts with the modern contributory fluvial system.

The alternation between stages of aggradation and erosion suggests can be promoted by variations in water and sediment supply due to climate changes affecting precipitation in the watershed (e.g. Vandenberghe 2003). The hierarchical classification of geomorphic units allows to define a relative chronology of the mapped

landforms. The geomorphic map presented in this study can be useful in environmental and socio-economic planning of activities connected with the Tocantins River and its floodplains since the delineation and characterization of mapping units give information about physical dynamics of the landscape under human interventions, including for example substrate types and susceptibility to seasonal or historical flooding. Floodplain areas commonly host urban populations or agriculture activities due to the characteristics of relief and soils (Ross, 2016). Part of the city of Marabá is located on the Proximal Floodplain (Main Map), which is seasonally flooded by the Tocantins and Itacaiúnas Rivers. This floodplain is the most extensive floodplain of the Tocantins River, and the place on which recruitment occur for migratory and non-migratory fishes (Akama, 2017). Therefore, it is an important habitat for conservation of aquatic ecosystems.

Historically, the Tocantins River main stem is the most impacted tributary of the Amazon fluvial system, with several already built dams, though the Araguaia River is still well-preserved due to absence of dams (Latrubesse et al., 2019). However, the building of the planned Marabá hydropower plant in the Tocantins River will affect both rivers, with potential severe effects on the studied floodplains and related aquatic ecosystems (Lees et al., 2016; Winemiller et al., 2016; ICMBio, 2018).

In summary, the geomorphological and morphometric analyses from satellite images, DEMs and field surveys allow to map three main geomorphic units named alluvial plain, fluvial terraces, and paleo-alluvial fan. The origin of the mapped landforms and their sedimentary deposits are related to active and ancient fluvial systems. The hierarchical organization of the geomorphic units provide new information about relative timing of landform formation, being potential archives to reconstruct environmental conditions of the terrains drained by Tocantins River and its tributaries.

SOFTWARE

QGIS 2.18.19 and Global Mapper 18 software was used for map data visualization and analysis purposes. Some output maps were redrawn using Inkscape 0.92. The map is designed to be color printed at A1 (594x841mm) size for optimum clarity of font, point size and shading.

FINANCING

This research had financial support of the projects “*Dimensions US-BIOTA-São Paulo: Assembly and evolution of the Amazonian biota and its environment: an integrated approach*” (São Paulo Research Foundation-FAPESP grant#2012/50260-6, US National Science Foundation and NASA grant#1241066) and “*The response of sedimentary dynamics of the Xingu and Tapajós Rivers to climate changes and hydropower dams: risks for biodiversity conservation and energy production in Amazonia*” (FAPESP grant#2016/02656-1). JJ is thankful to the Master’s scholarship from *Coordination of Superior Level Staff Improvement, Brazil (CAPES) - Finance Code 001*. FNP was supported for a postdoctoral fellowship FAPESP grant#2014/23334-4. FNP and AOS are supported by National Council for Scientific and Technological Development (CNPq, Brazil) grants #302411/2018-6 and #304727/2017-2, respectively. The opinions, hypotheses, conclusions, and recommendations expressed in this material are responsibility of the author (s) and do not necessarily reflect FAPESP's and CAPES vision.

ACKNOWLEDGMENT

JJ is grateful for Federal University of South and Southeast Pará (Unifesspa) for car support for field activity and Geologist Elianne Conde from Unifesspa for their help during field work.

6 LATE QUATERNARY EVOLUTION OF THE MIDDLE TOCANTINS RIVER IN EASTERN AMAZON

Article Submitted to Geomorphology

ABSTRACT

The Tocantins River drains the easternmost area the Amazonia. Most of its upper catchment is represented by bedrock channels, but the middle reach is marked by the extensive sediment accumulation that shows a diverse assembly of channel fluvial forms, wide floodplains and terrace levels, which is called Tocantins Paleochannel and Bico do Papagaio. However, the Quaternary history of the Tocantins River is poorly understood due the lack of geomorphological studies constrained by geochronological data. Therefore, we characterized the sedimentary deposits of the middle reach of the Tocantins River and applied optically stimulated luminescence dating (OSL) to understand how this fluvial landscape evolved during the late Quaternary. The analysis of satellite images and digital elevation models (DEMs) allowed the mapping of four distinct geomorphic units placed in different topographic levels: (i) channel, (ii) floodplain, (iii) fluvial terraces (T1 and T2), (iv) paleo-alluvial fan. The results from the morphosedimentary analysis integrated with OSL dating allow us to interpret the landscape evolution between 661 ± 42 and 160 ± 16.3 ka. The OSL ages permit to identify three main phases of sediment deposition and two phases of incision. The older depositional phase formed the Upper Terrace (T1) and part of the paleo-alluvial fans from 160 to 32 ka. Afterwards, an incision event took place around 31 ka, allowing the abandonment of T1, followed by a second depositional phase that built the Lower Terrace (T2) and promoted reactivation of the paleo-alluvial fans from 31 to 6 ka. The younger incision event occurred from 6 to 5 ka, allowing the abandonment of T2 and lowering the local base level until its present position. The modern floodplain has been built-up since 5 ka to the present, with deposition of sediments due frequent lateral channel migration of the Tocantins River channel. The OSL chronology of the depositional landforms indicates variations flow related to climate change were the main driver of the river dynamic, timing of incision and depositional, and landscape evolution since 160 ka of the middle Tocantins River, the largest river system of the eastern Amazon, during the Late Quaternary.

Keywords: Tocantins River, Marabá, Fluvial geomorphology, Dating OSL, Paleoclimate.

1 INTRODUCTION

The riverscapes Amazonian evolved under the influences of geological and climatic processes operating over millions to billions of years (Albert et al., 2018). The geomorphology of the old floodplains remains highly heterogeneous and is composed of a mosaic of abandoned river channels, oxbow lakes and sedimentary beds of different ages (Salo et al., 1986). This heterogeneity record signals of environmental changes from different temporal and spatial scales (Schumm, 1988). Over geologic timescale (10^3 - 10^6 years), tectonic and climate regimes play a fundamental role in the dynamics and development of fluvial systems (Maddy et al., 2001). The interplay between tectonic and climate modulates boundary conditions such as base level, water discharge and sediment supply, which drive alternating phases of aggradation and incision in the plains (Bull, 1991; Tofelde et al., 2019). Changes in boundary conditions can lead to channel metamorphosis and the formation of the terrace sequences along the evolutionary history of the fluvial system (Bridgland and Westaway, 2008).

Contrasts in morphological and sedimentary characteristics from different terrace levels suggest the occurrence of changes in regional environmental conditions (Pazzaglia, 2013). Therefore, the geomorphological and sedimentological study of sedimentary deposits preserved in terraces and fluvial plains, coupled to absolute chronology of sediment accumulation, are important tools for understanding the response of fluvial systems to tectonic or climate changes occurring on long-term temporal scales, exceptionally during the Late Quaternary (Merritts, 2007). The fluvial system formed by the Amazon River and its tributaries has been the target of many efforts with the aim to understand its evolution during the Quaternary. Most of these studies are focused in the western portion of the basin, where the occurrence of fluvial deposits at different levels of terraces is more abundant (Latrubblesse, 2002; Latrubblesse and Franzinelli, 2002, 2005; May et al., 2008; Rigsby et al., 2009; Soares et al., 2010; Rossetti et al., 2012, 2014, 2019a; Bertani et al., 2015; Cremon et al., 2016; Gonçalves Júnior et al., 2016; Pupim et al., 2019; Passos et al., 2020). However, the factors that govern the changes in these large fluvial systems are still controversial. Many authors have argued that climate fluctuations would be the main factor responsible for the formation of terraces sequences in the rivers of western Amazonia along the Late Quaternary (Räsänen et al., 1990; Latrubblesse, 2003; Rigsby et al., 2009) while other authors argue that tectonics (Costa et al., 2001; Latrubblesse and Franzinelli, 2002;

Franzinelli and Igreja, 2002a; Soares et al., 2010; Rossetti et al., 2014, 2015, 2017a; Bertani et al., 2015; Cremon et al., 2016) or relative sea level (Mertes and Dunne, 2007; Irion et al., 2009; Irion and Kalliola, 2010) are also important drivers of river courses and terraces building.

The alternation between humid and dry periods associated with changes in vegetation cover (more or less dense forests or forest *versus* savanna) (Hammen et al., 1992; Bush et al., 2004a; Cheng et al., 2013; D'Apolito et al., 2013) would lead to disturbances in the sediment-to-water-discharge ratio, promoting aggradational phases (dry period) and degradational (humid period) (Latrubesse, 2003). Important palynological and geochemical records from the east (Absy et al., 1991, 2014; Sifeddine et al., 1994; Cordeiro et al., 2008; Hermanowski et al., 2012, 2014; Guimarães et al., 2013, 2016, 2019b; Sahoo et al., 2015; Reis et al., 2017), south (Fontes et al., 2017), west (Behling and Hooghiemstra, 1999; Seltzer et al., 2000; Baker et al., 2005; Groot and Bogot, 2011; Cordeiro et al., 2011b; Cohen et al., 2014), central (Irion et al., 2001; Moreira et al., 2009) and northwestern (Behling, 2001; Sifeddine et al., 2003; Moreira et al., 2009; Zocatelli et al., 2013, 2016; Häggi et al., 2017; Augusto-Silva et al., 2019) Amazonia contribute to evidence of paleo-vegetation changes that probably reflects climate variability during the Late Quaternary in the region. In contrast, other studies indicate to the influence of recent tectonic control on the configuration and geometry of the Amazonian drainage system (Costa et al., 2001; Latrubesse and Franzinelli, 2002; Franzinelli and Igreja, 2002; Mertes and Dunne, 2007; Almeida-Filho and Miranda, 2007; Soares et al., 2010; Rossetti et al., 2019a, 2014, 2015, 2017; Bertani et al., 2015).

Terraces formation was also associated with relative changes in sea level since the Last Glacial Maximum (LGM). Irion et al., (2009) argue that the incision that originated the current fluvial valley of the Amazon River and tributaries occurred during the LGM due to relative lower sea level. According to these authors, the sea level rise until the Mid Holocene would have drowned the carved valley, increasing the accommodation space for sediment deposition that infill the current fluvial plain.

Despite recent studies added important chronological constraints to understand the factors that influence fluvial systems in Amazonia studies about fluvial deposits from the easternmost large Amazonian river, the Tocantins River, are absent. Available geological data are scarce (Valente and Latrubesse, 2012) and many questions are still under debate, notably about what are the roles of external drivers such as climate,

tectonic and sea level compared to internal factors for the evolution of large rivers draining the eastern Amazonia; the temporal and spatial scales that they act. However, paleoenvironmental that the precipitation and vegetation pattern was not homogeneous throughout the region drained by the Amazonian rivers, at least in the last 100 ka, with striking differences between east-west and north-south (Bush et al., 2004a; Cheng et al., 2013; Zhang et al., 2016; Wang et al., 2017). Thus, the working hypothesis is that the fluvial systems of eastern Amazonia, which drain terrains of central Brazil (Sawakuchi et al., 2015; Pupim et al., 2016; Bertassoli et al., 2019), such as the Tocantins River, present different responses from the rivers that drain Andeans terrains.

In this context, the aim of this research was to investigate geomorphological, sedimentological, and chronological aspects of the fluvial deposits on the middle Tocantins River in order to better understand its response to changes in external forces during the Late Quaternary. Our morphosedimentary mapping highlight the occurrence of different terrace levels and fluvial plains with high diversity of wetland environments. The optically stimulated luminescence (OSL) dating of the fluvial deposits allows us to constrain the timing of geomorphological shifts and propose an evolution model for the middle Tocantins River during the Late Quaternary. Moreover, our results filled a knowledge gap about the geological history of the fluvial systems in the most eastern Amazonia, contributing to the discussion about the impact of the Quaternary climate changes on river dynamics that drain eastern the edge of the Brazilian Amazon, Amazon (rain forest) – Cerrado (savanna) ecotone.

2 THE TOCANTINS RIVER SYSTEM

The Tocantins River and its main tributary, the Araguaia River, drain terrains that extends from 46° to 55° West and 2° to 18° South, comprising the largest entirely Brazilian river basin (Figure 1A; ANA, 2019). Due to the large latitudinal extension, there is an expressive difference of precipitation throughout the drainage basin with an increase of rainfall from south to north. Thus, the mean annual total precipitation varies from 1.869 mm/year in the headwaters to 2.565 mm/year at the river mouth (MMA, 2006). The climate is tropical with a mean annual temperature of 26 °C and two well-

defined climatic periods with a rainy season from October to April (90% of precipitation) and dry season from May to September.

The Tocantins River drains distinct landscapes, including the seasonally dry savannas (Cerrado) of the Central Plateau of Brazil, the Amazon rainforest and a transitional environment between them, called Pre-Amazonian environments (Figure 1A; Mérone et al., 2010). However, the Tocantins River Watershed has experiencing fast deforestation making way for planted pastures and croplands (MapBiomas, 2019). The most impacted regions are the headwaters in the Cerrado biome, where high deforestation rates lead to the increase of soil erosion and sediment supply to the rivers, losing ecosystem services provided by river (Latrubesse et al., 2019). The regional geology is represented by the Bacajá Domain, Araguaia Belt, Parnaíba Sedimentary Basin and Marajó Sedimentary Basin (Figure 1B).

Quaternary sedimentary deposits are restricted to alluvial plains associated with main rivers. They were deposited over different types of rocks, such as Cretaceous sandstones of the Itapecuru (Campbell, 1949) and Codó (Mesner and Wooldridge, 1964; Lima, 1982) formations related to the Marajó (Villegas, 1994) and Parnaíba Basins (Bigarella, 1973; Góes, 1995), high-grade metamorphic rocks of the Cajazeira Complex-Bacajá Domain (Brito Neves, B and Cordani, 1991) and phyllites and shales of the Couto Magalhães Formation of Province Tocantins (Figure 1C; Hasui et al., 1977).

Vasquez and Rosa-Costa, (2008) reported that the Quaternary deposits are divided into two macro units: 1) fluvial terraces: composed of unconsolidated and semi-consolidated clays, sands and gravels that occur in topographic levels higher than the current alluvial plains; and 2) alluvial deposits: composed of clastic sediments related to the current alluvial plains, which constitute deposits of channels and floodplains (Figure 1C).

Although they form a single watershed, the Tocantins and Araguaia rivers have many unique features (Mérone et al., 2010). The Tocantins River is dominantly a bedrock river with moderately high drainage density. Its headwaters are in the Brazilian Shield, about 1.000 m in altitude, and flows northwards over plateaus of sedimentary rocks for about 1.960 km until reach the Pará River, near the city of Belém/PA (MMA, 2006). The channel shows straight pattern, stable riverbanks, few and narrow floodplains, and generally clear waters, indicating a low sediment load (Gonçalves and Nicola, 2002). Several channels reach shows a strong lithological and structural control

from the basement rocks, expressed by channel straightness, anomalies, rapids and waterfalls (Várzea, 1942; RadamBrasil, 1974). The Araguaia River is a lowland river with low drainage density. Its headwaters are in the foothills of the Serra dos Caiapós at 850 m and flows almost parallel to the Tocantins River for about 2.600 km (Mérona et al., 2010). Downstream of the Bananal Island, the Araguaia channel also shows a bedrock river style, with some rapids and waterfalls, similar to Tocantins River (Gonçalves and Nicola, 2002).

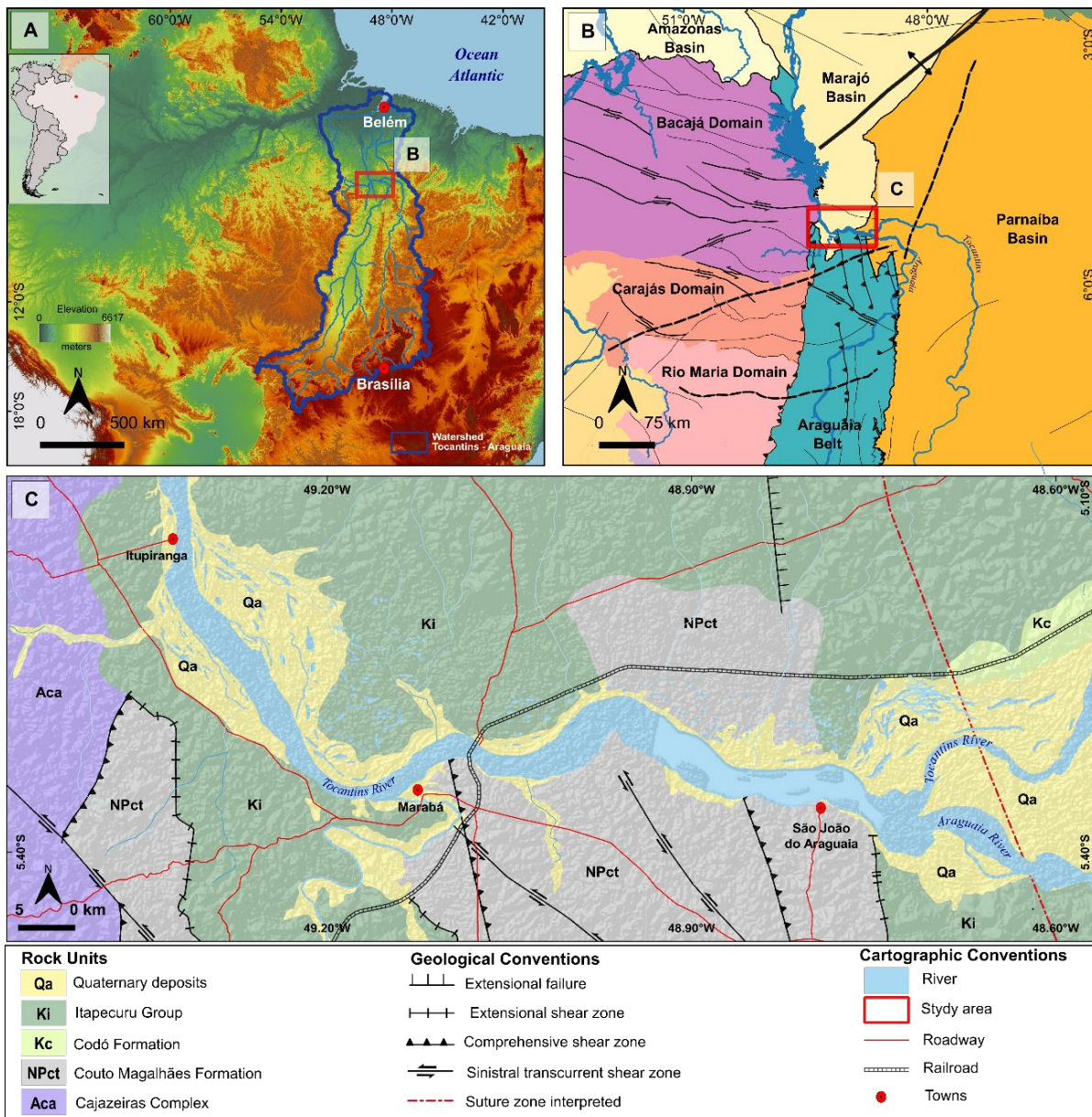


Figure 1 - Geological and topographical settings of the middle Tocantins River. (A) The Tocantins River watershed is highlighted by the blue line. The studied area is located in the middle stretch of the Tocantins River and includes the downstream reach of its main tributary, the Araguaia River (red square); (B) Regional tectonic domains setting and main structural configuration. The map is based on the South American Tectonic Map of the Geological Service of Brazil (CPRM, 2018); (C) Geologic map of the study area (Vasquez and Rosa-Costa 2008).

3 MATERIAL AND METHODS

3.1 Geomorphic Mapping and Remote Sensing

The mapping combined visual interpretation of geomorphic features and morphometric analysis through remote sensing images, digital elevation model (DEM) and field surveys. We use a 1 arc second resolution (~30 m) DEM derived from images from the Shuttle Radar Topography Mission (SRTM), (USGS, 2015) and a 3 arc second resolution DEM from Multi-Error Removed Improved-Terrain Digital Elevation Model (MERIT DEM) (Yamazaki et al., 2017) to characterize morphometric aspects, perform topographic profiles and mapping main landforms, as fluvial plains and terrace levels. Imagens from the Landsat-8 OLI, composition 432 (RGB), Google Earth™ and Esri World Imagery® were also used to recognition and interpretation of the geomorphic surface features in detailed scale. Digital image processing techniques were applied to enhance landforms of low topographic amplitude, following Merino et al., (2015). The color palettes were customized with local altimetric intervals, from 3 to 15 m, to highlight sets of elevation values of the geomorphic units. The criteria for image interpretation in fluvial landforms were applied as suggested by Fryirs and Brierley, (2012); Lewin and Ashworth, (2014); Akter et al., (2018). Geomorphic units were distinguished or correlated based on the topographic level, erosive or depositional characteristics, occurrence of morphological features and its preservation pattern. Field survey were carried out to verify the boundaries between units and describe landforms and geological material. The geomorphological classification was based on the hierarchical system proposed by Zinck (2016), which is constructed under the basic criteria of configuration, composition and hierarchical organization that reflects the level of the geoform in the landscape.

3.2 Sedimentological Descriptions

Sedimentological data consisted of facies descriptions in natural outcrops (e.g. riverbanks), road cut, trenches and shallow drillings. The drillings were performed using a borehole made with a hand auger. The sedimentary facies analysis was realized according to Miall, (2014). The sedimentary deposits were described, photographed and recorded on lithostratigraphic profiles, including characteristics

such as lithology, grain size, sedimentary structure and boundary surfaces. Grain size analysis was realized by the laser diffraction technique in a Malvern Mastersizer 2000.

Analyses of composition and sedimentological attributes of conglomerate clasts were based method of Graham, (1986) with adaptations, given the geometry of the outcropping deposits. Were classified and measured (short and longer axis, and height) 400 clasts, divided into 5 meshes of 1m² spaced along of the horizon of conglomerate. The minimum number of 400 clasts is proposed by Howard, (1993) so that the errors of sampling and counting can be minimized.

3.3 Optically Stimulated Luminescence Dating

The sampling strategy for OSL dating considered to collect at least two samples in two sedimentary profiles per geomorphic unit. We avoid the collection of samples above 1 m depth to prevent sediment mixing due pedogenetic processes. All samples were collected using opaque plastic tubes. Sample preparation for quartz isolation were performed under subdued light environment using the following steps: 1) wet-sieving to isolate the grain size fraction between 180 and 250 µm; 2) treatment with hydrogen peroxide (H₂O₂, 29%) to remove organic matter and hydrochloric acid (HCl, 10%) to eliminate potential carbonate minerals; 3) separation of quartz from heavy minerals and feldspar grains with lithium metatungstate (LMT) solution with densities of 2.75 g/cm³ and 2.62 g/cm³, respectively; 4) treatment with hydrofluoric acid (HF, 40%) for 40 min to remove remnant grains of feldspar and the external layer of quartz grains, eliminating the contribution of the alpha radiation to dose rate. For all aliquots used in luminescence measurements, the purity of the quartz concentrates was checked by the infrared depletion ratio (Duller, 2003).

Aliquots of quartz grains (~100-200 grains) were mounted on stainless steel discs. All luminescence measurements were carried out on two automated Risø TL/OSL Model DA-20 readers equipped with ⁹⁰Sr/⁹⁰Y beta sources with dose rates of 0.0768 ± 0.001 and 0.1197 ± 0.001 Gy/s, blue light emitting diodes (470 ± 20 nm) operated at 90% power (~40mW/cm²) for stimulation and Hoya U-340 filter for light detection in the ultraviolet band (290-340 nm) with a PM bialkali tube (Thorn EMI 9635QB). The Single-Aliquot Regenerative (SAR) dose protocol (Murray and Wintle, 2000, 2003) was used for estimates of the equivalent dose (De) (Table 01). The OSL data for calculation of De were analyzed using the Analyst software package (Duller,

2015). Only aliquots with recycling ratio between 0.9 and 1.1, recuperation less than 5% and insignificant infrared signal were considered in the calculation of equivalent doses (Murray and Wintle, 2003). OSL signal was calculated using the initial 0.8 s integral of light emission with subtraction of the normalized last 10 s of light emission as background. Dose-response curves were fitted using four regenerative doses with the aid of a single saturating exponential growth curve equation. The equivalent dose of each sample was calculated by the Central Age Model (CAM; Galbraith et al., 1999).

Dose recovery tests were performed to access an accurate pre-heat temperature used to estimate equivalent doses for the studied samples. The quartz aliquots were bleached in a solar simulator from 2 to 3 h. The dose recovery test was performed for given radiation doses in the same range of the expected equivalent doses (5, 30, 50 and 100 Gy) and using preheat temperatures of 200 °C.

The sediments (about 300-500g) for dose rate estimation were collected in the around of 30 cm of the samples collected for OSL measurements. The sample preparation involved the following procedures: 1) drying and weighing of sample to estimate the water content (water weight in relation to dry sample weight); 2) packaging in sealed plastic recipient and storage for at least 21 days for radon equilibration; 3) high-resolution gamma rays spectrometry for 24h to determine radionuclides (U, Th and K) concentrations; and 4) determination of background radiation in empty plastic recipient. Gamma ray spectrometry was performed using a high-purity germanium detector (HPGe Detector) with a 55% of relative efficiency, 2.1 keV of energy resolution at 1332 keV and encased in an ultralow background shield (Canberra Industries).

The calculation of dose rate considered conversion factors from Guérin et al., (2011). Water saturation was determined by the ratio between water weight and dry sample weight (Aitken, 1985). The contribution of cosmic radiation in the dose rate was calculated as described by Prescott and Hutton, (1994), considering the latitude, longitude, altitude, depth and density of each sample.

Table 1 - Measurement protocol used for equivalent dose estimation in quartz grains of the studied samples.

Step	Procedure*
1°	Dose (D_i)
2°	Pre-heat at 200° C for 10s
3°	Blue stimulation at 125° for 40s (L_i)
4°	Test dose
5°	Heat at 160°C
6°	Blue stimulation at 125° for 40s (T_i)
7°	Blue bleach at 280° for 40s
	Step Repeat 1-7 for growing series
8°	of D_i , $i = 0-7$, being D_0 =signal natural $D_1 < D_2 < D_3 < D_4$; $D_5 = 0$ Gy; $D_6 = D_7 = D_1$

* Regeneration doses D_i : $D_1 < D_2 < D_3 < D_4$; $D_5 = 0$ Gy, $D_6 = D_1$; $D_7 = D_6$, with additional infrared stimulation before blue stimulation for OSL measurement of D_7 . The test dose is kept constant throughout the SAR sequence. A corrected luminescence signal was calculated through the ratio between L_i and T_i . OSL signal was calculated using the integral of the first 0.8s of light emission with subtraction of the normalized last 10s of light emission as background. Source: (Murray and Wintle, 2000, 2003).

4 RESULTS

After the confluence with Araguaia River, the Tocantins River flows through two distinct geological provinces. The upstream reach is characterized by low grade metamorphic rocks (Neoproterozoic) consisting of phyllites, slates and metasiltites, gently dipping towards east and southeast. The downstream reach is developed over sedimentary rocks (Cretaceous), mostly arenites. The spatial distribution of this basement rocks and tectonic structures clearly control the occurrence of the Quaternary deposits from Tocantins River (Figure 2), which are better developed over the sedimentary rocks. The analysis of satellite images and DEMs allowed mapping four main geomorphic units placed in different topographic levels and with distinct morphologic characteristics: (i) alluvial plain, (ii) fluvial terraces (T1 and T2), (iii) paleo-alluvial fan (Figure 2C). The main geomorphic and sedimentologic characteristics of each are shown below. Details about small-scale morphological elements that characterized each geomorphic unit can be found in Article 1 – Submitted Journal of Maps.

The grains samples of the quartz collected are bright, signal rapidly decaying, exponential growth of dose-response curves and adequate ability to recover radiation doses. The calculated equivalent doses in the 32 samples range from 1.6 ± 0.1 to 166.1 ± 11.5 Gy, with 84% samples dispersion (OD) below 30%, commonly reported values for well-bleached sediment not affected by post-deposition mixing (Pupim et al., 2019) and only five samples showing relatively high OD values, between 35 and 60%. Dose rate Gy/ky ranged from 0.238 ± 0.015 to 3.02 ± 0.238 Gy/ky.

The OSL dating results show that the fluvial terraces (T1 and T2) and paleo-alluvial fans units were deposited from 160 ± 16.4 to 6.2 ± 0.4 ka. The deposits from the floodplain's unit showed ages from 4.8 ± 0.4 to 0.6 ± 0.04 ka (Table 2).

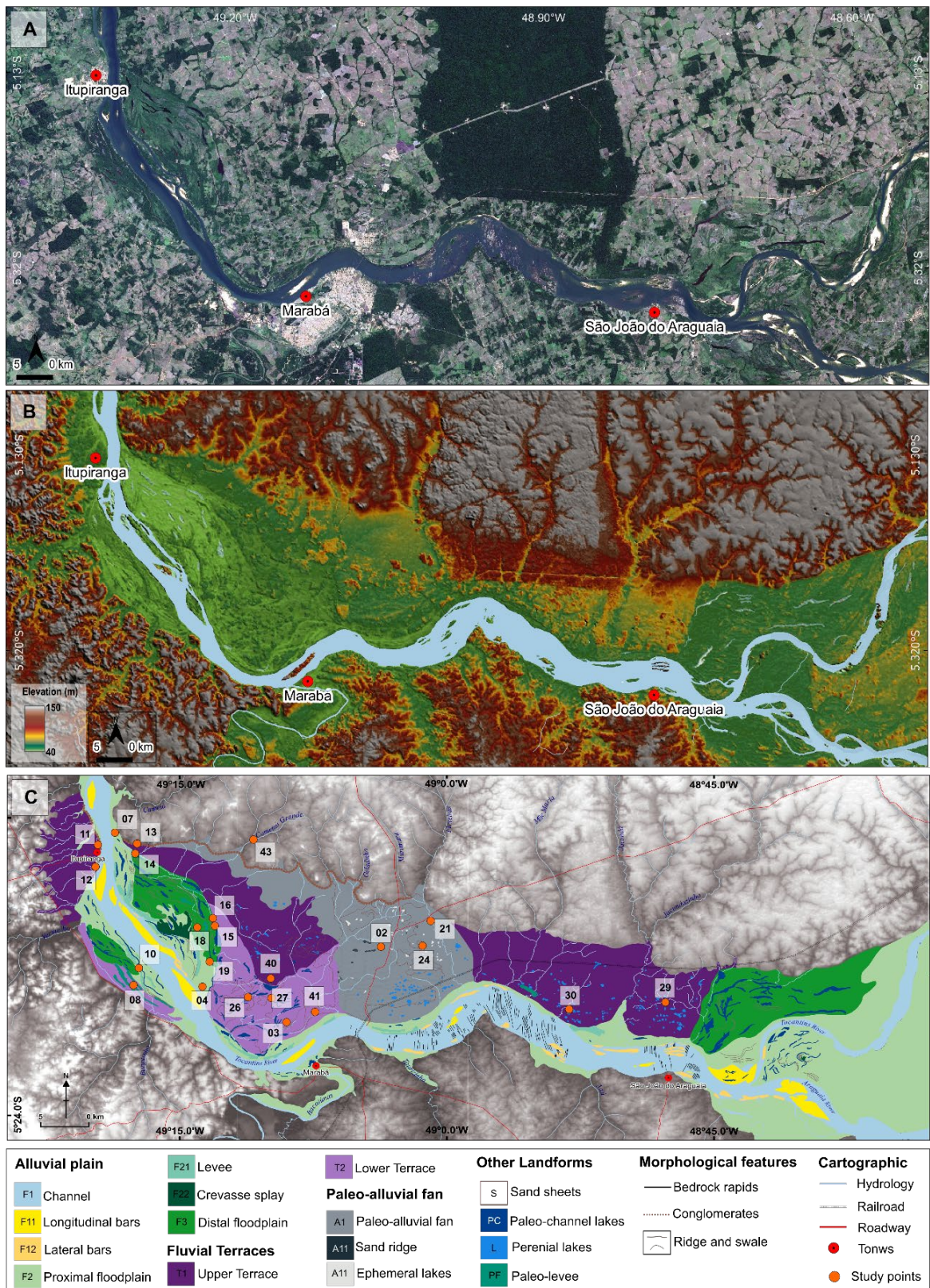


Figure 2 - Geomorphology of the middle Tocantins River. (A) Landsat imagem, composition RGB 432, 2019; (B) Digital Elevation Model (DEM) elaborated from MERIT DEM, with 3 arcsecond resolution (SRTM3 v2.1 and AW3D-30m v1); (C) Geomorphological map of the middle Tocantins River.

Table 2 - Data summary of the equivalent doses, dose rates and OSL ages. OD is the overdispersion of equivalent dose distributions.

Sample ID	Lab Code	Decimal Degree Lat /Long	Depth (m)	Dose rate (Gy/ka)	Number of aliquots*	Equivalent dose (Gy)	OD (%)	Age (years)	Geomorphological unit
MAB 04A	L0588	-5.27239/-49.2423	0.3	2.4 ± 0.1	24/24	1.5 ± 0.1	13.7	661 ± 42	F2
MAB 04B	L0589	-5.27239/-49.2423	0.7	2.4 ± 0.1	24/24	3.0 ± 0.1	5.6	1,233 ± 90	F2
MAB 10A	L1167	-5.253793/-49.28618	1.8	2.4 ± 0.1	23/24	1.6 ± 0.1	10.1	666 ± 67	F2
MAB 10B	L1168	-5.253793/-49.28618	2.1	1.6 ± 0.1	22/23	1.9 ± 0.1	22.6	1,152 ± 109	F2
MAB 12	L1170	-5.143639/-49.32603	1	2.3 ± 0.1	23/24	3.3 ± 0.0	3.3	1,391 ± 110	F2
MAB 14A	L1173	-5.137341/-49.28993	1.2	1.2 ± 0.09	24/24	4.4 ± 0.1	10.9	3,394 ± 249	F3
MAB 14B	L1174	-5.137341/-49.28993	3.7	1.5 ± 0.1	24/24	7.5 ± 0.2	10.7	4,885 ± 358	F3
MAB 15	L1175	-5.208499/-49.21710	3	1.2 ± 0.09	24/24	6.2 ± 0.1	5	4,785 ± 364	F3
MAB 16A	L1176	-5.208499/-49.21710	0.5	1.6 ± 0.1	23/24	3.9 ± 0.1	6.9	2,384 ± 199	F3
MAB 16B	L1177	-5.208499/-49.21710	3	1.5 ± 0.124	24/24	6.5 ± 0.3	22.2	4,135 ± 377	F3
MAB 18	L1178	-5.213901/-49.23044	0.6	1.2 ± 0.09	24/24	4.1 ± 0.1	13.3	3,404 ± 271	F3
MAB 19	L1179	-5.242607/-49.22004	1.25	1.3 ± 0.1	24/24	4 ± 0.1	5.8	2,976 ± 239	F3
MAB 11	L1169	-5.133029/-49.32432	3	0.5 ± 0.03	10/24	85.4 ± 6.4	22.8	149,897 ± 15,212	T1
MAB 13A	L1171	-5.116663/-49.28779	1.2	2.1 ± 0.1	24/24	5.5 ± 0.3	25	2,618 ± 242	T1
MAB 13B	L1172	-5.116663/-49.28779	1.5	3.0 ± 0.2	18/24	166.1 ± 11.5	28.5	54,847 ± 5.75	T1
MAB 29A	L1185	-5.285383/-48.79683	1.8	0.6 ± 0.04	22/24	73.6 ± 3.3	20.4	112,559 ± 8,689	T1
MAB 29B	L1186	-5.285383/-48.79683	1.2	0.7 ± 0.04	18/24	22.4 ± 1.2	22.1	31,626 ± 2,611	T1
MAB 30A	L1187	-5.299453/-48.88883	1.8	0.4 ± 0.02	23/24	48.2 ± 1.9	18.7	105,220 ± 7,439	T1
MAB 30B	L1188	-5.299453/-48.88883	1.2	0.3 ± 0.02	20/24	25.1 ± 1.4	24.3	70,602 ± 5,661	T1
MAB 40A	L1333	-5.29945/-49.16847	1.3	0.5 ± 0.03	27/36	26.3 ± 3.1	61.2	46,391 ± 6,175	T1
MAB 40B	L1334	-5.29945/-49.16847	0.75	0.5 ± 0.03	27/36	25.3 ± 2.9	59.7	45,133 ± 5,926	T1
MAB 03A	L0586	-5.31043/-49.15217	0.21	1.7 ± 0.1	24/24	18.6 ± 0.7	18.6	10,382 ± 821	T2
MAB 03B	L0587	-5.31043/-49.15217	0.96	0.4 ± 0.02	24/24	7.9 ± 0.3	16.6	16,738 ± 1,166	T2
MAB 08	L1166	-5.265488/-49.29539	2.5	1.8 ± 0.14	23/24	20.3 ± 1.1	25.5	10,776 ± 1,014	T2
MAB 26	L1182	-5.279815/-49.18118	1.25	0.7 ± 0.05	16/24	2.6 ± 0.1	17.8	3,424 ± 269	T2
MAB 27A	L1183	-5.282368/-49.15807	3	0.4 ± 0.02	24/24	13.6 ± 0.5	14.3	31,118 ± 2,138	T2
MAB 27B	L1184	-5.282368/-49.15807	1.5	0.8 ± 0.05	16/22	5.3 ± 0.2	10.7	6,255 ± 487	T2
MAB 41A	L1336	-5.29728/-49.12067	1.65	0.9 ± 0.06	21/22	85.4 ± 4.6	24.6	87,322 ± 7,418	T2/T1
MAB 41B	L1335	-5.29728/-49.12067	0.8	1.3 ± 0.09	24/24	35.6 ± 2.3	31	26,781 ± 2,616	T2
MAB 02A	L0584	-5.22796/-49.06001	0.25	0.2 ± 0.02	24/24	3.4 ± 0.3	41.6	13,668 ± 1,674	A1
MAB 02B	L0585	-5.22796/-49.06001	0.67	0.2 ± 0.01	23/24	7.4 ± 0.4	23.7	31,118 ± 2,637	A1
MAB 24A	L1180	-5.229146/-49.02164	3.6	0.4 ± 0.02	20/24	70.9 ± 6.0	36.8	159,296 ± 16,389	A1
MAB 24B	L1181	-5.229146/-49.02164	1.6	0.2 ± 0.01	18/22	30 ± 1.1	15.3	118,229 ± 8,707	A1

* Accepted/measured

4.1 Alluvial Plain

4.1.1 Channel

The studied reach of the middle Tocantins River comprises a mixed bedrock-alluvial channel. The main channel is cutting into a bedrock style in the upstream reach, with rapids and some lateral and attachment sand bars (Figure 3). The river style changes to a predominately sand rich and wide floodplain character from Marabá to Itupiranga. The geomorphic features recognized inside the channel unit are longitudinal bars, lateral bars and vegetated bars. Longitudinal bars are elongated sediment bodies in the direction of the water flow, that are not covered by vegetation.

The deposits are predominately sandy with decimetric to centimetric crossbedding sets and levels of well-selected and sub-pitched granules (Figure 4). The sediments are quartz-rich and grain size decreases from upstream to downstream. Lateral bars are sand bodies attached to rocky outcrops in the riverbed that consist in obstacles to transport of sediments. Restricted areas of wider bars can present cover vegetation. These deposits are composed of gravels in the base and coarse sand in the top (Figure 4D). Vegetated bars are associated with large longitudinal bars, which the continuous deposition builds up a relatively stable and high-altitude landform. This condition keeps the surface above seasonal inundation level for longer times and support the development of forest vegetation.

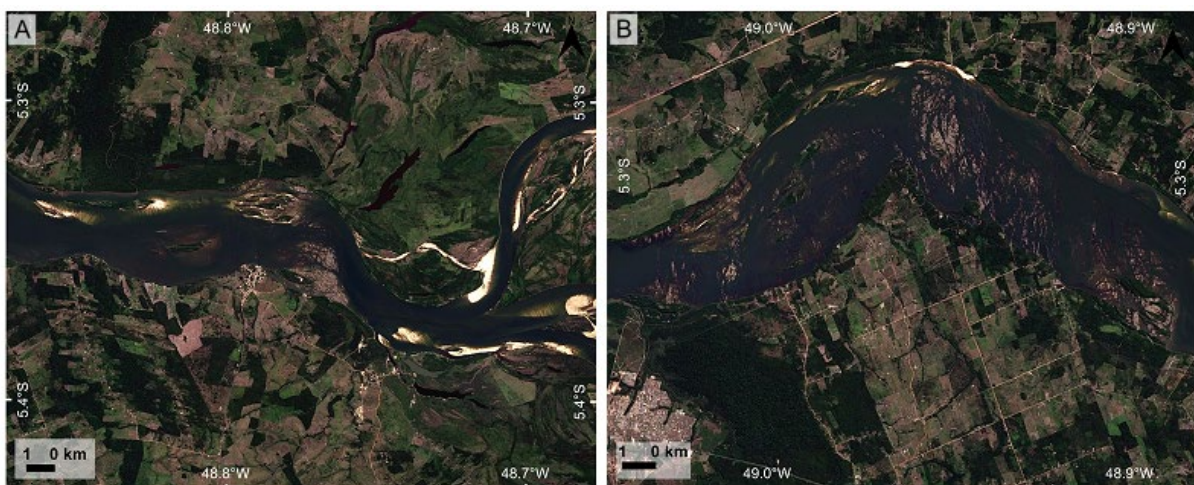


Figure 3 - Surface aspects of the fluvial channels in the study area. (A) Confluence of the Tocantins and Araguaia Rivers, with rapids and lateral and attachment sand bars; (B) Rapids developed over metamorphic rocks of the Couto Magalhães Formation (Image Landsat-8+Pan RGB 432, true color, 2017).

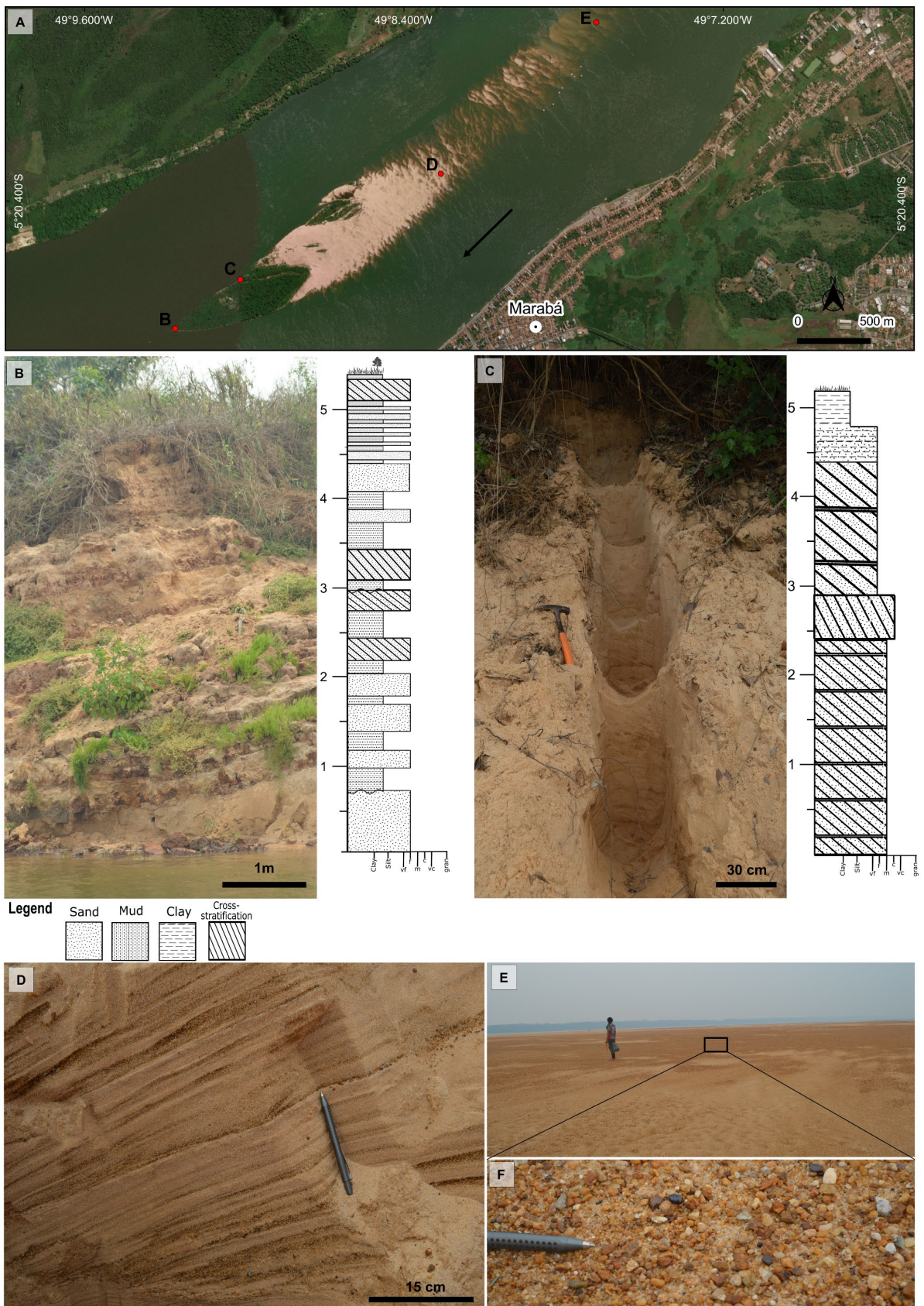


Figure 4 - Characteristic of the geomorphologic unit Channel. (A) Longitudinal bar (Esri's World Imagery, updated: Aug 8, 2019); (B) and (C) Sedimentary profiles in the downstream and lateral portions of the bar; (D) Set of cross-stratified sand with levels of granules; (E) Bar top with lag of granules and pebbles (F).

4.1.2 Floodplain

Floodplains were recognized in both margins of the Tocantins River, yet the plain of the right margin is broader and more complex in terms of landforms, with the presence of numerous lakes, paleo-channels, swamp areas, levees and crevasse splays. The terrain is almost flat, with local relief in which the highest elevations vary from 84 to 79 meters above sea level (m.a.s.l.) and the lowest from 78 to 66 m.a.s.l.. These are depositional areas with accumulation of mud and sand due to seasonal inundation of the Tocantins River. The floodplains were divided in proximal floodplain and distal floodplain.

Distal floodplain, is the lowest area of this geomorphic unit, with elevation from 66 to 78 m.a.s.l.. It corresponds to a flat surface with large and smooth depressions composed of thin layers of mud and fine sands (Fsm, Sh and Sm) (Table 3). This region is filled by water and suspended load during floods of the Tocantins River, that occur from December to May. Perennial lakes and paleo-channels, ridge and swale are diagnostic features of this geomorphic unit, but they also occur in proximal floodplains and younger terraces.

Proximal floodplain are periodically flooded terrains immediately adjacent to the Tocantins River. It has elongated geometry and parallel to the main channel, changes in width are controlled by marginal bedrocks and tectonic structures. Sedimentation in swampy areas are dominated by mud, but fine sands are not rare in other sub-environments that compose the plain as levees, paleo-levees, and crevasse splays (Figure 5). Distal Floodplain is markedly distinct from the Proximal floodplain in geomorphology and geochronology, witch all OSL ages were from 2.3 ± 0.2 to 4.8 ± 0.4 ka and the Proximal floodplain shows OSL ages from 0.6 ± 0.04 to 1.2 ± 0.1 ka (Table 2).

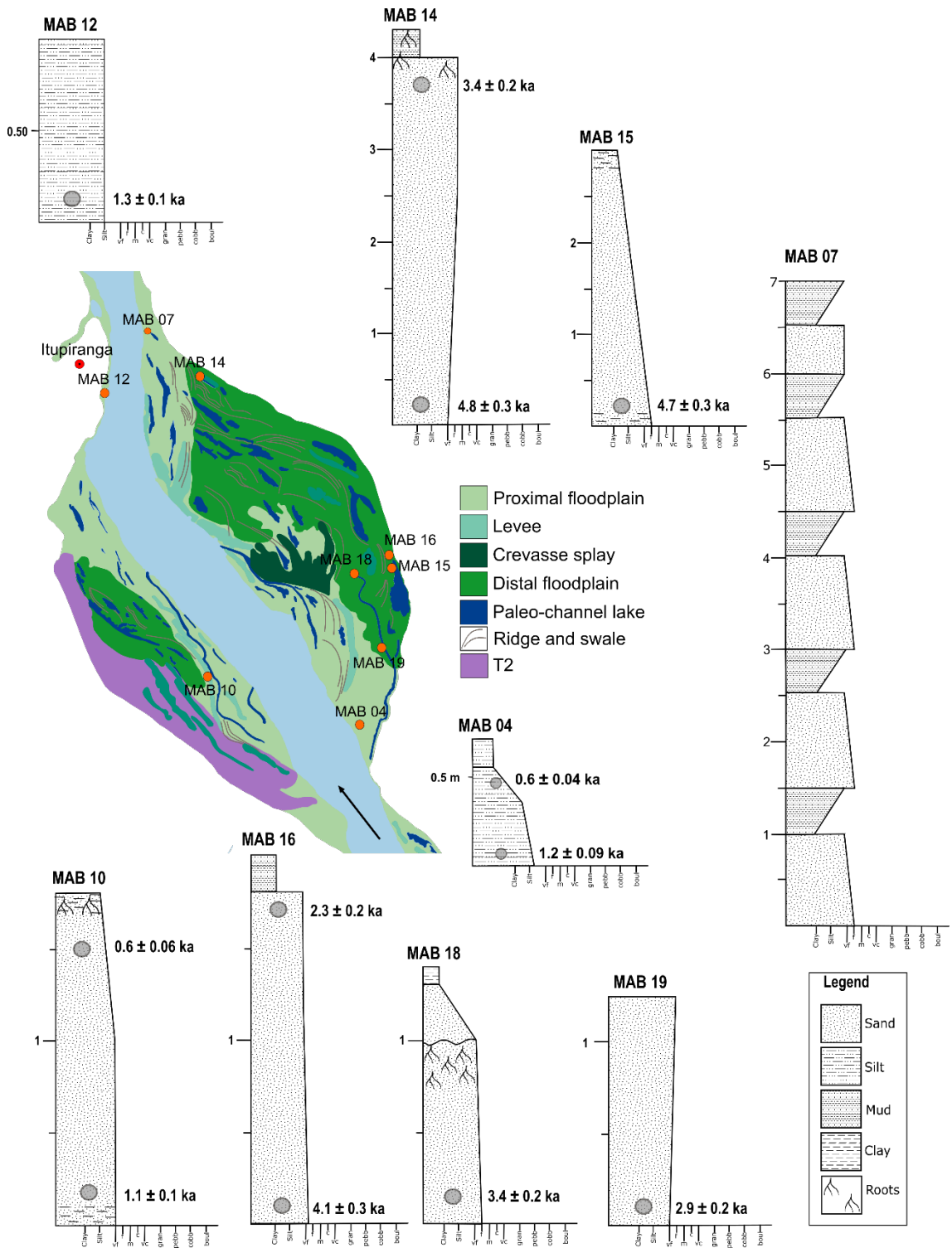


Figure 5 - Sedimentary sections described in the Floodplain units.

4.2 Fluvial Terraces

The Upper Terrace (T1) is related to fluvial deposits between 43 and 66 m above the Tocantins River channel (105-110 m.a.s.l.). The surface is almost flat with low drainage density sculpted by narrow and shallow valleys from modern streams. Upper terraces are characterized by shallow and ephemeral lakes and poor preserved paleo-levees; the occurrence of conglomerate layer at the base of the deposits; the lateral contacts between T1 deposits and Neoproterozoic basement are represented to linear features, which are coincident with local streams as Flexeiras and Taurizinho creeks (Figure 2 – Chapter 5).

Three sedimentary units were described in the T1 geomorphic unit. The Lower Unit (Fsm) with an average thickness of 40 cm is characterized by a mottled kaolinitic layer and iron oxide nodules, incipient stratification, with wavy top marked by sporadic lithoclasts ranging from pebble to granules of igneous, sedimentary and metamorphic rocks (Figure 6C). The intermediate Unit includes conglomerates (Gcm, Gmm and Gh) layers of around 1 meter thick but can reach up to 3 meters (Figure 6 D and E). At the base of this unit, occur Gcm facies, which consists of a massive deposit of polymitic conglomerate. Grain size varies from granules to blocks composed of sandstone, gneiss, quartzite, granitic, volcanic and metamorphic rocks. A systematic count made of 400 clasts larger than 3 cm show a contribution from rocks granite (46%), quartizite (9.7%), sandstone (9.7%) and quartz vein/others (25.7%). Paleocurrent data (49 measurements) from block imbrication indicate transport components for NW and NE. Facies Gmm, incipient, tabular geometry, base wavy top in contact with Gh facies, that consists rounded to subrounded, lenticular geometric, undulating base, predominantly granules, pebbles and boulders up to 15 cm length. The upper boundary of this facies corresponds to a wavy surface in contact with the Upper Unit, Sm facies, massive moderately sorted, medium-grained sand composed mainly of quartz and subordinate feldspar in gradual contact with facies Fr with roots and bioturbation. Two OSL ages were recorded in the intermediate unit: 1) Basal facies of the unit, Gcm facies, with OSL age of 150 ± 15.2 ka at 60 m.a.s.l and an age of 54.8 ± 5.7 ka corresponding to facies Gh. In the Upper Unit, 4 samples were dated from Sm facies and OSL ages ranged from 31.6 ± 2.6 to 112.5 ± 8.6 ka, and one sample from Fr facies aged 2.6 ± 0.2 ka (Table 2).

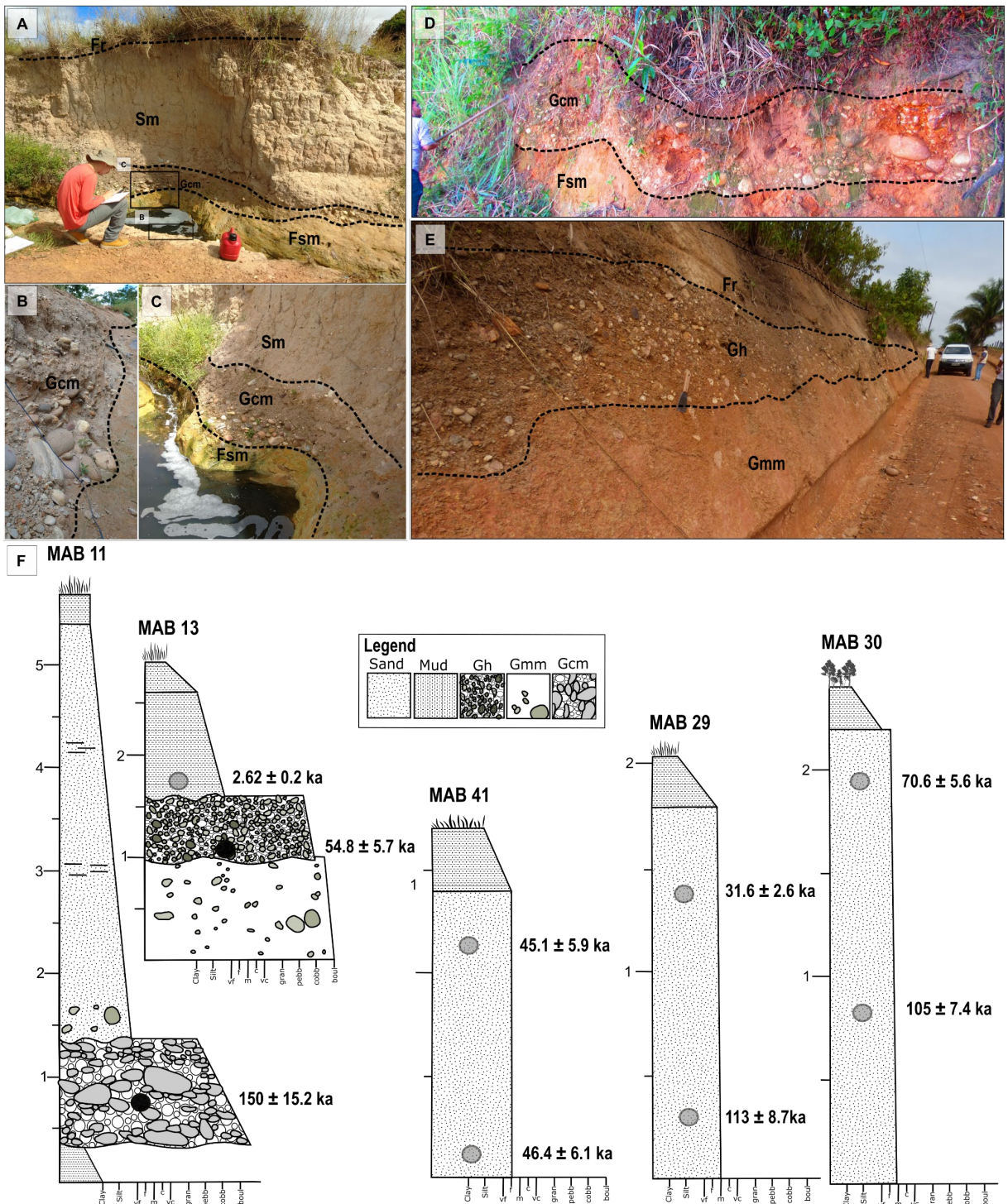


Figure 6 - Sedimentary facies of the Upper Terraces (T1). (A) General view and (B) detail facies Gcm association drainage; (C) Detail contact between Facies Fsm, Gcm and Sm; (D) Conglomerate horizon (Facies Gcm), clasts up 20 cm. (E) General view in facies Gh lenticular geometry; (F) Sedimentary profiles described in T1.

Lower Terraces (T2) are between 27 and 36 m above the river water level (84 and 86 m.a.s.l.), surface is slightly dipping towards the main channel. This unit is marked by the high density of dry and wet paleo-channels that remain the lakes on the

modern floodplain and younger terraces (Figure 7A). These levels of terraces are susceptible to exceptional floods, values above 14 m above normal level (MMA, 2006).

Two sedimentary facies were described: 1) basal facies (Sm) composed of fine to medium sand with sporadic occurrence of granules, yellowish to whitish, well selected and rounded in gradual contact with (Fr) (Table 3), predominantly on top composed of silt with gray to grayish clay (mud or incipient soil) (Figure 07B). The OSL ages for this unit were obtained from Sm facies, with the main ages varying from 10.4 ± 0.8 to 31.1 ± 2.1 ka (Table 2). Two samples from the upper part of these deposits showed OSL ages of 3.4 ± 0.2 and 6.2 ± 0.5 ka, suggesting reworking processes. Moreover, one sample presented an older age of 87.3 ± 7.4 ka.

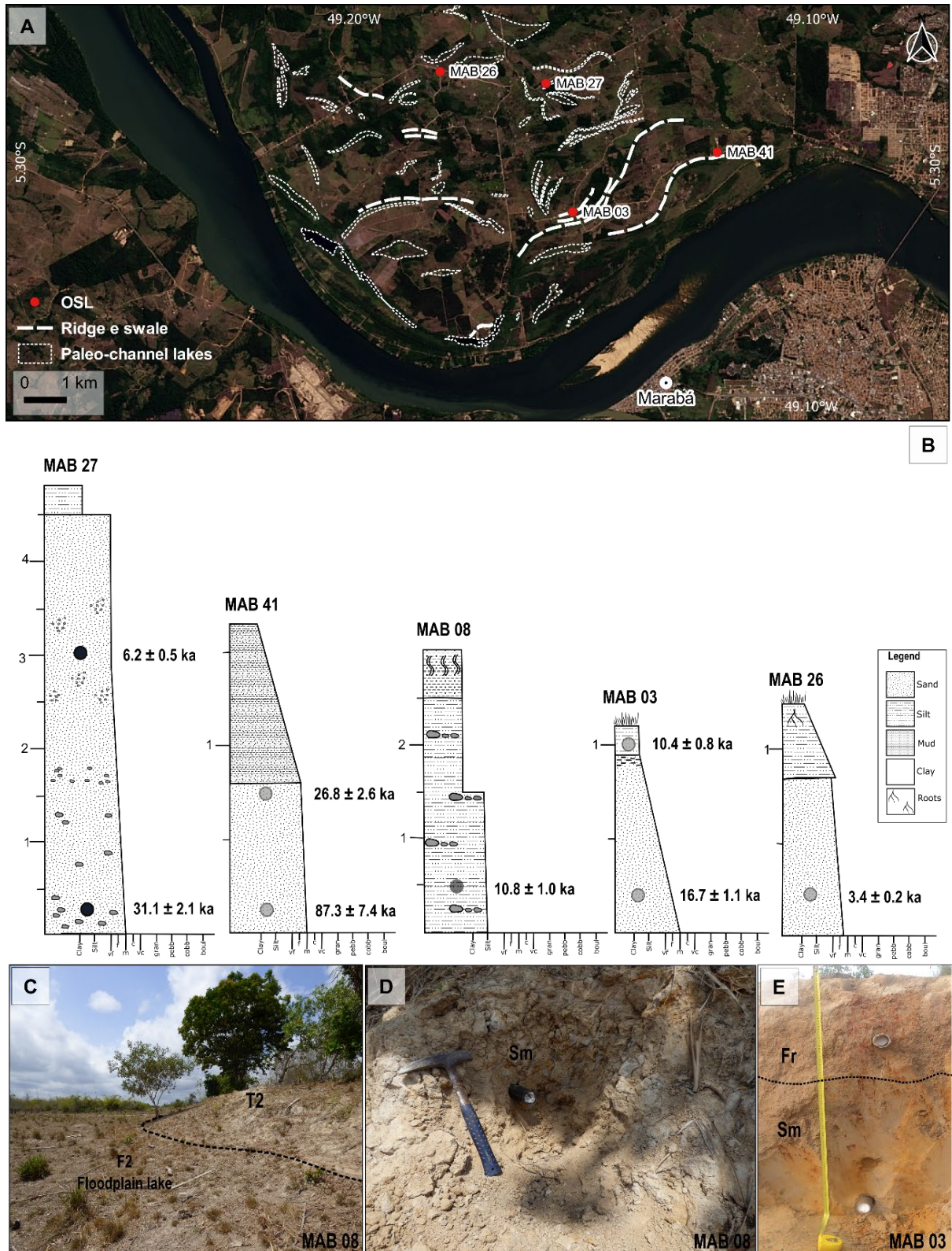


Figure 7 - Geomorphic features and sedimentology of the Lower Terraces (T2). (A) Unit T2 contains preserved geomorphological features such paleo-channel lakes and ridge e swale highlighted in white (Landsat-8+Pan RGB 432, true color, 2019); (B) Sedimentary profiles described in T2; (C) Inferred contact between T2 and floodplain, in detail (D) facies Sm; (D) Facies Sm and Fr.

Table 3 - Summary of lithofacies characteristics of the Late Quaternary deposits in middle Tocantins River, with corresponding interpretation of sedimentary processes.

Code	Facies	Description	Sedimentary process
Gmm	Matrix-supported massive gravel	Matrix-supported, reddish, massive conglomerate in beds to meters 1 to 3m thick with wavy top. Clasts range from 5 cm to 15 cm in diameter, and consist of granite, quartz, quartzite, gneiss.	Plastic debris flow, viscous flow, high internal cohesion
Gcm	Clast-supported massive gravel	Clast-supported, massive conglomerate in beds to meters thick with wavy top, tabular geometry. Subangular to subrounded, very poorly sorted. Clasts range from 1 mm to 30 cm in diameter, and consist of granite, quartz, quartzite, gneiss, BIF.	Turbulent flow, pseudoplastic debris flow
Gh	Clast-supported massive gravel, incipient bedding	Clast-supported, massive conglomerate in beds to decimeters thick, lenticular. Clasts range from 3 cm to 20 cm in diameter, and consist of quartz, quartzite, BIF.	Longitudinal bed shapes, lags
Sh	Sand very fine	Very fine-grained, yellowish, sandstone forms bodies that are up to 0.30 m thick, is well sorted with rounded grains. Interbedded with facies Fl. Sedimentary structures include flat lamination.	Plane-bed flow (critical flow)
Ss	Sand fine to medium	Fine to medium grained, grayish to whitish, sandstones with some granules and small pebbles. Filling wide area.	Scour fills
Sm	Sand fine to coarse, may be pebbles	Fine to coarse grained, yellowish, moderately sorted, sandstones with some pebbles. Massive or indistinct lamination.	Hyperconcentrated flow deposits, fluidization or intense bioturbation
Fl	Sand, mud	Mud and very fine-grained sand, yellowish. Interlaminations with facies Sh. The thickness bodies from 0.3 m more than 0.7m.	Overbank, abandoned channel, or waning flood deposits.
Fsm	Silt, mud	Silt and mud, grayish to reddish, mottled red, with iron oxide nodules and kaolinitic, massive and very compact. Bodies that are up to 0.40 m thick.	Backswamp or abandoned channel deposits.
Fr	Mud, massive with roots and bioturbation	Mud massive, grayish to yellowish, with roots and bioturbation.	Incipiente soil
C	Soil with carbonized matter organic	Fine to medium grained, dark brownish, sandstones with some granules, thin roots and branches. Abrupt contact with facies Ss.	Vegetated swamps deposits

4.3 Paleo-alluvial fan

The main paleo-alluvial fan occupies an area around 188 km² (Figure 8A) while the entire mapped paleo-alluvial fan system occupies 237 km². The paleo-alluvial fans are made up of unconsolidated sands accumulated in a relatively high elevation (90 - 100 m.a.s.l.). The present morphology shows a convex-up transversal profile and several ephemeral lakes. Those landforms have been dissected by a poorly density dendritic drainage network, with small streams incised in narrow and shallow valleys. The deposits comprise a well-rounded and well-sorted quartz-rich sands, and sporadic occurrence of sub-rounded granules of quartz. Withe sand layers are interbedded with organic-rich layers (5 to 10 cm) of the facies C, at 0.6, 1.3 and 1.8 m depth (Figure 08D). These organic-rich layers have homogeneous dark brown color, essentially composed of medium sand with few contents of clay and fine sand (Figure 8H). It resembles small fragments of roots and charcoal. Sedimentary reworking appears to be active in this units, promoting the formation of thin sand sheets due to eolian and / or sheet flow processes. Sand sheets are main composed of medium sands and they are not exclusive of the paleo-alluvial fan, also occurring in the surrounding fluvial terraces (T2). OSL dating in two sedimentary profiles shows ages from 160 ± 16.4 to 13.7 ± 1.6 ka (Table 2; Figure 8D).

Most of the paleo-alluvial fan surface is covered by open vegetation, that comprise a mosaic of grassland, shrubs and vegetated islands. Vegetation Vegetated islands are located preferably in the central portion of the unit, have a microtopography (1 m higher) compared to the surrounding sandy flat area. Seventeen features associated with forest islands were identified, with area ranging from 1 to 10 hectares (Figure 8B and C). The dominant vegetation is classified as forested campinaranas (IBGE, 2012). This phyto-physiognomy has an abrupt transition to grassy and shrubby grassland. The sedimentary deposit that support campinarana are composed of well-selected and well-rounded quartz sand with occurrences of gray mud (Figure 8G).

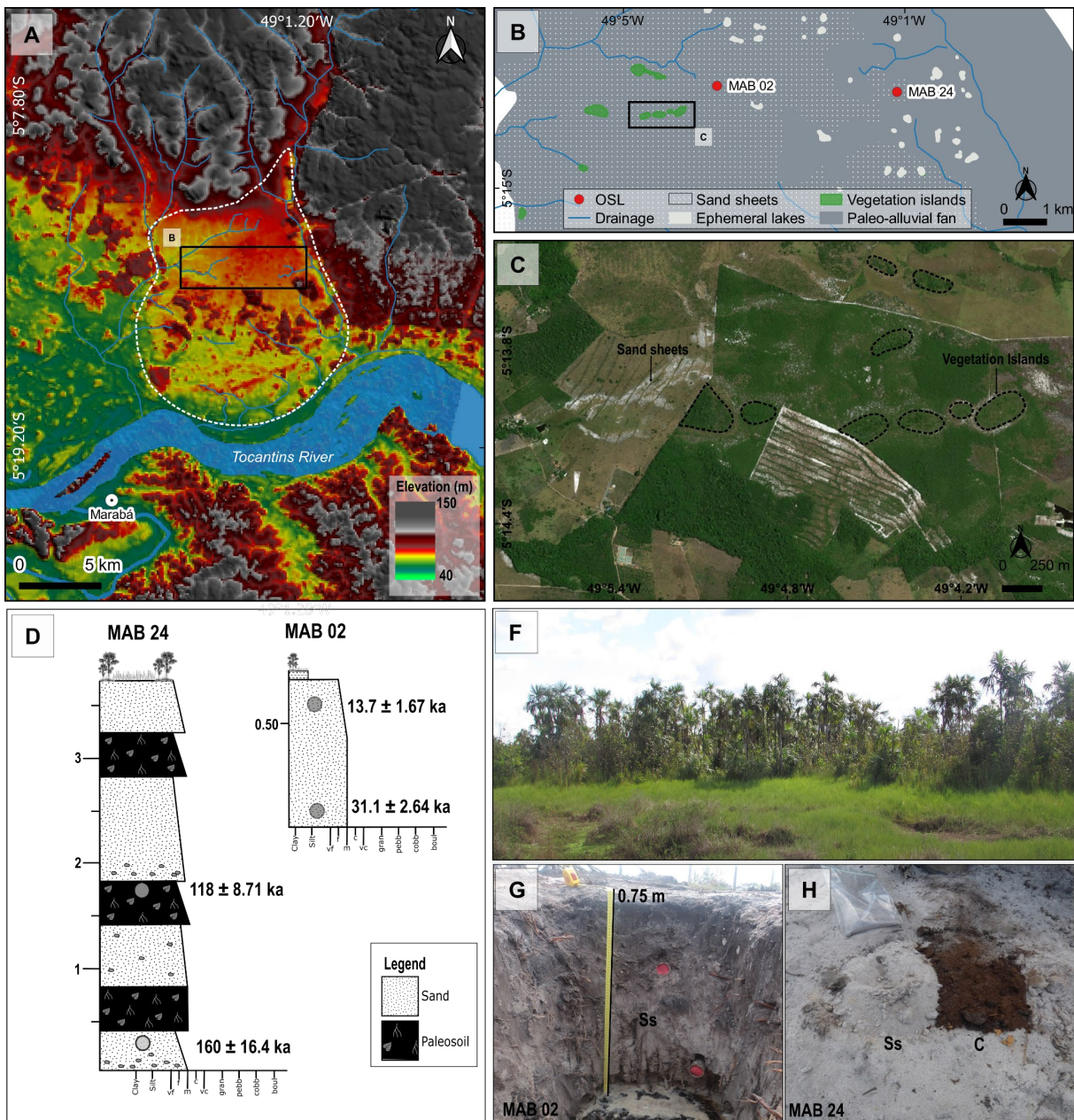


Figure 8 - Features of the geomorphologic unit Paleo-alluvial fan (A1). (A) DEM highlights the contrasting geomorphic with the fluvial terraces and floodplain; (B) Morphological characterization of the patches of open vegetation identified; (C) General view of the vegetation islands, line black. Area consolidated by human occupation and agricultural activities (ESRI's World Imagery, Updated: November, 2019); (D) Sedimentary profiles described in Paleo-alluvial fan (A1) in (G) Profile with 0.75m, features spodosol and (H) Detail of facies C e Ss with sampling for OSL dating; (F) Partial view of vegetation with shrubs.

5 DISCUSSION

5.1 Late Quaternary Evolution of the Tocantins River

The alluvial plain of the middle Tocantins River shows a wide variety of fluvial landforms, including floodplains, two terrace levels and a complexity of paleo-alluvial fans. The results from the morphosedimentary analysis integrated with OSL dating allow us to interpret that the landscape is constantly changing during the Late Quaternary (from 160 ka to present), with three main phases of deposition and two phases of erosion: 1) the first depositional phase that forms the Upper Terrace (T1) and part of the paleo-alluvial fans (160 to 32 ka); 2) incision event take place around 31 ka, allowing the abandonment of T1; 3) second depositional phase, with the deposition of the Lower Terrace (T2) and (re)activation of the paleo-alluvial fans (31 to 6 ka); 4) incision event from 6 to 5 ka, allowing the abandonment of T2 and lowering the local base level until its present position; 5) the modern floodplain has been built-up since 5 ka to the present, with deposition of sediments due frequent lateral channel migration of the Tocantins River. The interpretation regarding the evolution of middle Tocantins River are summarized in Figure 10.

The lithofacies described in the Upper Terrace (T1), mostly medium sands and occurrence of conglomerates, and the activity of (paleo)alluvial fans suggest a fluvial system with high bed load and high stream power by extreme water discharge events (Bull, 1991) from 112.6 ± 8.9 to 31.6 ± 2.6 ka. The massive medium sand sediments, without evidence of lateral discontinuity suggest sedimentation of channel bars. Whereas, the upper units can be related to the progressively decreasing of the flow energy and the deposition of finer sediments in floodplain environments. This fluvial dynamic provided conditions to deposition of sediments during long period, with no significant changes in the local base level (riverbed incision). Even though incisions would occur, they were shallow and followed by depositional period that covered all space created. These conditions are like the modern Tocantins River. Widespread aggradation dominated the period from 250 to 45 ka, which was followed by a stage of intensified incision punctuated by events of terrace aggradation inside the incised valleys after 45 ka. T1 deposits also exhibit conglomeratic sediments (Figure 6) that were not found in any other sedimentary units along the studied alluvial plain. The origin of theses conglomerates is not clear at all, but our sedimentary and paleocurrent analysis allow us to interpret that theses sediments appear to be deposited by small

tributaries of the Tocantins River. The geometry and internal architecture of conglomerate layers indicate that they were deposited as gravel bars (Figure 06 A, B and E). The preferred orientation of clasts imbrication indicates a paleo-flow direction NW-SE and NNW-SSE. This direction is like small streams that flow to Tocantins River in the present. Moreover, similar coarse sediments can be found in the nowadays tributaries (Figure 9), which are reworked only during torrential floods that increase substantially the stream power. The abrupt discontinuity between conglomerate facies and muddy layers below also suggest an episodic event to the deposition of the coarse sediments. Coarse-grained terraces from different localities of Amazonia are not necessarily time equivalent and does (Dumont et al., 1991; Latrubesse and Kalicki, 2002; Rigsby et al., 2009; Rossetti et al., 2014) not present characteristics similar to those described in this paper. Changes in the paleo-hydraulic conditions are interpreted to take place around 31 ka, which resulted in fluvial incision leading to the abandonment of the T1. This incision eroded the valley of the Tocantins River to at least 23 m deeper the T1, creating accommodation space to deposition of sediments that constitute the Lower Terrace (T2).

The interval between 31.6 and 25.3 ka are marked por downcutting terrace Madeira River (Rossetti et al., 2014). The depositional phase that built-up the T2 appears to have occurred from 31.1 ± 2.1 to 6.2 ± 0.4 ka. The predominance of deposits composed by medium sands in the base and muddy layers in the top and the occurrence of the planform elements as sinuous paleo-channels and oxbow lakes allow us to interpret a sinuous alluvial channel that migrates laterally. The lithofacies association suggest paleo-hydrological condition like that operate during the deposition of the T1 (the upper units), with a system with high capacity to transport sands in the bedload. This OSL age agrees with the OSL age interval of 30.9 ± 8 ka and 19.1 ± 6.3 ka furnished by Gonçalves et al. (2016) for their intermediate terrace in Central Amazonia. An extremely older OSL age of 87.3 ± 7.4 ka was reported to deposits related to the area of the T2 (MAB-41; Table 2), in sediments buried at 1,65 m deeper and near the boundary of T2 and paleo-alluvial fan unit. Because the depth and geomorphic position, we interpret that this older age can be related to sediments of the paleo-alluvial fan or T1, which were buried during the deposition of the T2. Younger age in shallow deposits (3.4 ± 0.3 ka) indicate sedimentary reworking. These shallow deposits can be formed by several surface process well reported in alluvial plains, including local erosion, sheet flow, episodic floods and eolian activity (Oliveira et al.,

2019; Pupim et al., 2017). Furthermore, T2 are not frequently flooded, but it may occur in high magnitude precipitation events, as in the historical flood of 1980 (MMA, 2006). The last major incision period occurred around 6 to 5 ka, which culminated in the abandonment of T2 and the establishment of the modern floodplain since 4.8 ± 0.4 ka. However, geomorphological analysis and OSL dating indicate at least two stages of sediment deposition. The OSL ages from Distal floodplain record the first stage from 4.8 ± 0.4 to 2.4 ± 0.2 ka and sediments from Proximal floodplain the second stage from 1.2 ± 0.1 ka to present. The gap of OSL ages between 2.4 and 1.2 ka are interpreted as a period of fluvial instability, with rapid channels lateral migration and erosion of the riverbanks. The main evidence that support this interpretation is the truncation/erosion of paleo-channels from the Distal floodplain units and the superposition by forms from Proximal floodplain (Figure 5). The presence of several scroll bars reinforces the interpretation of the frequent lateral channel migration of the Tocantins river. The unpaired features of terraces and plains indicate that a preferential channel migration from the right to the left margin. Moreover, the diversity of environments in the modern floodplain plays a key role in ecological processes (Stevaux et al., 2013). This diversity is supported by the flood seasonality and frequent geomorphic changes due to channel lateral migration, including the perennial and ephemeral lakes, paleo-channels connected with the main channel, and alluvial ridges-and-swale that support non flooded organisms during wet season.

Sedimentological and chronological data indicate that the Paleo-alluvial fan unit were formed by long term depositional phases simultaneously with both terrace levels (Table 2). Regardless of the limit of our geochronological control, the spatial distribution of the OSL ages suggest that the main depositional site change from east (MAB-24) to west (MAB-02) during the Late Pleistocene. The OSL age of 13.7 ± 1.7 ka obtained in the upper section of the profile MAB-02 indicate that the maximum age to the development of the open vegetation landcover. Another evidence of depositional change was observed in the sequence of white sands layers and paleosols horizons in MAB-24 (Figure 8D), suggesting at least three cycles of landscape instability (sedimentation pulses) and landscape stability (soil formation). Present OSL ages only allow us to interpret two instability periods around 160 ± 16.4 and 118 ± 8.7 , 31.1 ka, intercalated by to stability periods without absolute ages.

Morphological elements and the radial pattern of the unit suggest that the alluvial fans were formed by the interaction between tributary channels and the axial main river

(Tocantins River), which gives rise to a toe-cutting terraces (Leeder and Mack, 2001). The alluvial fans were fed by tributary channels that evolve by avulsions and the deposition alluvial lobes that prograde over the paleo floodplain of the axial river. Meanwhile, lateral migration of the axial river leads the erosion of the distal portion of the alluvial fans, and the vertical incision promote the abandonment of the alluvial fan. Similar landforms were observed in the Paraná River floodplain, where several modern tributary rivers are built-up alluvial fans over the main river floodplain (Oliveira et al., 2019).



Figure 9 - Gravel bars from the tributary drainage that filled the paleo-alluvial fans. (A) General view of the gravel bars in Flexeiras River; (B) General view in small stream without denomination. Lithic fragments are from sandstones, banded iron formation, gneiss, quartzite, granitic, volcanic.

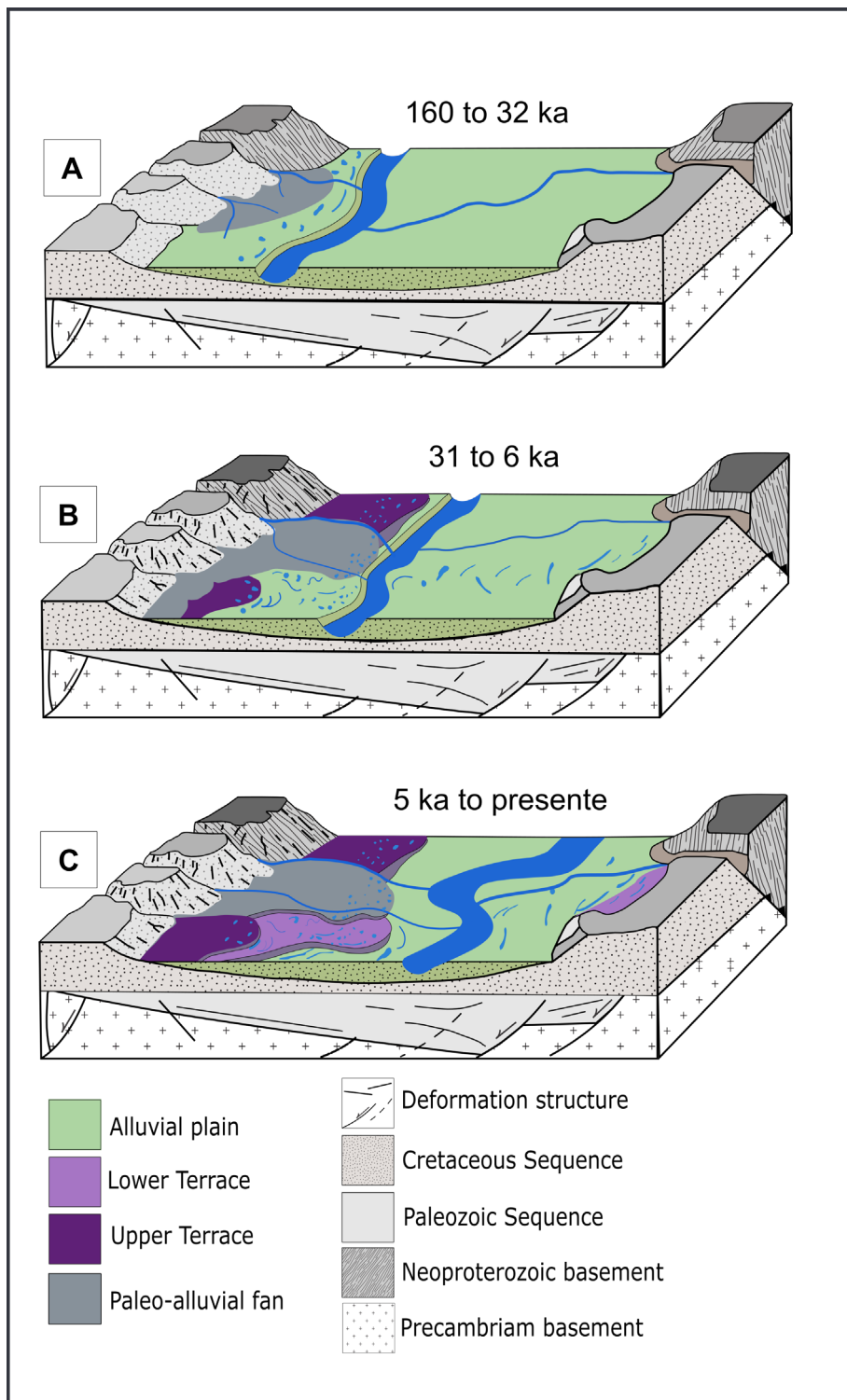


Figure 10 - Schematic diagrams illustrating the geomorphological evolution of the middle Tocantins River during the Late Quaternary. (A) During the Mid-Late Pleistocene (160 – 32 ka), the landscape was dominated by floodplain with contribution of tributaries rivers causing aggradation of the main valley. A regional incision cause the abandonment of the T1 around 31 ka; (B) The deposition of the T2 occurred from 31 and 6 ka, followed by another incision around 6-5 ka; (C) The modern landscape have been formed since 5 ka.

5.2 Climate and Tectonic Controls on the Fluvial History

The investigation about the Quaternary history of the Amazonian rivers have suggested that external factors are the main drivers of the fluvial changes and landscape evolution (Mertes and Dunne, 2007). However, there is a fruitful debate about the role of the climate, sea level and tectonic activity. Several authors have suggested that the main depositional and erosive phases were controlled by regional climate changes that lead to variation in upstream water discharge or sediment supply (e.g. Latrubblesse, 2003; Rigsby et al., 2009) or through downstream base-level fall (Irion et al., 2009). In contrast, other authors advocated that modern tectonic activity is the most important factor that control the landscape evolution (Costa et al., 2001; Rossetti et al., 2017). Our chronological framework allows us to investigate the influence of theses external forcing in the evolution of the middle Tocantins River during the Late Quaternary.

The OSL chronology of the depositional landforms of the middle Tocantins River indicate that climate changes were the main driver of the fluvial dynamic and landscape evolution since 160 ka. T1 and paleo-alluvial fan deposits indicate that a phase of deposition occurred during 160 to 32 ka. Despite dating spread from early MIS 6 to late MIS 3 (Marine Isotope Stage), most of the dating suggest predominance of deposition during MIS 5 (130 - 71 ka) and MIS 3 (57 - 29 ka) (time scale from Lisiecki and Raymo, 2005), thus during the Late Pleistocene. The sedimentology of the massive medium sand deposits, without evidence of lateral discontinuity of the T1 deposits and the activity of (paleo)alluvial fans suggest a fluvial system with high bed load and high stream power. In the tropical lowlands, rivers with such fluvial dynamic are frequently associated with boundary conditions of sparse vegetation cover and precipitation with high seasonality (Thomas, 2008). Alluvial deposits with similar characteristics and ages from 70.5 ± 8.0 and 34.0 ± 4.6 ka were reported in the Bananal Island, upper Araguaia River (Valente and Latrubblesse, 2012). Moreover, this depositional phase is also correlated with the formation of the Upper Terraces in the central and western Amazonia occurred from 250 to 45 ka (Pupim et al., 2019). This regional correlation leads the hypothesis that environmental conditions could be uniform throughout the Tocantins River Watershed, and maybe across a broad area of Amazon Basin.

Despite of the scarcity of paleoclimate records that dating back 50 ka, our data from the T1 and paleo-alluvial fan deposits agree with environmental conditions

interpreted from pollen and oxygen isotope ($\delta^{18}\text{O}$) records of speleothems from regional lowlands (Figure 12). $\delta^{18}\text{O}$ records of speleothems from the Paraíso Cave (eastern Amazonia) show strong millennial-scale variability in precipitation during the MIS 3, as a manifestation of Heinrich and Dansgaard–Oeschger (D/O) climate events (Wang et al., 2017).

However, even with variability in precipitation, the interpretation of pollen records suggest that environmental conditions were drier during MIS 3 than the present, with expansion of savanna vegetation in the transitional areas between Cerrado and Amazon biome (Figure 12). In core areas of the Amazon forest, most of the pollen records show that the forest cover appears to have no significant changes during the MIS 3 (Figure 12).

Vegetation changes in Tocantins River Watershed resulting from climatic variations may have influenced water and/or sediment supply and triggered the degradational and aggradation phases. The studied lakes on the Carajás mountain, at 700-800m elevation lies about 150 km south of study area. O record is about 60,000 ^{14}C yr B.P. shows several alternating periods dominated by arboreal and herbaceous savanna taxa. This has been interpreted as alternations between forest and edaphic savanna in the surrounding region (Absy et al., 1991). Savana extension, reflecting dry episodes, occurred at a 60,000 and ca 40,000 ^{14}C yrs B.P. (Figure 12). Core from lake Lagoa da Confusão, upper Araguaia River, inserted in the cerrado biome, during the period dated between 60,300 and 51,700 ^{14}C yr B.P. an landscape dominated by cerrado of the campo limpo type, a grass savanna with rare woody savanna shrubs and trees (Behling, 2002). The palynological records inserted in the Amazonia-Cerrado ecotone during construction of the Upper Terrace follow a trend of dry conditions with reduced tree vegetation and high supply sediments.

The first degradational phase (fluvial incision) around 32-31 ka correspond to the transition from MIS 3 to MIS 2 (Figure 12). Although our data do not support a definitive correlation between fluvial process and paleoclimate, we interpret that the river incision probably results from the disruption of the previous environmental conditions that allow the increase of the proportion between water discharge and sediment supply (Bull, 1991; Tofelde et al., 2019). This first degradational phase appears to synchronous with incisions reported in western and central Amazonian alluvial deposits, as Madeira and Solimões Rivers (Rossetti et al., 2015; Gonçalves Júnior et al., 2016). The period from

32,000 to cad 20,000 ^{14}C yr B.P. is interpreted as having wetter climatic conditions and lower temperatures than today.

The OSL ages from T2 deposits suggest that sediment supply and/or accommodation space were limited during the MIS 2, specially during the LGM. The absence of fluvial deposits dating from LGM is well documented across Amazon and central Brazil (Hammen and Hooghiemstra, 2000; Irion and Kalliola, 2010; Sant'Anna et al., 2017), but it supports contrasting interpretations. Latrubesse, (2003) interpreted the LGM gap in Brazilian Amazon rivers as a result of a dry period with limited water discharge and reduced sediment supply. In the Pantanal wetland (Central Brazil), the occurrence of paleo-channels with morphology that becomes narrower and straighter downstream suggests discharge loss due to high percolation and evapotranspiration, implying a relatively low effective precipitation and reduced vegetation cover in the depositional site (Assine et al., 2014; Pupim, et al., 2017). In contrast, Rigsby et al., (2009) advocate that the lack of fluvial deposits dating back to LGM in Madre de Dios River was due to high water discharge that allow the transport and evacuation of the sediments from river valleys.

The environmental conditions during the LGM in Amazon is still under debate. Our data make it possible to interpret that there was no sediment deposition / preservation during LGM (14 to 25 ka) due to a balance in the water discharge/sediment supply. This is interpreted as result of drier conditions in the Tocantins River Watershed (Cerrado / eastern Amazon) that decreased both sediment production and runoff.

The decrease in temperature during the LGM in the Amazon are supported by (Colinvaux et al., 1996; Bush et al., 2001) reduction in arboreal vegetation (e.g. (Anhuf et al., 2006) due to increased aridity and decreased temperature of landmasses (Figure 12). The dominance of hematite in fluvial deposits in the region of the junction of the Solimões-Amazon and Negro Rivers dated from 25.3 to 17.7 ka points to a dry phase in the center of the Amazon plain, during the LGM (Sant'Anna et al., 2017). As in the Amazon, the LGM is also marked in the Cerrado (Ferraz-Vicentini and Labouriau-Salgado, 1996; Barberi et al., 2000; Behling, 2002; De Oliveira et al., 2019)

Sedimentary gaps for the full glacial period, apparently are common in the tropical South American lowland cores (Ledru et al., 1998) and point to widespread dry climatic conditions.

The cluster of OSL ages from 16 to 6 ka suggests that the most significant depositional period of the T2 occurred during the last deglaciation and early Holocene (Figure 12). The environmental conditions reconstructed through pollen record interpreted for the Pleistocene-Holocene transition in Cerrado and eastern Amazonia biomes is a highly controversial issue. Most of these records indicate the predominance of savanna vegetation in the central Brazil (basin headwaters) (Barberi et al., 2000; De Oliveira et al., 2019). In contrast, a shift from savanna to forest cover around the Pleistocene-Holocene transition is documented in several pollen records from lakes across eastern Amazonia lowlands and lakes at the Carajás plateau in easternmost Amazonia (Figure 12). Speleothems records from Paraíso Cave show a decrease of oxygen isotopic ratio throughout the last deglaciation and the early Holocene (Figure 12) due to substantial increase in convection intensity and rainfall over the eastern Amazon basin (Wang et al., 2017). This is in agreement with the expansion of vegetation adapted to drier conditions such as savanna, as proposed by Barberi et al., (2000). Therefore, we interpret that the deposition of T1 was driven by the increase of sediment supply due the overall increase of precipitation and consequent erosion of the watershed hillslopes with sparse vegetation (Cerrado). Lower fluvial terraces deposited during the last deglaciation and early Holocene are common features in fluvial systems across north, western and central Amazon basin (Latrubblesse and Franzinelli, 2005; Rossetti et al., 2005a; Cremon et al., 2016; Gonçalves Júnior et al., 2016).

Higher precipitation combined with a substantial expansion of a denser vegetation cover may have increased the discharge and stream transport capacity during the early-mid Holocene, culminating in an incision around 6-5 ka in the middle Tocantins River. Lake located in the western part of the Amazon Basin too recorded periods avulsion between 5,600 and 2,600 cal yr BP (Aniceto et al., 2014). The wettest Holocene climatic conditions, after 5 ka, and has been registered in Cerrado too and indicates an expansion of Amazon forest tree population into the gallery forest and cerrado vegetation (Salgado-Labouriau et al., 1997; Barberi et al., 2000; Behling, 2002). The Paraíso cave record indicating a wetter regional climate at the mid-Holocene (Wang et al., 2017). The modern floodplain of the Tocantins River infill from 4.8 ± 0.4 ka likely accompanied a reduced stream capacity and stabilization of riverbanks by vegetation through the mid and early Holocene, under which fine-grained sediments and sand were deposited in fining-upward sequences by lateral meander

shifting. The Lake Marabá, record indicates a switch to a Humid Evergreen Tropical Forest (HETF; Smith and Mayle, 2018) dominated signal at ca. 5 ka (Guimarães et al., 2013). This fluvial dynamic is also common for several large fluvial systems across South American lowlands during since the mid Holocene (i.e. Stevaux, 2000; Assine et al., 2015).

Geomorphic features and OSL dating indicate that a fluvial instability occurred from 2.4 and 1.2 ka, resulting in the abandonment of the geomorphic unit Floodplain lake (from 2.4 ± 0.2 ka) and the subsequent deposition of the Proximal floodplain (1.2 ± 0.1 ka). The gap in fluvial sedimentation is synchronous with a change in sediment accumulation in the confluence between Xingu (Xingu Ria) and Amazon rivers (Bertassoli et al., 2019). The geochemical records show a decrease in water discharge of the Amazon River from about 2,600 to 1,400 cal yr BP, suggesting a decreasing of precipitation due to lower temperatures in the extratropical Southern Hemisphere that weakened the South American Summer Monsoon (Bertassoli et al., 2019). This drier condition could decrease the stream power and sediment supply, limiting the lateral accretion due channel migration. The reestablishment of the more humid climate since 1.2 ka allowed the return of hydrological conditions that lead the deposition of the Proximal floodplain.

Our data from the paleo-alluvial fans recorded at least three cycles of landscape instability (sedimentation pulses) and stability (soil formation) may be linked with high variability in precipitation across eastern Amazonia and central Brazil during the Mid-Late Pleistocene. The paleosol, in the paleo-aluvial fan, with OSL age of 118 ± 8.7 ka indicate a period with relative landscape stability that coincide with the peak of Eemian interglacial sub-stage (123 ka; Lisiecki and Raymo, 2005). Moreover, the younger OSL age of 13 ka suggest the final stage of sedimentation of the paleo-alluvial fans and the begun of the development of the open vegetation (white sands vegetation). We interpret that this patches of open vegetation is closely related to the abandonment of distributary river systems during the Pleistocene-Holocene (13-160 ka), sustaining a connection with sedimentary processes as well (Cordeiro et al., 2016; Rossetti et al., 2017b, 2019a). However, apparently, no deposit with horizons of paleosol, as we found, has been described in other regions of the Amazon, as well as the age measure of 160 ka.(Cordeiro et al., 2016; Rossetti et al., 2017a, 2019a) Although the relevance of alluvial deposits to paleoenvironmental reconstruction, our database is limited, and

a detailed facies analysis and robust geochronological framework are needed to investigate the linkages between past climate and surface processes.

The correlation between fluvial evolution of the Tocantins River and regional climate changes allow us to interpret that tectonic warping of the region has been minimal and has not actively influenced the fluvial dynamic during the last 160 ka. Although previous researchers had recognized evidences of tectonic displacement in Miocene sedimentary rocks (Barreiras Formation) (Felipe and Morales, 2017), these faults were not observed in the studied deposits or other Quaternary deposits in the region. However, this does not mean that long-term structural controls do not play a role in the morphology of the river channel and alluvial deposits. The abrupt shift in channel direction, from N-S to E-W, near the confluence of the Tocantins and Araguaia rivers, and the occurrence of rapids and bedrock reaches (Figure 2) are evidences of local effects of tectonic structures on fluvial features. The N-S structure also appears to control the shape of the eastern bank of the T1 and its boundary with the Holocene floodplain (Figure 2), but no evidence of displacement was observed. The occurrence and direction of all these geomorphic elements are coincident with regional shear zones observed in Precambrian basement rocks (Figure 1C), suggesting an inherited tectonic control that are sometimes interpreted as modern tectonic.

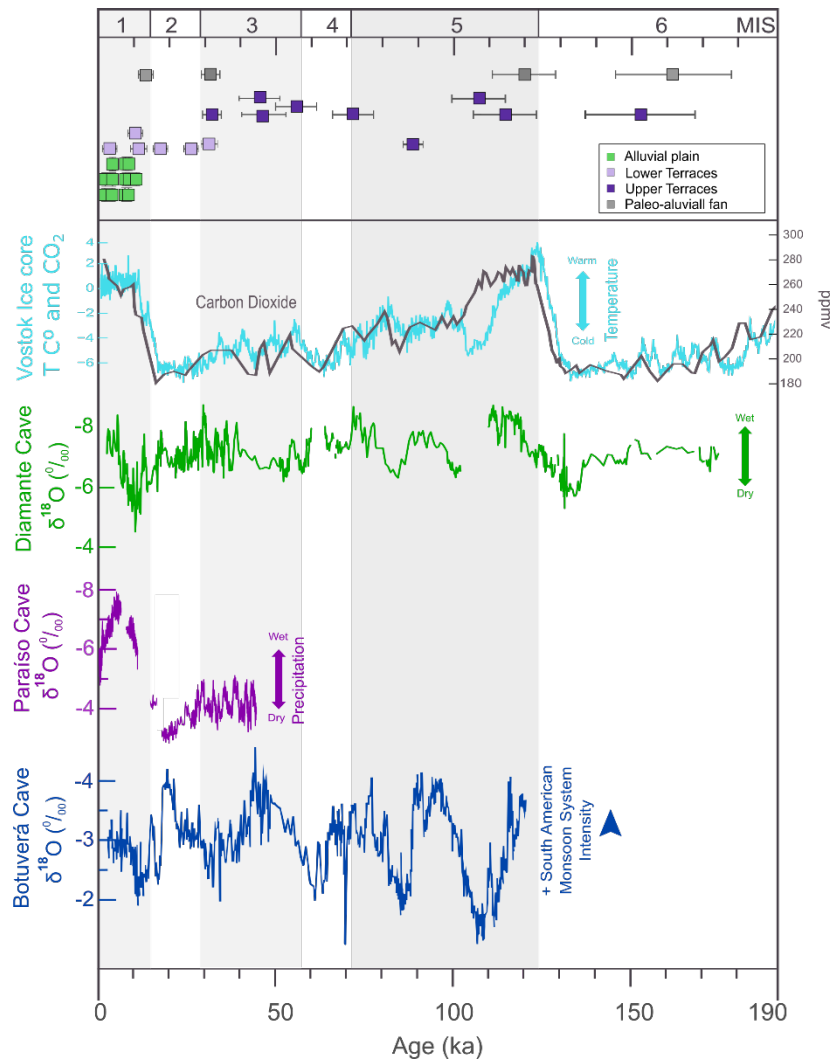


Figure 11 - Chronology of sediments of the geomorphologic units described in the middle Tocantins River compared with Quaternary climate records. The main domains are floodplains (green squares), Lower Terraces (lilac), Upper Terraces (purple) and paleo-alluvial fan (grey). The Vostok Ice core indicating changes in Temperature C° (light blue) and CO_2 (grey) (Petit et al., 1999). Speleothem $\delta^{18}O$ records from Cueva del Diamante cave (green line) indicating precipitation changes in western Amazonia (Cheng et al., 2013). Speleothem $\delta^{18}O$ records from Paraiso cave (purple line) indicating precipitation changes in eastern Amazonia (Wang et al., 2017). Speleothem $\delta^{18}O$ records from Botuverá cave (dark blue line) indicating intensity of the SASM (Cruz et al., 2005).

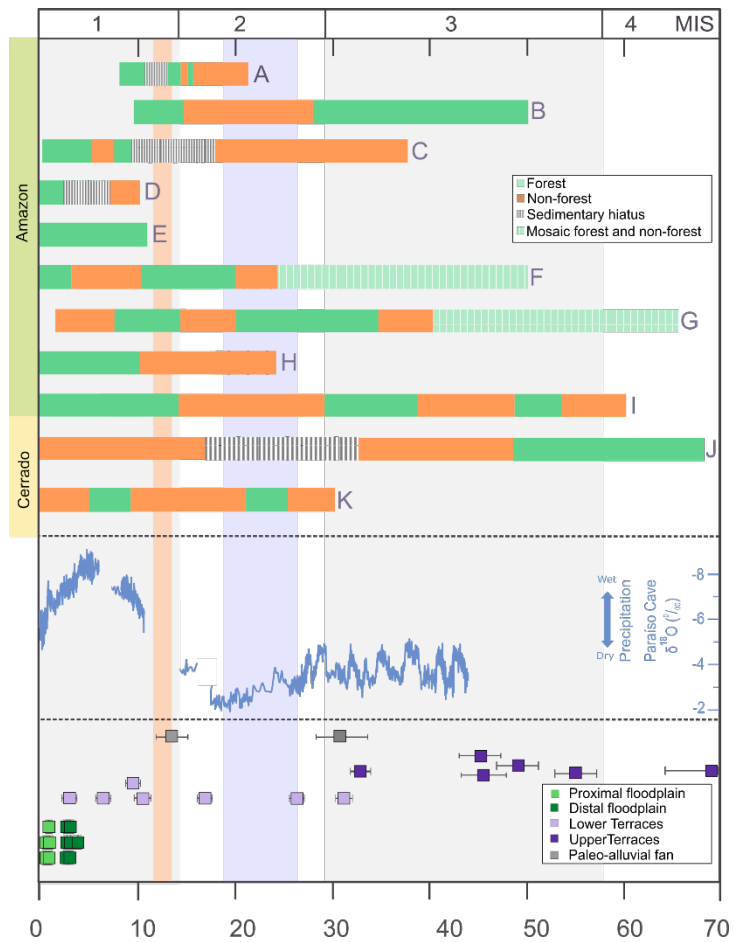


Figure 12 - Synthesis of the chronological evolution of fluvial terraces in the study area and its comparison with Quaternary palynology and speleothem records of the Eastern Amazon. (A) Caçó Lake (Sifeddine et al., 2003); (B) Hill of Six Lakes and Lagoa da Pata (Cordeiro et al., 2011a); (C) Lago do Saci (Fontes et al., 2017); (D) Comprido Lake (Moreira et al., 2013); (E) Lago Tapajós (Irion et al., 2006); (F) R2 Lake in Carajás (Reis et al., 2017); (G) R2 and R1 Lake (Guimarães et al., 2016); (H) Pântano da Mauritia in Carajás (Hermanowski et al., 2012), (I) CSS2 Core in Carajás (Absy et al., 1991), (J) Lake of Serra Negra in Southeastern of Brazil (De Oliveira et al., 2019) and (K) Plateau of Águas Emendadas Center-West of Brazil (Barberi et al., 2000).

6 CONCLUSION

The integrated approach using morphostratigraphic correlations and OSL dating provided the first robust chronological framework and an evolution model for the alluvial deposits of the middle Tocantins River, the largest fluvial system of the eastern Amazon. The geomorphological features, with depositional and erosion phases constrained by OSL ages, suggest that the current landscape was formed by the sedimentary dynamics of the Tocantins River and its tributaries in the last 160 ka as a result of water and sediments discharge variations due to climate change. The three main phases of deposition and two phases of erosion are result of alternation between humid and dry periods, promoting aggradational phases and degradational. The depositional phase of the Upper Terraces from 160 to 32 ka is correlated with the formation of the terraces in the central and western Amazonia described in the literature and reveal that the fluvial systems of eastern Amazonia, which drain terrains of central Brazil present similar responses from the rivers with headwaters drainning Andean terrains.

FINANCING

We acknowledge the financial support of the project “Dimensions US-BIOTA-Sao Paulo: Assembly and evolution of the Amazonian biota and its environment: an integrated approach”, a collaborative Dimensions of Biodiversity BIOTA grant supported by grant#2012/50260-6, Sao Paulo Research Foundation (FAPESP, Brazil), National Science Foundation (NSF, United States) and NASA (United States) 1241066. Support was also obtained from the FAPESP grant#2016/02656-1. JJ is thankful to the master’s degree scholarship from Coordination of Superior Level Staff Improvement, Brazil (CAPES) - Finance Code 001. FNP was supported for a postdoctoral fellowship FAPESP grant#2014/23334-4. FNP and AOS are supported by National Council for Scientific and Technological Development (CNPq, Brazil) grants #302411/2018-6 and #304727/2017-2. The opinions, hypotheses, conclusions, and recommendations expressed in this material are responsibility of the author (s) and do not necessarily reflect FAPESP's and CAPES vision.

ACKNOWLEDGMENT

JJ is grateful for Federal University of South and Southeast Pará for car support for field activity and Prof. Leonardo Felipe and geologists Elianne Conde, Romário, Ricardo and Josiel from Unifesspa for their help during field work. We are thankful to Thays and Luciana for the technical support to OSL dating in the Laboratory of Gamma Spectrometry and Luminescence (LEGaL), São Paulo University (USP).

7 CONCLUSÕES

A região do Bico do Papagaio e o Paleocanal do Tocantins localizados na região do médio rio Tocantins consiste em um importante registro geomorfológico fluvial do leste da Amazônia. Ocorre um emaranhado de feições geomorfológicas dominadas por lagos estreitos e extensos, paleodiques e paleocanais inseridos em extensos terraços e amplas planícies, e contrastes de ambientes de sedimentação e vegetação.

O mapa geomorfológico na escala de 1:100.000 dessa região oferece insights sobre os complexos processos geomorfológicos e sedimentológicos que moldam a paisagem fluvial atual e pode ser de utilidade para planejadores e tomadores de decisão em projetos de desenvolvimento regional e conservação.

Integração do mapeamento geomorfológico e o quadro cronológico obtido a partir dos sedimentos fluviais aliados as características sedimentológica coletados em terraços, planícies e leques aluviais possibilitaram apontar as principais fases de evolução geomorfológica dessa complexa paisagem.

Com base no mapeamento por sensoriamento remoto, de campo, levantamento bibliográfico, ainda escasso para essa região, e o nosso robusto registro geocronológico tornou-se possível propor que a paisagem atual foi formada pela dinâmica do rio Tocantins e seus afluentes nos últimos 160 ka, e apontam que o principal motor dessa evolução foram alterações no suprimento de água e sedimentos resultantes das mudanças climáticas.

As três principais fases de deposição e duas de incisão resultam da alternância entre períodos úmidos e secos, promovendo fases de agradação e incisão. As cinco principais fases são: 1) Formação dos Terraços Altos (T1) e parte do Paleoleque aluvial entre 32 a 160 ka; 2) Primeiro evento de incisão por volta de 31 ka com o abandono do T1; 3) Formação dos Terraços Baixos (T2) e reativação dos leques aluviais entre 6 e 31 ka; 4) Segundo evento de incisão entre 5-6 ka promove o abandono do T2 e a redução do nível de base local a posição atual do canal; e 5) Construção da planície aluvial desde 5 ka até o presente com e a migração lateral do canal.

A deposição e abandono dos terraços altos (T1) entre 32 e 160 ka se correlaciona diretamente com a formação dos terraços na Amazônia Central e Ocidental descritos na literatura e relevam que os sistemas fluviais da Amazônia Oriental, que drenam terrenos do Brasil Central apresentam respostas semelhantes

os rios com cabeceiras em terrenos andinos. Dessa forma nossa hipótese que esse sistema fluvial do leste da Amazônia teria uma dinâmica diferente vista o contexto geológico e biológico, no ecótono Cerrado-Amazônia não foi confirmada. Reforçando a influência das mudanças climáticas na construção da paisagem fluvial amazônica. Os registros fluviais encontrados nessa região seguem a tendência geral dos testemunhos palinológicos e paleoclimáticos de outros locais da Amazônia e de parte do Cerrado.

Apesar do avanço que esta pesquisa trouxe para o entendimento da dinâmica fluvial durante o Quaternário tardio frente as mudanças climáticas no médio rio Tocantins, leste da Amazônia, a área ainda possui registros sedimentares a serem explorados. Os inúmeros lagos e paleocanais apresentam grande potencial para o avanço de reconstruções paleoclimáticas em área de transição entre floresta amazônica e cerrado durante o Holoceno médio e tardio; assim como o sistema de paleoleques aluviais, composto de “white sands” que suportam enclaves de vegetação aberta com horizontes de paleossolos, são potencialmente promissores para reconstrução da dinâmica funcional e geobotânica dessa região, que ainda é limitado e por vezes controverso.

REFERÊNCIAS

- Ab'Saber, A.N., 2010, Zoneamento fisiográfico e ecológico do espaço total da Amazônia Brasileira: Estudos Avançados , p. 15–24, <http://www.scielo.br/pdf/ea/v24n68/04.pdf> (accessed October 2019).
- Absy, M.L. et al., 1991, Mise en évidence de quatre phases d'ouverture de la forêt dense dans le sud-est de l'Amazonie au cours des 60 000 dernières années. Première comparaison avec d'autres régions tropicales: Comptes Rendus de l'Académie des Sciences, v. 3, p. 673–678, <http://www.documentation.ird.fr/hor/fdi:31917>.
- Absy, M.L., Cleef, A.M., D'apolito, C., and Silva, M.F.F., 2014, Palynological differentiation of savanna types in Carajás, Brazil (southeastern Amazonia): Palynology, v. 38, p. 78–89, doi:10.1080/01916122.2013.842189.
- Aitken, M.J., 1985, An Introduction to Optical Dating- The Dating of Quaternary Sediments: New Yourk, Oxford University Press Inc., 279 p.
- Akama, A., 2017, Impacts of the hydroelectric power generation over the fish fauna of the Tocantins river, Brazil: Marabá dam, the final blow: Oecologia Australis, v. 21, p. 222–231, doi:10.4257/oeco.2017.2103.01.
- Akter, S., Ali, R.M.E., Karim, S., Khatun, M., and Alam, M., 2018, Geomorphological, Geological and Engineering Geological Aspects for Sustainable Urban Planning of Mymensingh City, Bangladesh: Open Journal of Geology, v. 08, p. 737–752, doi:10.4236/ojg.2018.87043.
- Albert, J.S., Val, P., and Hoorn, C., 2018, The changing course of the Amazon River in the Neogene: center stage for Neotropical diversification: Neotropical Ichthyology, v. 16, p. 1–24, doi:10.1590/1982-0224-20180033.
- Almeida-Filho, R., and Miranda, F.P., 2007, Mega capture of the Rio Negro and formation of the Anavilhas Archipelago, Central Amazônia, Brazil: Evidences in an SRTM digital elevation model: Remote Sensing of Environment, v. 110, p. 387–392, doi:10.1016/j.rse.2007.03.005.
- Almeida, F.F., Hasui, Y., Brito Neves, B., and Fuck, R.A., 1977, Províncias estruturais brasileiras. In: Simpósio de Geologia do Nordeste, 8, Campina Grande, PB:
- ANA, 2005, Cadernos de Recursos Hídricos - Aproveitamento do Potencial Hidráulico para Geração de Energia: Brasília-DF, 101 p., http://arquivos.ana.gov.br/planejamento/planos/pnrh/VF_GeraçaoEnergia.pdf.
- ANA, A.N. de Á., 2017, Plano Estratégico da Bacia Hidrográfica dos Rios Tocantins e Araguaia: , p. 204, <http://www3.ana.gov.br/portal/ANA/todos-os-documentos-do-portal/documentos-spr/planos-de-bacia/plano-estrategico-de-recursos-hidricos-da-bacia-hidrografica-dos-rios-tocantins-e-araguaia-relatorio-sintese>.
- Anhuf, D. et al., 2006, Paleo-environmental change in Amazonian and African rainforest during the LGM: Palaeogeography, Palaeoclimatology, Palaeoecology, v. 239, p. 510–527, doi:10.1016/j.palaeo.2006.01.017.
- Antoine, P., Lozouet, N.L., Chaussé, C., Lautridou, J.P., Pastre, J.F., Auguste, P., Bahain, J.J., Falguères, C., and Galehb, B., 2007, Pleistocene fluvial terraces from

northern France (Seine, Yonne, Somme): synthesis, and new results from interglacial deposits: *Quaternary Science Reviews*, v. 26, p. 2701–2723, doi:10.1016/j.quascirev.2006.01.036.

Assine, M.L., Corradini, F.A., Pupim, F. do N., and McGlue, M.M., 2014, Channel arrangements and depositional styles in the São Lourenço fluvial megafan, Brazilian Pantanal wetland: *Sedimentary Geology*, v. 301, p. 172–184, doi:10.1016/j.sedgeo.2013.11.007.

Assine, M.L., Merino, E.R., Pupim, F.N., Warren, L. V., Guerreiro, R.L., and McGlue, M.M., 2015, Geology and Geomorphology of the Pantanal Basin, *in* Dynamics of the Pantanal Wetland in South America. The Handbook of Environmental Chemistry, Springer, Cham, v. 37, p. 23–50, doi:10.1007/698_2015_349.

Augusto-Silva, P.B., MacIntyre, S., Rudorff, C.M., Cortés, A., and Melack, J.M., 2019, Stratification and mixing in large floodplain lakes along the lower Amazon River: *Journal of Great Lakes Research*, v. 45, p. 61–72, doi:10.1016/j.jglr.2018.11.001.

Baker, P.A., Fritz, S.C., Garland, J., and Ekdahl, E., 2005, Holocene hydrologic variation at Lake Titicaca , Bolivia / Peru , and its relationship to North Atlantic climate variation: v. 20, p. 655–662, doi:10.1002/jqs.987.

Bangen, S.G., Wheaton, J.M., Bouwes, N., Bouwes, B., and Jordan, C., 2014, A methodological intercomparison of topographic survey techniques for characterizing wadeable streams and rivers: *Geomorphology*, v. 206, p. 343–361, doi:10.1016/j.geomorph.2013.10.010.

Barberi, M., Salgado-Labouriau, M.L., and Suguio, K., 2000, Paleovegetation and paleoclimate of “Vereda de Aguas Emendadas”, central Brazil: *Journal of South American Earth Sciences*, v. 13, p. 241–254, doi:10.1016/S0895-9811(00)00022-5.

Behling, H., 2001, Late Quaternary environmental changes in the Lagoa da Curuça region (eastern Amazonia, Brazil) and evidence of Podocarpus in the Amazonon lowland: *Vegetation History and Archaeobotany*, v. 111, p. 1009–1010, doi:10.1192/bjp.111.479.1009-a.

Behling, H., 2002, Late Quaternary vegetation and climate dynamics in southeastern Amazonia inferred from Lagoa da Confusão Tocantins State, northern Brazil: *Amazoniana*, v. 17, p. 27–39.

Behling, H., and Hooghiemstra, H., 1999, Environmental history of the Colombian savannas of the Llanos Orientales since the Last Glacial Maximum from lake records El Pinal and Carimagua: *Journal of Paleolimnology*, v. 21, p. 461–476, doi:10.1023/A:1008051720473.

Behling, H., Keim, G., Irion, G., Junk, W., and Mello, J.N. de, 2001, Holocene environmental changes in the Central Amazon Basin inferred from Lago Calado (Brazil): *Palaeogeography, Palaeoclimatology, Palaeoecology*, v. 173, p. 87–101, doi:10.1016/s0031-0182(01)00321-2.

Bertani, T.C., Rossetti, D.F., Hayakawa, E.H., and Cohen, M.C.L., 2015, Understanding Amazonian fluvial rias based on a Late Pleistocene-holocene analog: *Earth Surface Processes and Landforms*, v. 40, p. 285–292, doi:10.1002/esp.3629.

Bertassoli, D.J. et al., 2019a, Spatiotemporal Variations of Riverine Discharge Within the Amazon Basin During the Late Holocene Coincide With Extratropical Temperature Anomalies: *Geophysical Research Letters*, v. 46, p. 9013–9022, doi:10.1029/2019GL082936.

Bertassoli, D.J., Sawakuchi, A.O., Chiessi, C.M., Schefuß, E., and Hartmann, G.A., 2019b, Spatiotemporal variations of riverine discharge within the Amazon Basin during the late Holocene coincide with extratropical temperature anomalies: , p. 0–3, doi:10.1029/2019GL082936.

Bigarella, J.J., 1973, Geology of the Amazon and Parnaiba Basins, *in* The South Atlantic, Boston, MA, Springer US, p. 25–86, doi:10.1007/978-1-4684-3030-1_2.

Brasil, 2012, Plano Decenal de Expansão de Energia 2021: Brasília-DF, Ministério de Minas e Energia, Empresa de Pesquisa Energética, 386 p.

Bridgland, D., and Westaway, R., 2008, Climatically controlled river terrace staircases: A worldwide Quaternary phenomenon: *Geomorphology*, v. 98, p. 285–315, doi:10.1016/j.geomorph.2006.12.032.

Bridgland, D.R., and Westaway, R., 2014, Quaternary fluvial archives and landscape evolution: A global synthesis: *Proceedings of the Geologists' Association*, v. 125, p. 600–629, doi:10.1016/j.pgeola.2014.10.009.

Brierley, G.J., and Fryirs, K.A., 2005, Geomorphology and river management: applications of the river styles framework: 387 p.

Brito Neves, B. B., and Cordani, U.G., 1991, Tectonic evolution of South America during the Late Proterozoic: *Precambrian Research*, v. 53, p. 23–40, doi:10.1016/0301-9268(91)90004-T.

Bull, W.B., 1991, Geomorphic Responses to Climatic Change: v. 83, 114–116 p.

Bush, M.B., De Oliveira, P.E., Colinvaux, P.A., Miller, M.C., and Moreno, J.E., 2004a, Amazonian paleoecological histories: One hill, three watersheds: *Palaeogeography, Palaeoclimatology, Palaeoecology*, v. 214, p. 359–393, doi:10.1016/S0031-0182(04)00401-8.

Bush, M.B., Silman, M.R., and Urrego, D.H., 2004b, 48,000 Years of Climate and Forest Change in a Biodiversity Hot Spot: *Science*, v. 303, p. 827–829, doi:10.1126/science.1090795.

Bush, M.B., Stute, M., Ledru, M., Behling, H., and Colinvaux, P. a, 2001, Paleotemperature Estimates for the Lowland Americas: *Americas*, The.,

Campbell, D.F., 1949, Revised report on the reconnaissance geology of the Maranhão Basin.: Conselho Nacional do Petróleo. 117p. Petrobras/DEPEX, Relatório Interno, v. 103.

Cheng, H., Sinha, A., Cruz, F.W., Wang, X., Edwards, R.L., D'Horta, F.M., Ribas, C.C., Vuille, M., Stott, L.D., and Auler, A.S., 2013, Climate change patterns in Amazonia and biodiversity: *Nature Communications*, v. 4, doi:10.1038/ncomms2415.

Cohen, M.C.L., Rossetti, D.F., Pessenda, L.C.R., Friaes, Y.S., and Oliveira, P.E., 2014, Late Pleistocene glacial forest of Humaitá-Western Amazonia: *Palaeogeography, Palaeoclimatology, Palaeoecology*, v. 415, p. 37–47,

doi:10.1016/j.palaeo.2013.12.025.

- Colinvaux, P.A., De Oliveira, P.E., Moreno, J.E., Miller, M.C., and Bush, M.B., 1996, A long pollen record from lowland Amazonia: Forest and cooling in glacial times: *Science*, v. 274, p. 85–88, doi:10.1126/science.274.5284.85.
- Cordeiro, C.L.O., Rossetti, D.F., Gribel, R., Tuomisto, H., Zani, H., Ferreira, C.A.C., and Coelho, L., 2016, Impact of sedimentary processes on white-sand vegetation in an Amazonian megafan: *Journal of Tropical Ecology*, v. 32, p. 498–509, doi:10.1017/S0266467416000493.
- Cordeiro, R.C., Turcq, B., Sifeddine, A., Lacerda, L.D., Silva Filho, E. V., Gueiros, B., Potty, Y.P., Santelli, R.E., Pádua, E.O., and Patchinelam, S.R., 2011a, Biogeochemical indicators of environmental changes from 50Ka to 10Ka in a humid region of the Brazilian Amazon: *Palaeogeography, Palaeoclimatology, Palaeoecology*, v. 299, p. 426–436, doi:10.1016/j.palaeo.2010.11.021.
- Cordeiro, R.C., Turcq, B., Sifeddine, A., Lacerda, L.D., Silva Filho, E.V., Gueiros, B., Potty, Y.P., Santelli, R.E., Pádua, E.O., and Patchinelam, S.R., 2011b, Biogeochemical indicators of environmental changes from 50Ka to 10Ka in a humid region of the Brazilian Amazon: *Palaeogeography, Palaeoclimatology, Palaeoecology*, v. 299, p. 426–436, doi:10.1016/j.palaeo.2010.11.021.
- Cordeiro, R.C., Turcq, B., Suguió, K., Oliveira da Silva, A., Sifeddine, A., and Volkmer-Ribeiro, C., 2008, Holocene fires in East Amazonia (Carajás), new evidences, chronology and relation with paleoclimate: *Global and Planetary Change*, v. 61, p. 49–62, doi:10.1016/j.gloplacha.2007.08.005.
- Costa, J.B.S., Bemerguy, R., Hasui, Y., and Borges, M.S., 2001, Tectonics and paleogeography along the Amazon river: *Journal of south American Earth Sciences*, v. 14, p. 335–347.
- Costa, J.B.S., Hasui, Y., Bemerguy, R.L., Soares-Júnior, A. V., and Villegas, J.M.C., 2002, Tectonics and paleogeography of the Marajó Basin, northern Brazil: *Anais da Academia Brasileira de Ciencias*, v. 74, p. 519–531, doi:10.1590/S0001-37652002000300013.
- Cremon, É.H., Rossetti, D. de F., Sawakuchi, A. de O., and Cohen, M.C.L., 2016, The role of tectonics and climate in the late Quaternary evolution of a northern Amazonian River: *Geomorphology*, v. 271, p. 22–39, doi:10.1016/j.geomorph.2016.07.030.
- Cruz, F.W., Karmann, I., Viana, O., Burns, S.J., Ferrari, J.A., Vuille, M., Sial, A.N., and Moreira, M.Z., 2005, Stable isotope study of cave percolation waters in subtropical Brazil: Implications for paleoclimate inferences from speleothems: *Chemical Geology*, v. 220, p. 245–262, doi:10.1016/j.chemgeo.2005.04.001.
- D'Apolito, C., Absy, M.L., and Latrubesse, E.M., 2013, The Hill of Six Lakes revisited: New data and re-evaluation of a key Pleistocene Amazon site: *Quaternary Science Reviews*, v. 76, p. 140–155, doi:10.1016/j.quascirev.2013.07.013.
- Dagosta, F.C.P., and Pinna, M., 2019, The Fishes of the Amazon : Distribution and Biogeographical Patterns , with a Comprehensive List of Species: *Bulletin of the American Museum of Natural History*, v. 2019, p. 1–163, doi:10.1206/0003-0090.431.1.1.

Deus, S.C.S., Neves, R.J.J., Jauche, E., Almeida, C., Faial, K.R.F., Medeiro, A.C., Mendes, R.A., Faial, K.C.F., Leite, J.C., and Deus, R.J.A., 2018, Streamflow forecasts due precipitation water in a tropical large watershed at Brazil for flood early warning, based on SWAT model: ITEGAM- Journal of Engineering and Technology for Industrial Applications, v. 4, p. 4–14, doi:10.5935/2447-0228.20180027.

Duller, G.A.T., 2003, Distinguishing quartz and feldspar in single grain luminescence measurements: Radiation Measurements, v. 37, p. 161–165, doi:10.1016/S1350-4487(02)00170-1.

Duller, G.A.T., 2015, The Analyst software package for luminescence data: overview and recent improvements, *in* Ancient TL, v. 33, p. 35–42.

Dumont, J.F., Deza, E., and Garcia, F., 1991, Morphostructural provinces and neotectonics in the Amazonian lowlands of Peru: Journal of South American Earth Sciences, v. 4, p. 373–381, doi:10.1016/0895-9811(91)90008-9.

Dunne, T., Mertes, L.A.K., Meade, R.H., Richey, J.E., and Forsberg, B.R., 1998, Exchanges of sediment between the flood plain and channel of the Amazon River in Brazil: Bulletin of the Geological Society of America, v. 110, p. 450–467, doi:10.1130/0016-7606(1998)110<0450:EOSBTF>2.3.CO;2.

Esri, 2019, World Imagery, , p. <https://www.arcgis.com/home/webmap/viewer.html?use>.

Felipe, L.B., 2012, Geologia, Geomorfologia e Morfotectônica da Região de Marabá-PA: Universidade Estadual Paulista (UNESP), 158 p., <https://repositorio.unesp.br/handle/11449/103038>.

Felipe, L.B., and Morales, N., 2017, Influência neotectônica na evolução geomorfológica e geológica da região de Marabá-PA: Contribuições à Geologia da Amazônia, v. 10, p. 145–161, <http://www.sbg-no.org.br/>.

Ferraz-Vicentini, K.R., and Labouriau-Salgado, L.M.L., 1996, Palynological analysis of a palm swamp in Central Brazil: Journal of South American Earth Sciences, v. 9, p. 207–209.

Fisch, G., Marengo, J.A., and Nobre, C., 1998, Uma revisão geral sobre o clima da amazônia: Acta Amazonica, v. 28, p. 101–126, <http://www.scielo.br/pdf/aa/v28n2/1809-4392-aa-28-2-0101.pdf>.

Fontes, D., Cordeiro, R.C., Martins, G.S., Behling, H., Turcq, B., Sifeddine, A., Seoane, J.C.S., Moreira, L.S., and Rodrigues, R.A., 2017, Paleoenvironmental dynamics in South Amazonia, Brazil, during the last 35,000 years inferred from pollen and geochemical records of Lago do Saci: Quaternary Science Reviews, v. 173, p. 161–180, doi:10.1016/j.quascirev.2017.08.021.

Franzinelli, E., and Igreja, H., 2002a, Modern sedimentation in the Lower Negro River, Amazonas State, Brazil: Geomorphology, v. 44, p. 259–271, doi:10.1016/S0169-555X(01)00178-7.

Franzinelli, E., and Igreja, H., 2002b, Modern sedimentation in the Lower Negro River ,: v. 44, p. 259–271.

Fryirs, K.A., and Brierley, G.J., 2012, Geomorphic Analysis of River Systems:,

doi:10.1002/9781118305454.

- Galbraith, R.F., ROBERTS, R.G., LASLETT, G.M., YOSHIDA2, H., and OLLEY, J.M., 1999, Optical Dating of Single and Multiple Grains of Quartz From Jinmium Rock Shelter, Northern Australia: Part I, Experimental Design and Statistical Models: *Archaeometry*, v. 41, p. 339–364.
- Garreaud, R.D., Vuille, M., Compagnucci, R., and Marengo, J., 2009, Present-day South American climate: Palaeogeography, Palaeoclimatology, Palaeoecology, v. 281, p. 180–195, doi:10.1016/j.palaeo.2007.10.032.
- Geosage, 2018, Spectral Transformer GUI Landsat-8 Imagery®, , p. http://www.geosage.com/highview/features_landsat8.. http://www.geosage.com/highview/features_landsat8.
- Goés, A.M., 1981, Estudo sedimentológico dos Sedimentos Barreiras, Ipixuna e Itapecuru, no Nordeste do Pará e Noroeste do Maranhão: Universidade Federal do Pará, 52 p.
- Góes, A.M., 1995, Formação Poti (Carbonífero inferior) da Bacia do Parnaíba: Universidade de São Paulo, 204 p., doi:10.11606/T.44.1995.tde-11022014-105309.
- Gonçalves Júnior, E.S., Soares, E.A.A., Tatumi, S.H., Yee, M., and Mittani, J.C.R., 2016, Pleistocene-Holocene sedimentation of Solimões-Amazon fluvial system between the tributaries Negro and Madeira, Central Amazon: *Brazilian Journal of Geology*, v. 46, p. 167–180, doi:10.1590/2317-4889201620160009.
- Gonçalves, J., and Nicola, R., 2002, Araguaia - Do tranqüilo balanço das águas à turbulência anunciada: lutar é preciso: Mobilização para Conservação das Áreas Úmidas do Pantanal e Bacia do Araguaia, p. 32.
- Google Earth Pro®, 2019, Google Earth Pro®: , p. kh.google.com, kh.google.com.
- Graham, S.A., 1986, Provenance modelling as a technique for analysing source terrane evolution and controls on foreland sedimentation.: *Foreland basins*, p. 425–436, doi:10.1002/9781444303810.ch23.
- Groot, M.H.M., and Bogot, R.G., 2011, of the Past Ultra-high resolution pollen record from the northern Andes reveals rapid shifts in montane climates within the last two glacial cycles: , p. 299–316, doi:10.5194/cp-7-299-2011.
- Guérin, G., Mercier, N., and Adamiec, G., 2011, Dose-rate conversion factors : Update Dose-rate conversion factors : update:
- Guimarães, J.T.F. et al., 2019a, Upland lakes of the Carajás region : origin and development through time: *Preprints*, p. 1–25, doi:10.20944/preprints201905.0214.v1.
- Guimarães, J.T.F., Cohen, M.C.L., França, M.C., Alves, I.C.C., Smith, C.B., Pessenda, L.C.R., and Behling, H., 2013, An integrated approach to relate Holocene climatic, hydrological, morphological and vegetation changes in the southeastern Amazon region: *Vegetation History and Archaeobotany*, v. 22, p. 185–198, doi:10.1007/s00334-012-0374-y.
- Guimarães, J.T.F., Sahoo, P.K., Souza-Filho, P.W.M., Costa de Figueiredo, M.M.J.,

Reis, L.S., da Silva, M.S., and Rodrigues, T.M., 2019b, Holocene history of a lake filling and vegetation dynamics of the Serra sul Dos Carajás, southeast Amazonia: Anais da Academia Brasileira de Ciencias, v. 91, p. 1–17, doi:10.1590/0001-3765201720160916.

Guimarães, J.T.F., Sahoo, P.K., Souza-Filho, P.W.M., Maurity, C.W., Silva Júnior, R.O., Costa, F.R., and Dall'Agnol, R., 2016, Late Quaternary environmental and climate changes registered in lacustrine sediments of the Serra Sul de Carajás, south-east Amazonia: Journal of Quaternary Science, v. 31, p. 61–74, doi:10.1002/jqs.2839.

Gupta, A., 2007, Large rivers: Geomorphology and management (A. Gupta, Ed.): Singapore, 661 p., doi:10.1002/rra.1204.

Häggi, C., Chiessi, C.M., Merkel, U., Mulitza, S., Prange, M., Schulz, M., and Schefuß, E., 2017, Response of the Amazon rainforest to late Pleistocene climate variability: Earth and Planetary Science Letters, v. 479, p. 50–59, doi:10.1016/j.epsl.2017.09.013.

Hamilton, S.K., Kellndorfer, J., Lehner, B., and Tobler, M., 2007, Remote sensing of floodplain geomorphology as a surrogate for biodiversity in a tropical river system (Madre de Dios, Peru): Geomorphology, v. 89, p. 23–38, doi:10.1016/j.geomorph.2006.07.024.

Hammen, T., Duivenvoorden, J.F., Lips, J.M., Urrego, L.E., and Espejo, N., 1992, Late quaternary of the middle Caquetá River area (Colombian Amazonia): Journal of Quaternary Science, v. 7, p. 45–55, doi:10.1002/jqs.3390070105.

Van Der Hammen, T., and Hooghiemstra, H., 2000, Neogene and Quaternary history of vegetation, climate, and plant diversity in Amazonia: Quaternary Science Reviews, v. 19, p. 725–742, doi:10.1016/S0277-3791(99)00024-4.

Hasui, Y., Abreu, F.D.A.M. de, and Silva, J.M.R. da, 1977, Estratigrafia da faixa de dobramentos Paraguai-Araguaia no centro-norte do Brasil: Boletim IG, v. 8, p. 107, doi:10.11606/issn.2316-8978.v8i0p107-117.

Hermanowski, B., Costa, M.L., and Behling, H., 2012, Environmental changes in southeastern Amazonia during the last 25,000yr revealed from a paleoecological record: Quaternary Research, v. 77, p. 138–148, doi:10.1016/j.yqres.2011.10.009.

Hermanowski, B., Costa, M.L., and Behling, H., 2014, Possible linkages of palaeofires in southeast Amazonia to a changing climate since the Last Glacial Maximum: Vegetation History and Archaeobotany, v. 24, p. 279–292, doi:10.1007/s00334-014-0472-0.

Herz, N., Hasui, Y., Costa, J.B.S., and Matta, M.A.S., 1989, The Araguaia fold belt, Brazil: A reactivated Brasiliano-Pan-African cycle (550 Ma) geosuture: Precambrian Research, v. 42, p. 371–386, doi:10.1016/0301-9268(89)90020-X.

Hoorn, C. et al., 2010, Amazonia through time: Andean uplift, climate change, landscape evolution, and biodiversity: Science, v. 330, p. 927–931, doi:10.1126/science.1194585.

Howard, J.L., 1993, The statistics of counting clasts in rudites: a review, with examples

from the upper Palaeogene of southern California, USA: *Sedimentology*, v. 40, p. 157–174, doi:10.1111/j.1365-3091.1993.tb01759.x.

IBGE, 2009a, Manual Técnico de Geomorfologia (Coordenação de Recursos Naturais e Estudos Ambientais, Ed.): Rio de Janeiro, 2009, 182 p., <https://biblioteca.ibge.gov.br/visualizacao/livros/liv66620.pdf>.

IBGE, 2009b, Manual Técnico de Geomorfologia: Rio de Janeiro , 182 p., <https://biblioteca.ibge.gov.br/visualizacao/livros/liv66620.pdf> (accessed October 2019).

ICMBio, 2018, Livro Vermelho da Fauna Brasileira Ameaçada de Extinção: Volume VI - Peixes, *in* Instituto Chico Mendes de Conservação da Biodiversidade (Org.). Livro Vermelho da Fauna Brasileira Ameaçada de Extinção, Brasília, DF, v. VI-Peixes, p. 1232.

IDESP, 1992, Instituto de Desenvolvimento Econômico, Social e Ambiental do Pará: v. Edição Esp.

Inkscape, 2007, Inkscape Project™ 0.92.3.: , p. <http://inkscape.org/>.

Irion, G., Bush, M.B., Nunes de Mello, J.A., Stüben, D., Neumann, T., Müller, G., Morais de, J.O., and Junk, J.W., 2006, A multiproxy palaeoecological record of Holocene lake sediments from the Rio Tapajós, eastern Amazonia: *Palaeogeography, Palaeoclimatology, Palaeoecology*, v. 240, p. 523–535, doi:10.1016/j.palaeo.2006.03.005.

Irion, G., Junk, W., Keim, G., Nunes de Mello, J., and Behling, H., 2001, Holocene environmental changes in the Central Amazon Basin inferred from Lago Calado (Brazil): *Palaeogeography, Palaeoclimatology, Palaeoecology*, v. 173, p. 87–101, doi:10.1016/s0031-0182(01)00321-2.

Irion, G., and Kalliola, R., 2010, Long-Term Landscape Development Processes in Amazonia: *Amazonia, Landscape and Species Evolution: A Look into the Past*, v. 1, p. 185–197, doi:10.1002/9781444306408.ch11.

Irion, G., Müller, J., Morais, J.O., Keim, G., Mello, J.N., and Junk, W.J., 2009, The impact of Quaternary sea level changes on the evolution of the Amazonian lowland: *Hydrological Processes*, v. 23, p. 3168–3172, doi:10.1002/hyp.7386.

Jesus, J.S., 2016, Geocronologia por Luminescência dos depósitos fluviais do Médio Tocantins - SE do Pará: Implicações Paleogeográficas e Paleoclimáticas: Universidade Federal do Sul e Sudeste do Pará, 62 p.

Jones, A.F., Brewer, P.A., Johnstone, E., and Macklin, M.G., 2007, High-resolution interpretative geomorphological mapping of river valley environments using airborne LiDAR data: *Earth Surface Processes and Landforms*, v. 32, p. 1574–1592, doi:10.1002/esp.1505.

Kodama, Y.-M., 1993, Large-Scale Common Features of Sub-Tropical Convergence Zones (the Baiu Frontal Zone, the SPCZ, and the SACZ) Part II : Conditions of the Circulations for Generating the STCZs: *Journal of the Meteorological Society of Japan. Ser. II*, v. 71, p. 581–610, doi:10.2151/jmsj1965.71.5_581.

Kodama, Y., 1992, Large-Scale Common Features of Subtropical Precipitation Zones (the Baiu Frontal Zone, the SPCZ, and the SACZ) Part I: Characteristics of

- Subtropical Frontal Zones: Journal of the Meteorological Society of Japan. Ser. II, v. 70, p. 813–836, doi:10.2151/jmsj1965.70.4_813.
- Latrubblesse, E.M., 2002, Evidence of quaternary palaeohydrological changes in middle Amazonia: The Aripuanã-Roosevelt and Jiparaná “fans”: *Zeitschrift fur Geomorphologie*, Supplementband, v. 129, p. 61–72.
- Latrubblesse, E.M., 2003, The Late Quaternary Paleohydrology of Large South American Fluvial Systems, *in* Gregory, K; Benito, G. ed., *Palaeohydrology: Understanding Global Change*, Wiley & Sons, p. 193–213.
- Latrubblesse, E., Arima, E., Ferreira, M., Nogueira, S., Wittmann, F., Dias, M.S., Dagosta, F., and Baye, M., 2019, Fostering water resource governance and conservation in the Brazilian Cerrado biome: *Conservation Science and Practice*, v. 1, doi:10.1111/csp2.77.
- Latrubblesse, E.M., and Franzinelli, E., 2002, The Holocene alluvial plain of the middle Amazon River, Brazil: *Geomorphology*, v. 44, p. 241–257, doi:10.1016/S0169-555X(01)00177-5.
- Latrubblesse, E.M., and Franzinelli, E., 2005, The late Quaternary evolution of the Negro River, Amazon, Brazil: Implications for island and floodplain formation in large anabranching tropical systems: *Geomorphology*, v. 70, p. 372–397, doi:10.1016/j.geomorph.2005.02.014.
- Latrubblesse, E.M., and Kalicki, T., 2002, Late Quaternary Palaeohidrological Changes in the Upper Purus Basin, South-western Amazonia, Brazil: *Boletim Goiano de Geografia*, v. 19, doi:10.5216/bgg.v19i1.15311.
- Latrubblesse, E.M., and Stevaux, J.C., 2002, Geomorphology and environmental aspects of the Araguaia fluvial basin, Brazil: *Zeitschrift fur Geomorphologie*, Supplementband, v. 129, p. 109–127.
- Ledru, M.P., Bertaux, J., Sifeddine, A., and Suguio, K., 1998, Absence of Last Glacial Maximum Records in Lowland Tropical Forests: *Quaternary Research*, v. 49, p. 233–237, doi:10.1006/qres.1997.1953.
- Leeder, M.R., and Mack, G.H., 2001, Lateral erosion ('toe-cutting') of alluvial fans by axial rivers: Implications for basin analysis and architecture: *Journal of the Geological Society*, v. 158, p. 885–894, doi:10.1144/0016-760000-198.
- Lees, A.C., Peres, C.A., Fearnside, P.M., Schneider, M., and Zuanon, J.A.S., 2016, Hydropower and the future of Amazonian biodiversity: *Biodiversity and Conservation*, v. 25, p. 451–466, doi:10.1007/s10531-016-1072-3.
- Lewin, J., and Ashworth, P.J., 2014a, The negative relief of large river floodplains: *Earth Science Reviews*, v. 129, p. 1–23, doi:10.1016/j.earscirev.2013.10.014.
- Lewin, J., and Ashworth, P.J., 2014b, The negative relief of large river floodplains: *Earth-Science Reviews*, v. 129, p. 1–23, doi:10.1016/j.earscirev.2013.10.014.
- Lewin, J., Davies, B., and Wolfenden, P., 1977, Interactions between channel change and historic mining sediments: *River Channel Changes*, p. 353–367, [https://hwbdocuments.env.nm.gov/Los Alamos National Labs/General/14434.pdf](https://hwbdocuments.env.nm.gov/Los%20Alamos%20National%20Labs/General/14434.pdf).
- Lima, M.R. de, 1982, PALINOLOGIA DA FORMAÇÃO CODÓ NA REGIÃO DE CODÓ,

MARANHÃO: Bol. IG. Instituto de Geociências, v. 13, p. 116–128.

- Lima, F.C.T., and Caires, R.A., 2011, Fishes from the Serra Geral do Tocantins Ecological Station, Rio Tocantins and Rio São Francisco basins, with remarks on the biogeographical implications of the common headwater between the Rio Sapão and Rio Galheiros: Biota Neotropical, v. 11, <http://www.biota-neotropica.org.br/v11n1/en/abstract?article+bn03411012011.%0AAbstract>.
- Lima, F.C.T., and Ribeiro, A.C., 2011, Continental-Scale Tectonic Controls of Biogeography and Ecology: Historical biogeography of Neotropical freshwater fishes, p. 145–164, doi:10.1525/9780520268685.003.0009.
- Lisiecki, L.E., and Raymo, M.E., 2005, A Pliocene-Pleistocene stack of 57 globally distributed benthic $\delta^{18}\text{O}$ records: Paleoceanography, v. 20, p. 1–17, doi:10.1029/2004PA001071.
- Maddy, D., Bridgland, D., and Westaway, R., 2001, Uplift-driven incision and climate-controlled river terrace development in the Thames Valley, UK: Quaternary International, v. 79, p. 23–36, doi:10.1016/S1040-6182(00)00120-8.
- MapBiomas, 2019, Project MapBiomas. Brazilian Land Cover & Use Map Series:, <http://mapbiomas.org/> (accessed December 2019).
- Marengo, J.A., and Espinoza, J.C., 2016, Extreme seasonal droughts and floods in Amazonia: Causes, trends and impacts: International Journal of Climatology, v. 36, p. 1033–1050, doi:10.1002/joc.4420.
- Mascarenhas, A.L.S., Vidal, M.R., and Silva, E.V., 2015, O Uso do SIG para Definição de Aspectos Geomorfológicos no Médio Curso do Rio Tocantins Parte Oriental da Bacia Amazônica: Revista Geoamazônia, v. 2, p. 68–78, doi:10.17551/2358-1778/geoamazonia.n1v2p68-78.
- Mattos, M.V.B. de, 2014, Projeto Paleocanal, in Coordenação Noé von Atzingen ed., O Penta - Revista 30 anos Fundação Casa da Cultura de Marabá - FCCM, Marabá, Halley Gráfica e Editora, p. 100, https://issuu.com/amauryaquino/docs/revista_fccm_420x280mm_ebookbaixa (accessed October 2019).
- May, J.H., Zech, R., and Veit, H., 2008a, Late Quaternary paleosol-sediment sequences and landscape evolution along the Andean piedmont, Bolivian Chaco: Geomorphology, v. 98, p. 34–54, doi:10.1016/j.geomorph.2007.02.025.
- May, J.-H., Zech, R., and Veit, H., 2008b, Late Quaternary paleosol-sediment sequences and landscape evolution along the Andean piedmont, Bolivian Chaco: Geomorphology, v. 98, p. 34–54, doi:10.1016/j.geomorph.2007.02.025.
- Merino, E.R., Pupim, F.N., Macedo, H.A., and Assine, M.L., 2015, Enhancement and integration of optical satellite images with SRTM data for mapping and study of large fluvial plains: Examples in the Brazilian Pantanal: Revista Brasileira de Geomorfologia, v. 16, p. 49–62.
- Merona, B., 1987, Aspectos Ecológicos da Ictiofauna no Baixo Tocantins: Acta Amazonica, v. Único, p. 109–124.

- Mérona, B., Juras, A.A., Santos, G.M., and Cintra, I.H.A., 2010, Os peixes e a pesca no Baixo Rio Tocantins Vinte anos depois da UHE Tucuruí: 208 p.
- Merritts, D., 2007, Fluvial Environments | Terrace Sequences, *in* Encyclopedia of Quaternary Science, Pennsylvania, USA, Elsevier, p. 694–704, doi:10.1016/b0-44-452747-8/00116-2.
- Mertes, L.A.K., and Dunne, T., 2007, Effects of Tectonism, Climate Change, and Sea-level Change on the Form and Behaviour of the Modern Amazon River and its Floodplain, *in* Avijit Gupta ed., Large Rivers: Geomorphology and Management, Chichester, John Wiley & Sons Ltd, p. 115–140.
- Mertes, L.A.K., Dunne, T., and Martinelli, L.A., 1996, Channel-floodplain geomorphology along the Solimões-Amazon River, Brazil: Bulletin of the Geological Society of America, v. 108, p. 1089–1107, doi:10.1130/0016-7606(1996)108<1089:CFGATS>2.3.CO;2.
- Mesner, J.C., and Wooldridge, L.C.P., 1964, Maranhão Paleozoic Basin and Cretaceous Coastal Basins, North Brazil: Bulletin of the American Association of Petroleum Geologists, v. 48, p. 1475–1512.
- Miall, A.D., 2014, Fluvial depositional systems: Toronto, 1–316 p., doi:10.1007/978-3-319-00666-6.
- Miklín, J., and Galia, T., 2017, Detailed fluvial-geomorphologic mapping of wadeable streams: A proposal of universal map symbology: Journal of Maps, v. 13, p. 698–706, doi:10.1080/17445647.2017.1355275.
- MMA, 2006, Caderno da Região Hidrográfica do Tocantins-Araguaia: Brasília-DF, Ministério do Meio Ambiente, Secretaria de Recursos Hídricos, 132 p.
- Molian, L.C.B., 1993, Amazonia rainfall and its variability: Hydrology and water management in the humid tropics, p. 99–111.
- Moreira, L.S., Moreira-Turcq, P.F., Cordeiro, R.C., and Turcq, B.J., 2009, Reconstituição paleoambiental do Lago Santa Ninha, Várzea do Lago Grande de Curuai, Pará, Brasil: Acta Amazonica, v. 39, p. 609–616, doi:10.1590/s0044-59672009000300016.
- Moreira, L.S., Moreira-Turcq, P., Cordeiro, R.C., Turcq, B., Caquineau, S., Viana, J.C.C., and Brandini, N., 2013, Holocene paleoenvironmental reconstruction in the Eastern Amazonian Basin: Comprido Lake: Journal of South American Earth Sciences, v. 44, p. 55–62, doi:10.1016/j.jsames.2012.12.012.
- Murray, A.S., and Wintle, A.G., 2000, Luminescence dating of quartz using an improved single-aliquot regenerative-dose protocol: Radiation Measurements, v. 32, p. 57–73, doi:10.1016/S1350-4487(99)00253-X.
- Murray, A.S., and Wintle, A.G., 2003, The single aliquot regenerative dose protocol: Potential for improvements in reliability: Radiation Measurements, v. 37, p. 377–381, doi:10.1016/S1350-4487(03)00053-2.
- Nanson, G.C., and Croke, J.C., 1992, A genetic classification of floodplains: Geomorphology, v. 4, p. 459–486, doi:0169-555X/92/.
- Nobre, P., and Shukla, J., 1996, Variations of SST, wind stress and rainfall over the

- tropical Atlantic and South America.: *J.Climate*, v. 9, p. 2464–2479, doi:10.1175/1520-0442(1996)009<2464.
- Nogueira, A.C.R., Silveira, R., and Guimarães, J.T.F., 2013, Neogene-Quaternary sedimentary and paleovegetation history of the eastern Solimões Basin, central Amazon region: *Journal of South American Earth Sciences*, v. 46, p. 89–99, doi:10.1016/j.jsames.2013.05.004.
- Oliveira-Filho, A.T., 1995, A study of the origin of central Brazilian forests by the analysis of plant species distribution patterns: *Edinburgh Journal of Botany*, p. 55, doi:10.1017/S0960428600000949.
- De Oliveira, P.E., McMichael, C.N.H., Pinaya, J.L.D., and Bush, M.B., 2019, Climate change and biogeographic connectivity across the Brazilian cerrado: , p. 1–12, doi:10.1111/jbi.13732.
- Oliveira, P.S., and Marquis, R.J., 2002, *The Cerrados of Brazil: Ecology and Natural History of a Neotropical Savanna*: New York Chichester, Columbia University Press, 373 p.
- Oliveira, S.C., Pupim, F.N., Stevaux, J.C., and Assine, M.L., 2019, Luminescence Chronology of Terrace Development in the Upper Paraná River , Southeast Brazil: v. 7, p. 1–17, doi:10.3389/feart.2019.00200.
- Park, E., and Latrubblesse, E.M., 2019, A geomorphological assessment of wash-load sediment fluxes and floodplain sediment sinks along the lower Amazon River: *Geology*, v. 47, p. 403–406, doi:10.1130/G45769.1.
- Park, E., and Latrubblesse, E., 2017, The hydro-geomorphologic complexity of the lower Amazon River floodplain and hydrological connectivity assessed by remote sensing and field control: *Remote Sensing of Environment*, v. 198, p. 321–332, doi:10.1016/j.rse.2017.06.021.
- Passos, M., Soares, E., Tatumi, S., Yee, M., Mittani, J., Hayakawa, E., and Salazar, C., 2020, Pleistocene-Holocene sedimentary deposits of the Solimões-Amazonas fluvial system, Western Amazonia: *Journal of South American Earth Sciences*, v. 98, p. 102455, doi:10.1016/j.jsames.2019.102455.
- Pazzaglia, F.J., 2013, Fluvial Terraces, *in* Shroder, J.F. ed., *Treatise on Geomorphology*, p. 379–412, <http://citeseerx.ist.psu.edu/viewdoc/download?doi=10.1.1.211.535&rep=rep1&type=pdf> (accessed August 2019).
- Petit, J.R. et al., 1999, Climate and atmospheric history of the past 420,000 years from the Vostok ice core, Antarctica: *The Future of Nature: Documents of Global Change*, p. 348–358.
- Prescott, J.R., and Hutton, J.T., 1994, Cosmic ray contributions to dose rates for luminescence and ESR dating: Large depths and long-term time variations: *Radiation Measurements*, v. 23, p. 497–500, doi:10.1016/1350-4487(94)90086-8.
- Pupim, F. N., Assine, M.L., and Sawakuchi, A.O., 2017, Late Quaternary Cuiabá megafan, Brazilian Pantanal: Channel patterns and paleoenvironmental changes: *Quaternary International*, v. 438, p. 108–125, doi:10.1016/j.quaint.2017.01.013.
- Pupim, F.N. et al., 2019, Chronology of Terra Firme formation in Amazonian lowlands

- reveals a dynamic Quaternary landscape: *Quaternary Science Reviews*, v. 210, p. 154–163, doi:10.1016/j.quascirev.2019.03.008.
- Pupim, F. do N., Sawakuchi, A.O., Mineli, T.D., and Nogueira, L., 2016, Evaluating isothermal thermoluminescence and thermally transferred optically stimulated luminescence for dating of Pleistocene sediments in Amazonia: *Quaternary Geochronology*, v. 36, p. 28–37, doi:10.1016/j.quageo.2016.08.003.
- RadamBrasil, 1974, Radam Brasil Folha SB.22 Araguaia e parte da Folha SC.22 Tocantins: Rio de Janeiro, 521 p., <https://biblioteca.ibge.gov.br/visualizacao/livros/liv24021.pdf> (accessed October 2019).
- RadamBrasil, 1986, RadamBrasil Folha SB.22-X-D Marabá: Programa Levantamentos Geológicos Básicos do Brasil. Carta Geológica - Escala 1:250.000 - Anexo I, v. SB.22-X-D.
- Räsänen, M.E., Salo, J.S., Jungnert, H., and Pittman, L.R., 1990, Evolution of the Western Amazon Lowland Relief: impact of Andean foreland dynamics: *Terra Nova*, v. 2, p. 320–332, doi:10.1111/j.1365-3121.1990.tb00084.x.
- Reis, L.S., Guimarães, J.T.F., Souza-Filho, P.W.M., Sahoo, P.K., Figueiredo, M.M.J.C., de Souza, E.B., and Giannini, T.C., 2017, Environmental and vegetation changes in southeastern Amazonia during the late Pleistocene and Holocene: *Quaternary International*, v. 449, p. 83–105, doi:10.1016/j.quaint.2017.04.031.
- Ribas, C.C., Aleixo, A., Nogueira, A.C.R., Miyaki, C.Y., and Cracraft, J., 2012, A palaeobiogeographic model for biotic diversification within Amazonia over the past three million years: *Proceedings of the Royal Society B: Biological Sciences*, v. 279, p. 681–689, doi:10.1098/rspb.2011.1120.
- Ribeiro, M.C.L.B., Petrere, M., and Juras, A., 1995, Ecological integrity and fisheries ecology of the Araguaia—Tocantins River Basin, Brazil: *Regulated Rivers: Research & Management*, v. 11, p. 325–350, doi:10.1002/rrr.3450110308.
- Rigsby, C.A., Hemric, E.M., and Baker, P.A., 2009, Late Quaternary Paleohydrology of the Madre de Dios River, southwestern Amazon Basin, Peru: *Geomorphology*, v. 113, p. 158–172, doi:10.1016/j.geomorph.2008.11.017.
- Rosa, M.B., and Silva, L.T., 2016, Alguns Aspectos Climatológicos da ZCIT sobre o Atlântico: Centro de Previsão de Tempo e Estudos Climáticos/Instituto Nacional de Pesquisas Espaciais(CPTEC/INPE), São Paulo, Brasil, p. 37–42.
- Ross, J.L.S., 2016, Relevo brasileiro no contexto da América do Sul: *Revista Brasileira de Geografia*, doi:10.21579/issn.2526-0375_2016_n1_art_2.
- Rossetti, D.F. et al., 2015, Mid-Late Pleistocene OSL chronology in western Amazonia and implications for the transcontinental Amazon pathway: *Sedimentary Geology*, v. 330, p. 1–15, doi:10.1016/j.sedgeo.2015.10.001.
- Rossetti, D.F., Bertani, T.C., Zani, H., Cremon, E.H., and Hayakawa, E.H., 2012, Late Quaternary sedimentary dynamics in Western Amazonia: Implications for the origin of open vegetation/forest contrasts: *Geomorphology*, v. 177–178, p. 74–92, doi:10.1016/j.geomorph.2012.07.015.
- Rossetti, D.F., Cohen, M.C.L., Bertani, T.C., Hayakawa, E.H., Paz, J.D.S., Castro,

- D.F., and Friaes, Y., 2014, Late Quaternary fluvial terrace evolution in the main southern Amazonian tributary: *Catena*, v. 116, p. 19–37, doi:10.1016/j.catena.2013.11.021.
- Rossetti, D.F., and Goés, A.M., 2004, O Neógeno da Amazônia Oriental: Museu Paraense Emílio Goeldi, Coleção Friederich Katzer, p. 13–52.
- Rossetti, Gribel, R., Cohen, M., Valeriano, M., Tatumi, S.H., and Yee, M., 2019a, The role of Late Pleistocene-Holocene tectono-sedimentary history on the origin of patches of savanna vegetation in the middle Madeira River, southwest of the Amazonian lowlands: *Palaeogeography, Palaeoclimatology, Palaeoecology*, v. 526, p. 136–156, doi:10.1016/j.palaeo.2019.04.017.
- Rossetti, D., Peter, Mann de Toledo, and Góes, A.M., 2005a, New geological framework for Western Amazonia (Brazil) and implications for biogeography and evolution: *Quaternary Research*, v. 63, p. 78–89, doi:10.1016/j.yqres.2004.10.001.
- Rossetti, D.F., Toledo, P.M., and Góes, A.M., 2005b, New geological framework for Western Amazonia (Brazil) and implications for biogeography and evolution: *Quaternary Research*, v. 63, p. 78–89, doi:10.1016/j.yqres.2004.10.001.
- Rossetti, D.F., Toledo, P.M., and Valeriano, M.M., 2019b, Neotectonics and tree mortality in a forest ecosystem of the Negro basin: Geomorphic evidence of contemporary seismicity in the intracratonic Brazilian Amazonia: *Geomorphology*, v. 329, p. 138–151, doi:10.1016/j.geomorph.2018.12.028.
- Rossetti, D.F., and Truckenbrodt, W., 1997, Revisão estratigráfica para os depósitos do albano-terciário inferior (?) na Bacia de São Luís, Maranhão: *Bol. Mus. Para. Emílio Goeldi*, sér. Ciênc. da Terra, v. 9, p. 29–41.
- Rossetti, D.F., Valeriano, M.M., Gribel, R., Cohen, M.C.L., Tatumi, S.H., and Yee, M., 2017a, The imprint of Late Holocene tectonic reactivation on a megafan landscape in the northern Amazonian wetlands: *Geomorphology*, v. 295, p. 406–418, doi:10.1016/j.geomorph.2017.07.026.
- Rossetti, D.F., Valeriano, M.M., Gribel, R., Cohen, M.C.L., Tatumi, S.H., and Yee, M., 2017b, The imprint of Late Holocene tectonic reactivation on a megafan landscape in the northern Amazonian wetlands: *Geomorphology*, v. 295, p. 406–418, <http://dx.doi.org/10.1016/j.geomorph.2017.07.026>.
- Sahoo, P.K., Souza-Filho, P.W.M., Guimarães, J.T.F.S., Silva, M.S., Costa, F.R., Manes, C.L.O., Oti, D., Júnior, R.O.S., and Dall'Agnol, R., 2015, Use of multi-proxy approaches to determine the origin and depositional processes in modern lacustrine sediments: Carajás Plateau, Southeastern Amazon, Brazil: *Applied Geochemistry*, v. 52, p. 130–146, doi:10.1016/j.apgeochem.2014.11.010.
- Salo, J., Kalliola, R., Häkkinen, I., Mäkinen, Y., Niemelä, P., Puhakka, M., and Coley, P.D., 1986, River dynamics and the diversity of Amazon lowland forest: *Nature*, v. 322, p. 254–258, doi:10.1038/322254a0.
- Sant'Anna, L.G., Soares, E.A. do A., Riccomini, C., Tatumi, S.H., and Yee, M., 2017, Age of depositional and weathering events in Central Amazonia: *Quaternary Science Reviews*, v. 170, p. 82–97, doi:10.1016/j.quascirev.2017.06.015.

Santos, J.O.S., Hartmann, L.A., Gaudette, H.E., Groves, D.I., Mcnaughton, N.J., and Fletcher, I.R., 2000, A New Understanding of the Provinces of the Amazon Craton Based on Integration of Field Mapping and U-Pb and Sm-Nd Geochronology: *Gondwana Research*, v. 3, p. 453–488, doi:10.1016/S1342-937X(05)70755-3.

Sawakuchi, A.O. et al., 2015, The Volta Grande do Xingu: Reconstruction of past environments and forecasting of future scenarios of a unique Amazonian fluvial landscape: *Scientific Drilling*, v. 20, p. 21–32, doi:10.5194/sd-20-21-2015.

Schumm, S., 1988, Variability of the fluvial system in space and time: Scales and global change, p. 225–250.

Seltzer, G., Rodbell, D., and Burns, S., 2000, Isotopic evidence for late Quaternary climatic change in tropical South America: , p. 35–38.

Sifeddine, A. et al., 2003, A 21 000 cal years paleoclimatic record from Caçó Lake, northern Brazil: evidence from sedimentary and pollen analyses: *Palaeogeography, Palaeoclimatology, Palaeoecology*, v. 189, p. 25–34, doi:10.1016/S0031-0182(02)00591-6.

Sifeddine, A., Frohlich, F., Fournier, M., Martin, L., Servant, M., Soubiès, F., Turcq, B., Suguio, K., and Volkmer-Ribeiro, C., 1994, La sédimentation lacustre indicateur de changements des paléoenvironnements au cours des 30000 dernières années (Carajas, Amazonie, Brésil): *Comptes Rendus de l'Académie des Sciences de Paris*, v. 318, p. 1645–1652.

Sinha, R., Jain, V., Babu, G.P., and Ghosh, S., 2005, Geomorphic characterization and diversity of the fluvial systems of the Gangetic Plains: *Geomorphology*, v. 70, p. 207–225, doi:10.1016/j.geomorph.2005.02.006.

Slingerland, R., and Smith, N.D., 2004, River Avulsions and Their Deposits: *Annual Review of Earth and Planetary Sciences*, v. 32, p. 257–285, doi:10.1146/annurev.earth.32.101802.120201.

Smith, R.J., and Mayle, F.E., 2018, Impact of mid- to late Holocene precipitation changes on vegetation across lowland tropical South America: A paleo-data synthesis: *Quaternary Research* (United States), v. 89, p. 134–155, doi:10.1017/qua.2017.89.

Soares, E.A.A., Tatumi, S.H., and Riccomini, C., 2010, OSL age determinations of Pleistocene fluvial deposits in Central Amazonia: *Anais da Academia Brasileira de Ciencias*, v. 82, p. 691–699, doi:10.1590/S0001-37652010000300017.

Souza, D.F., 2015, Evolução sedimentar do tabuleiro do Embaubal, baixo rio Xingu: , p. 64.

Souza, E.B., and Ambrizzi, T., 2003, Pentad precipitation climatology over Brazil and the associated atmospheric mechanisms: *Climanálise*, https://www.researchgate.net/profile/Everaldo_De_Souza/publication/228582482_Pentad_precipitation_climatology_over_Brazil_and_the_associated_atmospheric_mechanisms/links/57442f0008aea45ee84d20c7/Pentad-precipitation-climatology-over-Brazil-and-the-associa.

Steiaux, J.C., 2000, Climatic events during the Late Pleistocene and Holocene in the Upper Parana River: Correlation with NE Argentina and South-Central Brazil:

- Quaternary International, v. 72, p. 73–85, doi:10.1016/S1040-6182(00)00023-9.
- Stevaux, J.C., Corradini, F.A., and Aquino, S., 2013, Connectivity processes and riparian vegetation of the upper Paraná River, Brazil: Journal of South American Earth Sciences, v. 46, p. 113–121, doi:10.1016/j.jsames.2011.12.007.
- Tassinari, C.C.G., and Macambira, M.J.B., 1999, Geochronological provinces of the Amazonian Craton: Episodes, v. 22, p. 174–182.
- Thom, G., Xue, A., Sawakuchi, A.O., Ribas, C.C., Hickerson, M.J., Aleixo, A., and Miyaki, C., 2020, Quaternary climate changes as speciation drivers in the Amazon floodplains: Science Advances, v. 6, doi:10.1126/sciadv.aax4718.
- Thomas, M.F., 2008, Understanding the impacts of Late Quaternary climate change in tropical and sub-tropical regions: Geomorphology, v. 101, p. 146–158, doi:10.1016/j.geomorph.2008.05.026.
- Tobler, W., 1987, Measuring spatial resolution: Land Resources Information Systems Conference, p. 12–16.
- Tofelde, S., Savi, S., Wickert, A.D., Bufe, A., and Schildgen, T.F., 2019, Alluvial channel response to environmental perturbations: fill-terrace formation and sediment-signal disruption: , p. 609–631.
- USGS, 2015, USGS EROS Archive - Digital Elevation - Shuttle Radar Topography Mission (SRTM) 1 Arc-Second Global: US Geological Survey, doi:10.5066/F7PR7TFT.
- Valente, C.R., and Latrubesse, E.M., 2012a, Fluvial archive of peculiar avulsive fluvial patterns in the largest Quaternary intracratonic basin of tropical South America: The Bananal Basin, Central-Brazil: Palaeogeography, Palaeoclimatology, Palaeoecology, v. 356–357, p. 62–74, doi:10.1016/j.palaeo.2011.10.002.
- Valente, C.R., and Latrubesse, E.M., 2012b, Fluvial archive of peculiar avulsive fluvial patterns in the largest Quaternary intracratonic basin of tropical South America: The Bananal Basin, Central-Brazil: Palaeogeography, Palaeoclimatology, Palaeoecology, v. 356–357, p. 62–74, doi:10.1016/j.palaeo.2011.10.002.
- Vandenberghhe, J., 2003, Climate forcing of fluvial system development: an evolution of ideas: Quaternary Science Reviews, v. 22, p. 2053–2060, doi:10.1016/S0277-3791(03)00213-0.
- Várzea, A., 1942, Relevo do Brasil: Revista Brasileira de Geografia, p. 97–135.
- Vasquez, M.L., 2006, Geocronologia em Zircão, Monazita e Granada e Isotópos de Nd das Associações Litológicas da Porção Oeste do Domínio Bacajá: Evolução Crustal da Porção Meridional da Província Maroni-Itacaiúnas - Sudeste do Cratón Amazônico: Universidade Federal do Pará, 212 p.
- Vasquez, M.L., and Rosa-Costa, L.T., 2008, Geologia e Recursos Mineirais do Estado do Pará: Sistema de Informações Geográficas - SIG (Programa Geologia do Brasil (PGB). Integração e Difusão de Dados da Geologia do Brasil. Mapas Geológicos Estaduais, Ed.): Belém, CPRM, 328 p.
- Vera, C. et al., 2006, Toward a Unified View of the American Monsoon Systems: American Meterological Society, p. 4977–5000.

Verstappen, H.T., 1977, Remote sensing in geomorphology: Elsevier Scientific Publishing Company, v. 4.

Villegas, J.M.C., 1994, Geologia Estrutural da Bacia do Marajó: Universidade Federal do Pará, 128 p.

Wang, X., Edwards, R.L., Auler, A.S., Cheng, H., Kong, X., Wang, Y., Cruz, F.W., Dorale, J.A., and Chiang, H.W., 2017, Hydroclimate changes across the Amazon lowlands over the past 45,000 years: *Nature*, v. 541, p. 204–207, doi:10.1038/nature20787.

Wheaton, J.M., Fryirs, K.A., Brierley, G., Bangen, S.G., Bouwes, N., and O'Brien, G., 2015, Geomorphic mapping and taxonomy of fluvial landforms: *Geomorphology*, v. 248, p. 273–295, doi:10.1016/j.geomorph.2015.07.010.

Williams, R.D., Brasington, J., Vericat, D., and Hicks, D.M., 2014, Hyperscale terrain modelling of braided rivers: Fusing mobile terrestrial laser scanning and optical bathymetric mapping: *Earth Surface Processes and Landforms*, v. 39, p. 167–183, doi:10.1002/esp.3437.

Winemiller, K.O. et al., 2016, Balancing hydropower and biodiversity in the Amazon, Congo, and Mekong: *Science*, v. 351, p. 128–129, doi:10.1126/science.aac7082.

Yamazaki, D., Ikeshima, D., Tawatari, R., Yamaguchi, T., O'Loughlin, F., Neal, J.C., Sampson, C.C., Kanae, S., and Bates, P.D., 2017, A high-accuracy map of global terrain elevations: *Geophysical Research Letters*, v. 44, p. 5844–5853, doi:10.1002/2017GL072874.

Zhang, Y. et al., 2016, Equatorial Pacific forcing of western Amazonian precipitation during Heinrich Stadial 1: *Scientific Reports*, v. 6, p. 1–7, doi:10.1038/srep35866.

Zhou, J., and Lau, K.M., 1998, Does a monsoon climate exist over South America? *Journal of Climate*, v. 11, p. 1020–1040, doi:10.1175/1520-0442(1998)011<1020:DAMCEO>2.0.CO;2.

Zinck, J.A., 2016, Geopedology:, doi:10.1007/978-3-319-19159-1.

Zocatelli, R., Moreira-Turcq, P., Bernardes, M., Turcq, B., Cordeiro, R.C., Gogo, S., Disnar, J.R., and Boussafir, M., 2013, Sedimentary evidence of soil organic matter input to the curuai amazonian floodplain: *Organic Geochemistry*, v. 63, p. 40–47, doi:10.1016/j.orggeochem.2013.08.004.

Zocatelli, R., Moreira-Turcq, P., Jacob, J., Cordeiro, R.C., Boussafir, M., Le Milbeau, C., Bernardes, M., and Turcq, B., 2016, Holocene land cover dynamics in the Curuai Floodplain inferred from lacustrine biomarkers: *Palaeogeography, Palaeoclimatology, Palaeoecology*, v. 443, p. 237–248, doi:10.1016/j.palaeo.2015.11.046.

Zular, A., Sawakuchi, A.O., Chiessi, C.M., D'Horta, F.M., Cruz, F.W., Demattê, J., Ribas, C.C., Hartmann, G., Giannini, P.C., and Soares, E.A.A., 2019, The role of abrupt climate change in the formation of an open vegetation enclave in northern Amazonia during the late Quaternary: *Global and Planetary Change*, v. 172, p. 140–149, doi:10.1016/j.gloplacha.2018.09.006.

APÊNDICE – Mapa Geomorfológico

